Loughborough University

Thesis Access Form

Copy No……...……**Location**……

Author……RADHI ALAZMI……..…….
Title…The effect of wastewater components on the fouling of ceramic membrane.

Status of access OPEN / RESTRICTED / CONFIDENTIAL

Moratorium Period:……years,
ending……../……200…….

Conditions of access approved by (CAPITALS):……V. NASSEHI..…

Supervisor (Signature)……...……
Department of……Chemical Engineering……..……..

Author's Declaration: *I agree the following conditions:*

Open access work shall be made available (in the University and externally) and reproduced as necessary at the discretion of the University Librarian or Head of Department. It may also be digitised by the British Library and made freely available on the Internet to registered users of the EThOS service subject to the EThOS supply agreements.

*The statement itself shall apply to **ALL** copies including electronic copies:*

This copy has been supplied on the understanding that it is copyright material and that no quotation from the thesis may be published without proper acknowledgement.

Restricted/confidential work: All access and any photocopying shall be strictly subject to written permission from the University Head of Department and any external sponsor, if any.

Author's signature…….Date……...……...……...

users declaration: for signature during any Moratorium period (Not Open work): ***I undertake to uphold the above conditions:***			
Date	Name (CAPITALS)	Signature	Address

The effect of wastewater components on the fouling of ceramic membranes

By

Radhi Alazmi

Doctoral Thesis

Submitted in partial fulfilment of the requirements for the award of Doctor of Philosophy of Loughborough University

Certificate of Originality

This is to certify that I am responsible for the work submitted in this thesis, that the original work is my own except as specified in acknowledgments or in footnotes, and that neither the thesis nor the original work contained therein has been submitted to this or any other institution for a higher degree.

Author's signature ……

Date ……..

Acknowledgements

I would like to begin with thanking almighty Allah (God) for all his blessing and grace upon me in this life.

I wish to thank my family especially my wife for all the patient and encouragement they showed during the years I spent doing this work.

I wish to thank my supervisors Professor Richard Wakeman and Professor Vahid Nassehi for their guidance and advice which helped me to identify the crucial and the most important areas in membrane filtration to concentrate my research in.

I would like to thank Chris Manning the Experimental Officer in the Chemical Engineering Department at Loughborough University for his help with the experimental apparatus design and maintenance. I also would like to thank the Laboratory supervisor Sean Creedon and Dave Smith for all their training and help with the laboratory equipments.

ABSTRACT

In this work, the effect of wastewater feed composition on the membrane fouling rate of 5 and 20 kD ultrafiltration ceramic membranes was investigated using statistical analysis of the experimental results (two way factorial design), with particular regard to the protein (meat extract and peptone), sodium alginate and calcium chloride components. A mathematical model was used to determine the major membrane blocking mechanisms and the effect of different feed components concentration on the blocking mechanisms.

Polysaccharides are the major fouling compounds in extracellular polymeric substance (EPS), while protein compounds are an important part of EPS membrane fouling, their effect increases in the presence of polysaccharides. Sodium alginate calcium solutions fouled the membrane more severely, causing twice the increase of resistance (on average) than did meat extract calcium solutions. This study showed that irreversible fouling was the major fouling type in alginate calcium filtration experiments, while less of the fouling in the meat extract calcium filtration experiments was irreversible.

The effect of changing the artificial wastewater components concentration on the fitting accuracy of the blocking models for the 20 kD pore size membrane was almost the opposite of the 5 kD pore size membrane. Increasing the calcium concentration increased the predication accuracy of the intermediate and complete blocking models, while the increase in alginate concentration reduced the cake filtration model prediction accuracy.

After each experiment, the membrane was cleaned using different cleaning chemical concentrations. The best cleaning was achieved with increasing sodium hydroxide concentration in the cleaning solution. In general higher cleaning temperature and increasing cleaning time improved the membrane recovery, nevertheless; the effect was not as noticeable as the effect of increasing sodium hydroxide concentration.

Table of Contents

List of Tables

List of Figures

1.0 Introduction

1.1 Global Water Shortage

One of the biggest problems facing the world in this century is the shortage of potable water, especially in the developing countries. Global water consumption has increased six fold from 1900 to 1995 (Singh, 2006). The water shortage is so severe that, according to the World Health Organisation (WHO), almost 60% of human illnesses are caused by contaminated water or the lack of sewer treatment (Singh, 2006).

Fresh water is a fundamental need for most aspects of life. Fresh water is needed in agriculture, for drinking water, or as process water in various industries. Groundwater and/or surface water is not always sufficiently available and there are often many impurities contained in water. Water impurities may be classified by their size (Aptel, 1994):
True solutes: small molecules, with a size less than one nanometre, and macromolecules with sizes between 1 and 10 nanometres.
Colloidal suspensions: heterogeneous systems, in which the dispersed compounds generally measure less than 100 nm.
Particles: suspended solids visible under an optical microscope, with sizes more than 200 nm.

1.2 Water treatment

Water treatment processes are needed to remove these impurities so that communities can use water safely. A number of classical separation processes are already used as cleaning technologies, such as sand filtration, sedimentation, coagulation, flocculation, precipitation, distillation, disinfection, oxidation and ion exchange. The technique used depends largely on the specific application, and in many cases more research is needed to determine the appropriate technique to be applied and on the process parameters.

Different kinds of pollution present in waters used for various purposes result in a situation where their treatment is not easy to perform, and the treatment system may need to be specified individually for each type of water. In order to guarantee the quality required of potable water or water used for industrial purposes, often unconventional or high efficiency processes must be applied (e.g., membrane techniques) which are expected to improve consumer safety despite the higher costs involved.

1.3 Membrane Wastewater treatment

Membrane technology offers the advantages of higher effluent quality and a reduction of treatment plant size compared to traditional wastewater treatment technology The fouling of membranes by wastewater components is a major disadvantage, responsible for slowing the implementation of membrane separation technology in wastewater treatment (Judd and Jefferson, 2003; Singh, 2006).

In addition to the higher effluent quality and smaller plant footprint of membrane separation technology, a major advantage is the smaller sludge volume produced using membrane bioreactor technology in wastewater treatment (Judd and Jefferson, 2003).

In traditional activated sludge wastewater treatment processes, aggregation of microbials into flocs, bioflocculation, is a very important and desired process. Bioflocculation is believed to improve solid/liquid separation, which in turn leads to improved settling and dewatering in the bioreactor (Sobeck and Higgins, 2002; Steiner *et al.*, 1976; Houghton *et al.*, 2001).

From an operational point of view, a large amount of excess sludge presents a serious drawback for wastewater treatment plants (Neyens *et al.*, 2004). From an economic point of view it is estimated that 25-50 % of wastewater treatment cost is associated with sludge waste management (Baeyens *et al.*,

1997). Therefore, dewatering of sludge in wastewater plants is a costly as much as an essential process (Houghton *et al.*, 2001). Membrane bioreactor technology can reduce the amount of sludge production in wastewater yet achieve a high quality effluent.

1.4 Research Aims and Objectives

The aim of this work is to explore the problem of membrane fouling by wastewater components in depth. Understanding the effect of changing wastewater components concentration on membrane fouling, the specific fouling blocking mechanisms, type of fouling and extant of fouling caused by different components, will help in solving the membrane fouling problem. The objectives of this study are:

- To relate membrane fouling to wastewater organic and non-organic components concentration,
- To relate membrane fouling mechanisms to wastewater components concentration,
- To relate membrane fouling Type to wastewater components concentration and
- To identify an efficient cleaning procedures.

2.0 Literature Review

2.1 Wastewater Technology

2.1.1 Conventional activated sludge process

Recycling and reuse of industrial and municipal wastewater is one way of dealing with the water shortage problem.

Table 1 lists several undesirable water contaminants, the conventional solutions for them and corresponding membrane processes that can do the job.

Table 1 Conventional and membrane process solutions to common water problems. Ho and Sirkar (1992).

Constituents of concern	Conventional Process	Membrane Process
Turbidity Suspended Solids Biological Contamination	Coagulation/Flocculation Media Filtration Disinfection	Microfiltration
Colour Odour Volatile Organics	Activated carbons Media Filtration Aeration	Ultrafiltration
Hardness Sulphates Manganese Iron Heavy Metals	Lime Softening Ion Exchange Oxidation Filtration Coagulation/Flocculation	Nanofiltration
Total Dissolved Solids Nitrate	Distillation Ion Exchange	Reverse Osmosis Electrodialysis

Membrane bioreactors (MBR) are increasingly replacing the old conventional activated sludge process in wastewater treatment plants. Traditional activated sludge schemes consist of an aeration tank and a secondary clarification tank (Figure 1).

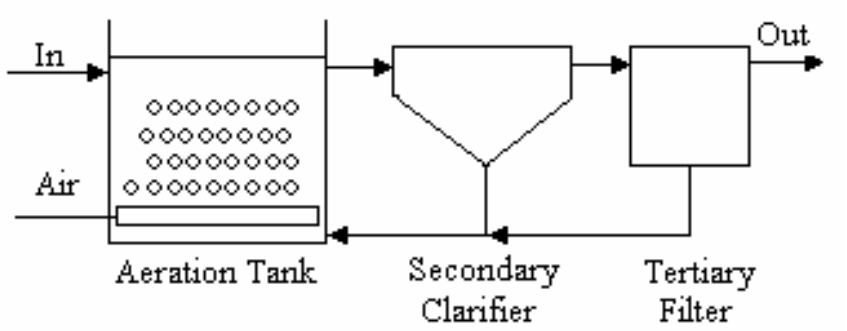

Figure 1. Conventional activated sludge schematic. Water Environment Federation (2006)

2.2 Membrane technology

Membrane technology has become a significant separation technology over the last decades of the twentieth century (Judd and Jefferson 2003). The main strength of membrane technology is the fact that the membrane separation works without the addition of chemicals, with a relatively low energy use and easy and well organised process conditions.

The membrane separation process is based on the use of semi permeable membranes. The membrane acts as a specific filter that will let water flow through, while retaining suspended solids and other substances. There are various methods that are used as the driving force to enable substances to penetrate a membrane. Examples of these are a pressure difference, a concentration gradient, or an electric potential (Judd and Jefferson, 2003)

Treating high turbidity and high total organic carbon (TOC) municipal wastewater using membrane filtration gives more stable and superior water quality compared to coagulation sedimentation techniques (Singh 2006).

Membrane filtration can be divided into microfiltration and ultrafiltration on one hand and nanofiltration and reverse osmosis (RO or hyper filtration) on the other hand. When membrane filtration is used for the removal of larger particles (10-0.1 and 0.1-0.001 μm) microfiltration and ultrafiltration are applied, respectively. Due to the open character of these membranes, the productivity is high while the pressure differentials are low.

When salts need to be removed from water, nanofiltration or reverse osmosis are applied (Singh 2006). Nanofiltration and RO membranes do not work according to the pores size separation; separation takes place by diffusion through the membrane (Singh 2006). The pressure that is required to perform nanofiltration and reverse osmosis is much higher than the pressure required for micro and ultrafiltration, while the productivity is much lower.

Membrane filtration has a number of benefits over existing water purification techniques. Filtration is a process that can take place at low temperatures. This is mainly important because this enables the treatment of heat sensitive matter, thus these methods are widely used for food products. For a high temperature process (higher than 40 ºC), a ceramic membrane is used (Singh 2006).
Membrane separation processes have low energy costs. Most of the energy that is required is used to pump liquids through the membrane. The total amount of energy that is used is minor compared to alternative techniques such as evaporation. The process can easily be expanded.

2.2.1 Membrane bioreactor

In the MBR system, the aeration and the clarification steps are combined; they can be pressure driven, in which case the membrane module is located externally to the bioreactor, or vacuum driven, in which case the membrane module is submerged in the bioreactor; see Figure 2 (Water Environment Federation, 2006).

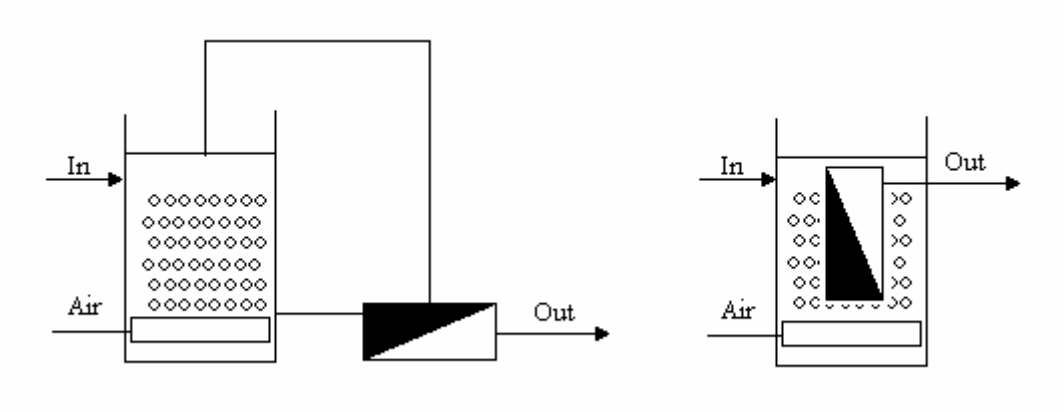

Figure 2. External and Immersed MBR Schematic (Water Environment Federation, 2006).

The advantages of using membrane bioreactors to treat industrial and municipal wastewater are numerous; some of the benefits are (Singh, 2006):

- High quality effluent due to complete biomass retention.
- Small footprint. The elimination of secondary clarifiers resulting in a smaller wastewater plant.
- Due to the modular nature of the membrane systems they provide ease of expansion and flexibility in configuration.
- Wide range of solids retention time (SRT) operation thus giving flexibility and greater options to optimise the system operation.
- MBR processes can be easily automated resulting in a reduction in operator requirements.
- High quality effluent reduces the need for downstream disinfection.

2.2.2 Membrane structure

Membranes are categorised according to the way by which separation is achieved (Table 2):

Dense: where a high degree of selectivity is achieved. The separation relies on the physicochemical interactions between the membrane material and the permeating components.

Porous: the separation is mechanically achieved by size exclusion. Materials with sizes larger than the pore size are rejected.

Table 2. Dense and porous membranes for water treatment (Judd and Jefferson 2003).

Dense	**Porous**
Reverse osmosis (RO) Separation achieved by virtue of differing solubility and diffusion rates of water (solvent) and solutes in water. *Electrodialysis (ED)* Separation achieved by virtue of differing ionic size, charge and charge density of solute ions using ion exchange membranes. *Pervaporation (PV)* Same mechanism as RO but with the (volatile) solute partially vapourised across the membrane by partially evacuating the permeate side. *Nanofiltration (NF)* Formerly called "leaky reverse osmosis". Separation achieved through a combination of charge rejection, solubility diffusion and sieving through micropores (<2 nm).	*Ultrafiltration (UF)* Separation by sieving through mesopores (2-50 nm) *Microfiltration (MF)* Separation of suspended solids from water by sieving through macropores (>50 nm) *Gas transfer (GT)* Gas transferred under a partial pressure gradient into or out of water in molecular form.
Membrane materials limited to polymeric materials.	Both polymeric and inorganic materials available.

The common types of membrane elements used in wastewater treatment are flat sheet, hollow fibres (Figure 3), tubular and spiral wound (Figure 4) (Water Environment Federation 2006).

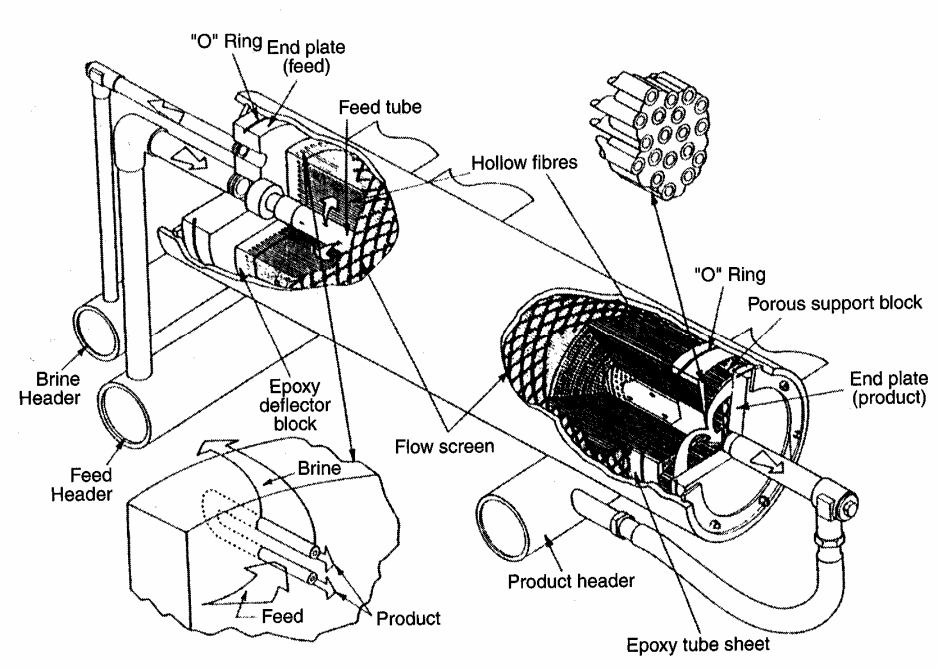

Figure 3 Hollow fibre RO membrane module assembly (Singh 2006).

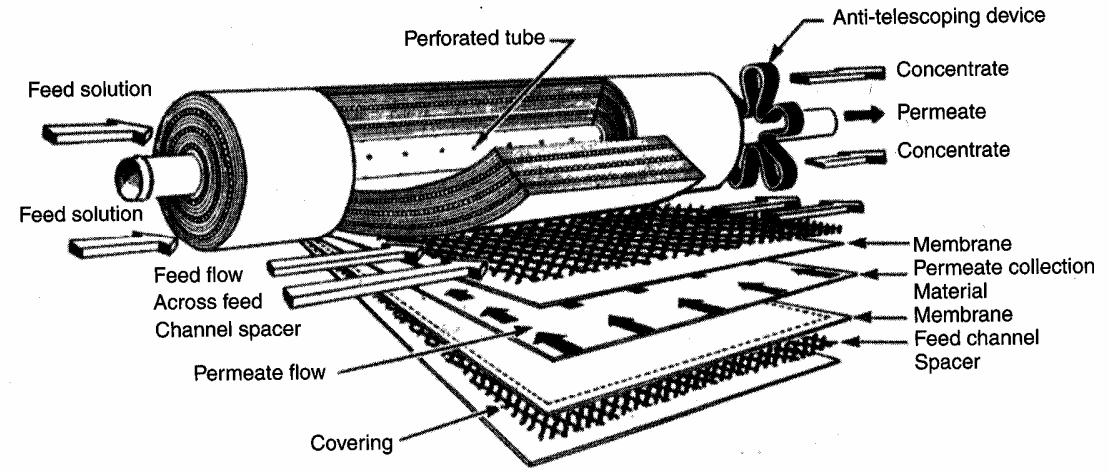

Figure 4 Spiral wound membrane module (Singh 2006).

2.2.3 Membrane materials

Membranes can be categorised as organic (polymeric) or inorganic (ceramic or metallic) depending on their material composition. Moreover, membranes can be categorised according to their physical structure (morphology).

The morphology of a membrane depends on the material and process in which they were manufactured. Membranes in which a pressure driven process is used for their construction are usually anisotropic, which means that they have symmetry in a single direction. The pore size changes with depth for an asymmetric membrane. A skin, a thin permselective layer, is to minimise the hydraulic resistance (Table 3) (Judd and Jefferson, 2003).

Table 3. Membrane materials by type (Judd and Jefferson 2003).

Membrane	Manufacturing procedure	Applications
Ceramic	Pressing, sintering of fine powders followed by sol gel coating	MF, UF. Aggressive and/or highly fouling media
Stretched polymers	Stretching of partially crystalline foil	MF. Aggressive, sterile filtration, medical technology
Track etched polymers	Radiation followed by acid etching	MF (polycarbonate (PET) materials). Analytical and medical chemistry, sterile filtration
Supported liquid	Formation of liquid film in inert polymer matrix	Gas separations, carrier mediated transport
Integral asymmetric, microporous	Phase inversion	MF, UF, NF, GT
Composite asymmetric microporous	Application of thin film to integral asymmetric microporous membrane to produce TFC	NF, RO, PV
Ion exchange	Functionalisation of polymer material	ED

2.3 Microfiltration and ultrafiltration

The principle of microfiltration and ultrafiltration is physical separation. The extent to which dissolved solids, turbidity and micro organisms are removed is determined by the size of the pores in the membranes. Substances that are larger than the pores in the membranes are fully removed. Substances that are smaller than the pores of the membranes are partially removed, depending on the construction of the rejection layer on the membrane.

Typical ranges of particle sizes and membrane processes used to separate them are described in Figure 5. Microfiltration and ultrafiltration are pressure

dependent processes, which remove dissolved solids and other substances from water to a lesser extent than nanofiltration and reverse osmosis.

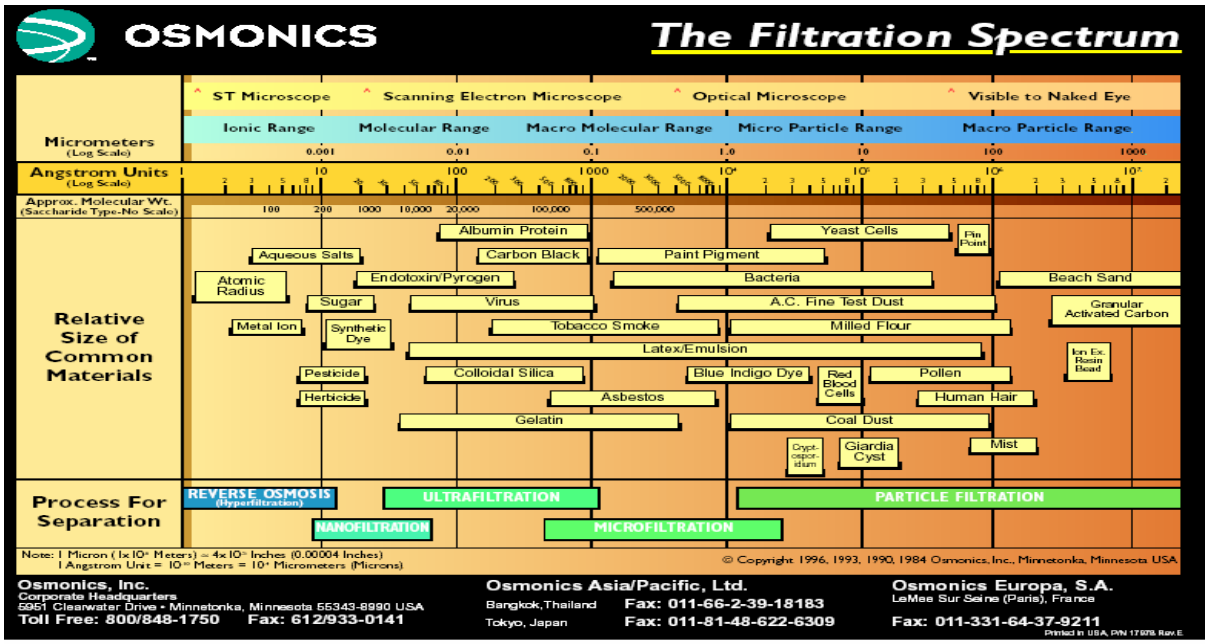

Figure 5 The filtration spectrum. Osmonics, Inc. (2002).

2.3.1 Microfiltration

Membranes with a pore size of 0.1 – 10 µm are used to perform microfiltration. Microfiltration membranes can remove all bacteria. A part of the viral contamination is removed in the process, even though viruses are smaller than the pores of a microfiltration membrane. This is because viruses can attach themselves to a bacterial biofilm. Microfiltration can be implemented in many different water treatment processes when particles with diameters greater than 0.1 mm need to be removed from a liquid.

In terms of characteristic particle size, this range covers the lower portion of the conventional clays and the upper half of the range for humic acids (Judd and Jefferson, 2003). This is smaller than the size range for bacteria, algae and cysts, and larger than that of viruses. A distinction should be made here between ‘dead end filtration’ (where clarified fluid is forced perpendicularly

through the filter) and 'crossflow filtration' (where the bulk suspension flows tangentially to the surface of the membrane).

The separation mechanism in microfiltration is based on a sieving mechanism. This means that the membrane will separate many substances in the feed solution based on their size compared with the size of the membrane pores. Substances larger than the pore size will be excluded by the membrane, while smaller substances will pass through the membrane.

The pressure driven permeate flux through this cake layer and the membrane may be described by Darcy's law (Ho and Sirkar, 1992; Coulson *et al,*. 1991).

$$J = \frac{1}{A}\frac{dV}{dt} = \frac{\Delta p}{\eta_o (R_m + R_c)} \tag{2.1}$$

where J is the permeate flux, V is the total volume of the permeate, t is the filtration time, Δp is the pressure drop imposed across the cake and membrane, η_o is the viscosity of the suspending fluid, R_m is the membrane resistance and R_c is the cake resistance.

2.3.2 Ultrafiltration

For the complete removal of viruses, ultrafiltration is required. The pores of ultrafiltration membranes can remove particles of 0.001 – 0.1 µm from fluids. Ultrafiltration can also be applied for pre-treatment of water for nanofiltration or reverse osmosis.

The most important membrane properties are obviously the flux and the rejection. The volumetric flux is given by Darcy's law, while the observed solute rejection R_i for a given species i is given by (Coulson *et al*. 1991):

$$R_i = 1 - \frac{c_{ip}}{c_{ir}} \tag{2.2}$$

where c_{ip} and c_{ir} are the concentration in the permeate and retentate sides, respectively.

Microfiltration and ultrafiltration are used in combination with other membrane processes. Bodzek *et al*. (2002) used ultrafiltration as a pretreatment before water containing chloroform was processed by nanofiltration and reverse osmosis. Ultrafiltration has also been used for sludge concentration before dewatering (Ho *et al*. 1992). The major barrier to the use of ultrafiltration in water treatment is the cost of the water produced.

2.4 Theories of bioflocculation mechanisms

Three theories exist that describe the mechanisms of cations in bioflocculation; the Derjaguin, Landau, Verwey, and Overbeek (DLVO) theory, the Divalent Cation Bridging (DCB) theory, and the Alginate Theory (Sobeck and Higgins, 2002). In the DLVO theory particles are surrounded with a double layer of counterions, a first, tightly associated, layer of counterions called the Stern layer and a second layer of less tightly associated counterions called the diffuse layer. The negative cloud surrounding the particles results in repulsion forces between particles. According to this theory, increasing cation concentration should compress the double layer thus allowing particles to aggregate.

In the Alginate theory, alginate, which is a polysaccharide made up of a linear copolymer of monomers of 1-4 linked β-D- mannuronic and α-L-guluronic acids (Draget *et al*., 2002), forms a gel in the presence of Ca^{++}. The gel is formed in what is called an egg-box model (Figure 6). According to this theory, this model is unique to the alginate composition (Bruus *et al*., 1992). Polysaccharides such as alginate are unprotonated at the typical pH of activated sludge. The unprotonated carboxyl groups contribute to the negative charge of the biofloc (Frolund *et al*.,1996; Horan and Eccles, 1986).

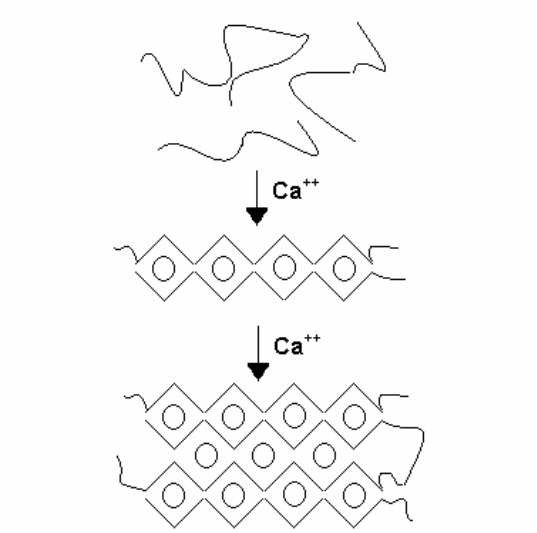

Figure 6 Alginate calcium cation “egg-box” model (Sobeck and Higgins, 2002).

Finally, the DCB theory emphasises the role of cations such as Ca^{++} and Mg^{++} in bridging between the negatively charged functional groups of EPS (Figure 7). The bridging causes biopolymers to aggregate into bioflocs (Sobeck and Higgins, 2002).

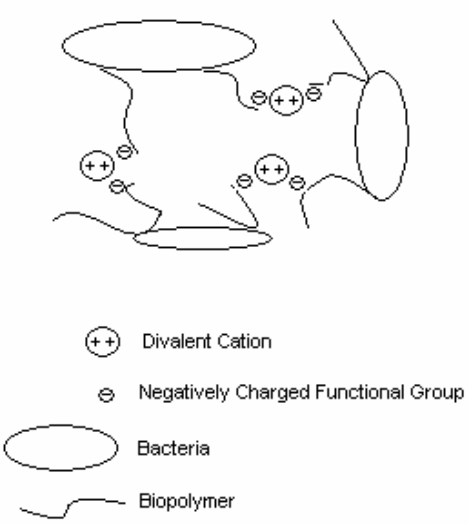

Figure 7 Divalent cation bridging (Sobeck and Higgins, 2002).

2.4.1 Effect of particle size and particle size distribution

Tarleton and Wakeman (1993) studied the effect of fine particle size and particle size distribution on flux decline in microfiltration. They found that

although smaller particle size resulted in a more rapid flux decline, at longer filtration times the flux for 'large' and 'small' particle systems were almost of the same magnitude (see Figures 8 and 9). This phenomenon was more noticeable with higher crossflow velocities and higher particle concentrations.

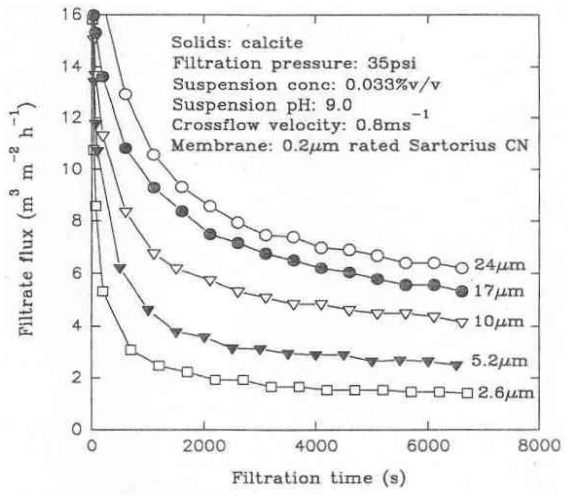

Figure 8 Effect of particle size on flux decline at lower crossflow velocity. Tarleton and Wakeman (1993).

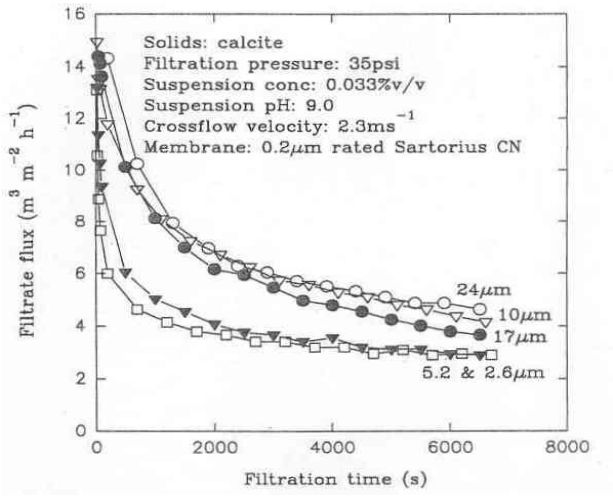

Figure 9 Effect of particle size on flux decline at higher crossflow velocity. Tarleton and Wakeman (1993).

Furthermore, Tarleton and Wakeman (1993) reported that unlike conventional dead end filtration, where small particles form the highest resistance cake, the lack of static cake formation complicated the identification of the fouling cake layer structure. Nevertheless, the authors hypothesised that smaller particles in the feed were mainly responsible for the fouling cake formation (Figure 10).

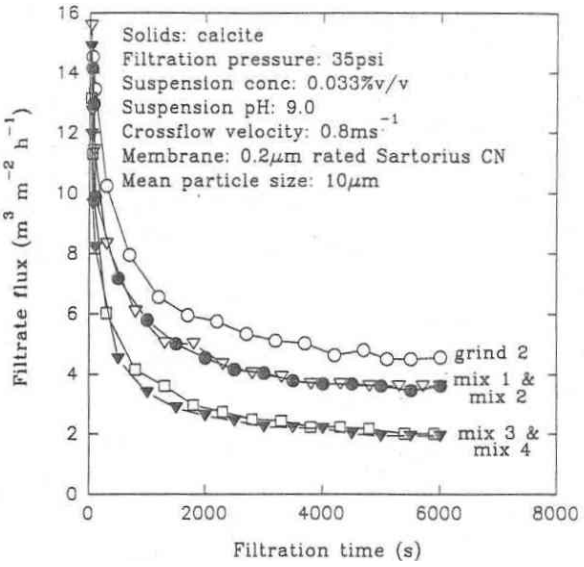

Figure 10 Effect of particle size distribution on flux decline. Tarleton and Wakeman (1993).

2.4.2 Effect of crossflow velocity on microfiltration flux

Zhong *et al.* (2007) used an ultrafiltration membrane with a pore size of 0.05 μm to recover titanium silicalite (TS-1) catalysts with particle diameters in the range of 1-7 μm from slurry (Figure 11).

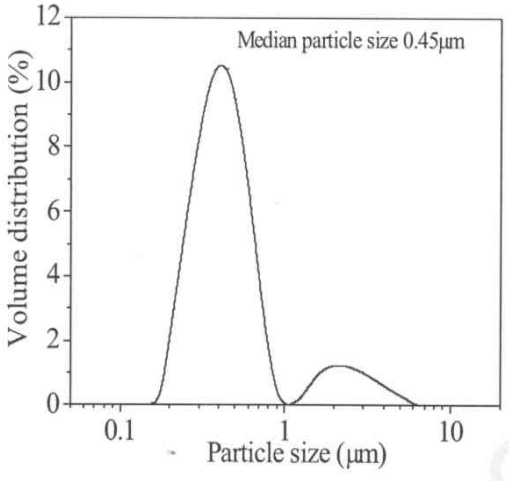

Figure 11 Size distribution of TS-1 particles. Zhong *et al.* (2007).

The researchers reported that dense cake layers formed on the membrane surface as a result of the interaction between TS-1 particles, a silica additive

and iron precipitation, leading to a large flux decline during the filtration process (Figure 12).

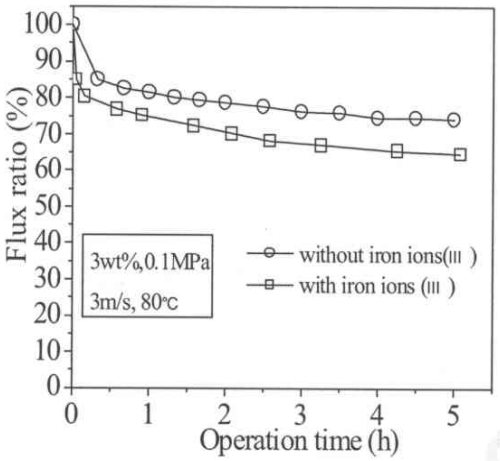

Figure 12 Effect of iron ions on the decline of flux. Zhong *et al.* (2007).

The authors reported that although an estimation of hydrodynamic forces acting on a single TS-1 particle (Figure 13) indicated that crossflow velocity (CFV) has a significant effect on the deposition of the particle, increasing CFV after the strong and dense cake layer has formed could not resuspend the TS-1 particle (Figure 14).

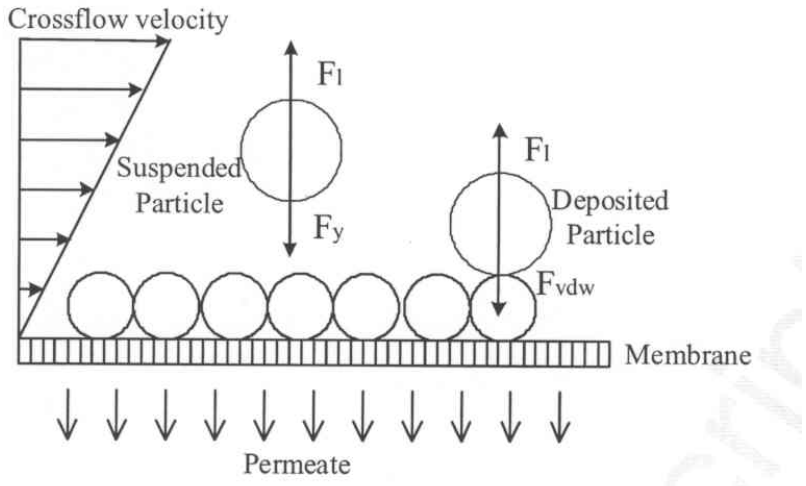

Figure 13 Forces acting on a single particle. Zhong *et al.* (2007).

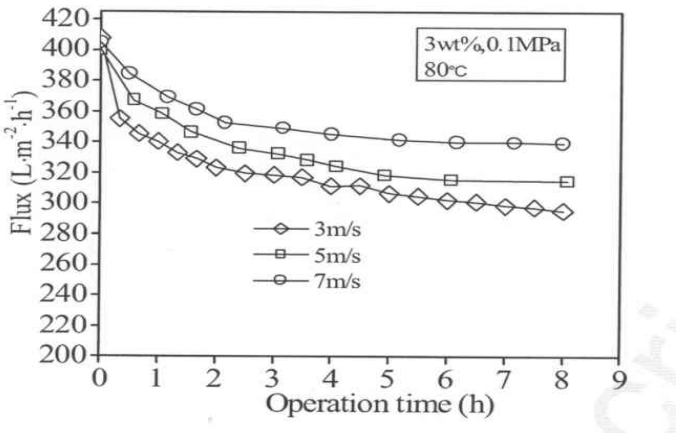

Figure 14 Effect of crossflow velocities on the decline of flux. Zhong *et al.* (2007).

2.4.3 Effect of yeast cells on microfiltration flux

Güell *et al.* (1999) studied the effect of yeast on dead end microfiltration of protein mixtures. In their work, Güell *et al.* (1999) used a 0.2 µm cellulose acetate membrane to filter an equal amounts mixture of bovine serum albumin, lysozyme and ovalbumin proteins. Yeast was added as suspension or as a cake on top of the membrane to study its effect. The researchers reported that a 0.022 g/L yeast concentration in suspension enhanced the permeate flux and kept the protein transmission at nearly 100% (Table 4).

Table 4 Permeate flux at different times and total permeate. Güell *et al.* (1999).

	Permeate flux (L/m^2 h) at different times (s)			Total permeate (L)
	100	1,800	10,800	
Water	9,800±600	9,200±300	n/a	n/a
Protein only	10,000±1500	360±100	70±30	0.48±0.03
0.022 g/L Yeast only	10,000±500	1,700±300	600±100	1.40±0.12
0.043 g/L Yeast only	6,900±750	1,300±150	700±50	1.20±0.13
0.28 g/L Yeast only	2,900±600	720±50	450±15	0.65±0.05
Protein+0.022 g/L yeast	8,500±1000	1,600±200	275±150	1.21±0.05
Protein+0.043 g/L yeast	5,300±1000	400±130	50±20	0.36±0.07
Protein+0.18 g/L yeast	3,700±1200	300±150	35±8	0.28±0.09

Although the proteins used in their study were much smaller in diameter than the pores of the microfiltration membrane, the authors attributed the severe fouling to the denaturation and aggregation of a fraction of proteins in the mixture. Furthermore, they hypothesised that adding yeast to the suspension formed a secondary membrane that helped retain protein aggregates (Figure 15).

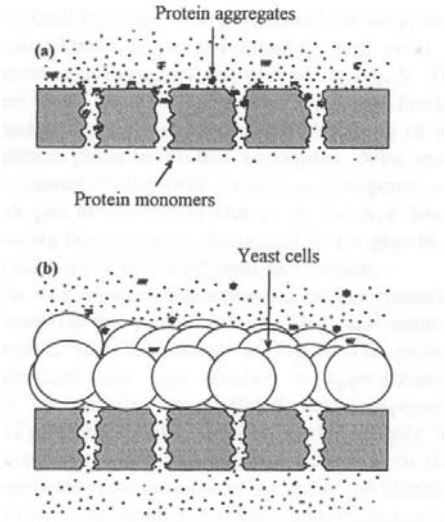

Figure 15 Proposed mechanisms of protein aggregation (a) without and (b) with yeast cells. Güell *et al.* (1999).

It was found that after plotting the resistance for the protein mixtures with different yeast concentrations that internal fouling dominates initially and after some time the external fouling due to cake growth was dominant (Güell *et al.,* 1999).

2.4.4 Biomass effect on membrane fouling

The effect of biomass characteristics on membrane fouling has also been studied. In their study, Fane *et al.* (1981) showed that membrane resistance increased linearly with the mixed liquor suspended solids (MLSS) content. Yamamoto *et al*. (1989) reported that when MLSS concentration exceeded

40,000 mg L^{-1} the flux decreased rapidly in a submerged membrane bioreactor system.

Different models have been suggested to predict the effect of MLSS on membrane resistance. Shimizu *et al*. (1993) described the impact of MLSS on cake layer resistance as:

$$R_c = \alpha \cdot v \cdot C_b \qquad (2.3)$$

where α is the specific cake resistance (m kg^{-1}); v is the permeate volume per unit area (m^3 m^{-2}); and C_b is the bulk MLSS or mixed liquor suspended solids concentration (kg m^{-3}).

The concentration of MLSS in an aerobic MBR usually ranges anywhere from 3,000 to 31,000 mg L^{-1} (Brindle and Stephenson, 1996); however, Lubbecke *et al.* (1995) reported that MLSS concentrations as high as 30,000 mg L^{-1} were not responsible for irreversible MBR fouling.

Several researchers have proposed empirical relations predicting the effect of MLSS concentration on the flux and resistance of an MBR system.

2.4.5 Role of Extracellular Polymeric Substances (EPS) in membrane fouling

Although some studies have not found a clear relationship between the concentration of extracellular polymeric substances and membrane fouling (Evenblij *et al*., 2005), it is generally accepted that EPS, which consists of biopolymers (polysaccharides, proteins, humic substances and lipids) produced by microorganisms by cell lysis or active transport, are the major fouling substance in the membrane bioreactor process (Neyens *et al*., 2004; Rosenberger and Kraume, 2003; Rosenberger *et al*., 2005; Tarnacki *et al*., 2005; Katsoufidou *et al*., 2007; Al-Halbouni *et al*., 2009; Chang *et al*., 2002; Bin *et al*., 2008; Ye *et al*., 2005a; Arabi and Nakhla, 2008). EPS constitutes

80% of the activated sludge mass (Frolund *et al*, 1996). Furthermore, polysaccharides are the major constituent of EPS. Forster (1971a) reported that polymer extracted from an activated sludge was almost totally polysaccharide. Another study found that polysaccharides constitute about 60% of EPS (Neyens *et al*., 2004).

A clear relationship between the concentration of dissolved polysaccharides and membrane permeate flux under constant filtration conditions has been found by many researchers (Tarnacki *et al*., 2005; Rosenberger and Kraume, 2003; Rosenberger *et al*., 2005; Jarusutthirak *et al*., 2002; Lesjean *et al*., 2005). A decrease in membrane permeate flux was reported with increasing dissolved polysaccharides concentration (Tarnacki *et al*., 2005). Other researchers have reported that sludge filterability always decreased with increasing suspended EPS concentration (Rosenberger and Kraume, 2002). Moreover, Rosenberger *et al*. (2005) reported that the main influence on membrane performance comes from soluble polysaccharides and organic colloids.

Proteins are an important component of EPS. Zhou *et al.* (2007) reported that proteins and polysaccharides were the major components comprising the fouling layer. Moreover, Kimura *et al.* (2005) found that proteins and polysaccharides were the dominant foulants.

The interaction between the different components of EPS is an interesting subject to many researchers. Many researchers widely believe that even a substance having only a minor influence individually might have a larger effect in a mixed system (Ye *et al*., 2005b). More severe irreversible fouling caused by a mixture of alginate, humic acid and calcium compared to the individual solutions of each of these components was reported (Jermann *et al*., 2007). Another study in which the fouling behaviour of bicomponent solutions of BSA-alginate, alginate-unwashed yeast, washed yeast and alginate-bentonite were compared with mono-solutions of alginate, BSA, unwashed yeast, washed yeast and bentonite, found that the alginate-BSA solution caused the highest irreversible fouling (Negaresh *et al*., 2007). However, Ye *et al*. (2005b)

did not find a significant difference between the fouling caused by a mono-solution of alginate and a bicomponent solution of alginate-BSA, although the fouling of the bicomponent solution was higher than for the BSA mono-solution.

2.4.6 Role of cations in membrane fouling

The role of divalent cations is an unclear and controversial one. Some researchers have reported a reduction of membrane fouling with increased calcium cation concentration (Kim and Jang, 2006). Aspelund *et al*. (2008) studied the effect of cationic polyelectrolyte concentration on permeate flux and rejection of bacterial cell suspension in stirred and unstirred cell, dead end and crossflow microfiltration, reporting that an increase in the cationic polyelectrolyte dosage resulted in the formation of larger flocculated particles and increased membrane permeate flux (Aspelund *et al*., 2008; Nguyen *et al.*, 2008b). On the other hand, several studies on the interaction effects of cations, especially divalent calcium cations and EPS components such as polysaccharides, proteins and humic acids, have reported that they form complexes with the organic molecules that form a compacted fouling layer on the membrane surface, causing severe flux decline (Costa *et al*., 2006; Hong and Elimelech, 1997; Schäfer *et al*., 1998; Li and Elimelech, 2004; Yoon *et al*., 1998). To complicate the matter further, Arabi and Nakhla (2008) reported that using a control membrane bioreactor (MBR) with a calcium concentration of 35 mg/L and two test MBRs with calcium concentrations of 280 mg/L and 830 mg/L respectively, the first MBR fouled the membrane less than the control MBR while the second test reactor, with the highest calcium concentration, fouled the membrane the most. The researchers speculated that cationic bridging with EPS by the calcium created a larger floc size in the first test MBR that improved permeate flux and lowered the fouling, whilst the excess of calcium cations in the second test MBR led to significant inorganic fouling.

It seems that the disagreement between researchers is not limited to stating either that cations improve or worsen membrane fouling in the presence of EPS but also extend to what type of fouling is caused by their interaction with EPS. Some researchers reported an increase in the reversibility of the membrane fouling with increasing calcium concentration, attributing this to the elimination of EPS adsorption onto the membrane and the cake fouling becoming the controlling fouling, with increased flocculation influenced by increased calcium cation concentration (Katsoufidou *et al*., 2007). Other researchers have reported opposite behaviours (van de Ven *et al*., 2008; Abrahamse *et al*., 2008). In a surface water ultrafiltration study by Abrahamse et al., (2008) the authors found that irreversible fouling increased linearly with increasing calcium and magnesium concentrations.

2.4.7 Morphology effects on membrane fouling

Hwang and Lin (2002) studied the effects of polymeric micro filtration membrane morphology on crossflow performance. In this study three membranes, MF Millipore (made of mixed cellulose esters), Durapore (made of modified polyvinylidene difluoride) and Isopore (made of bisphenol polycarbonate), with the same mean pore size of 0.1 μm were used (Figure 16).

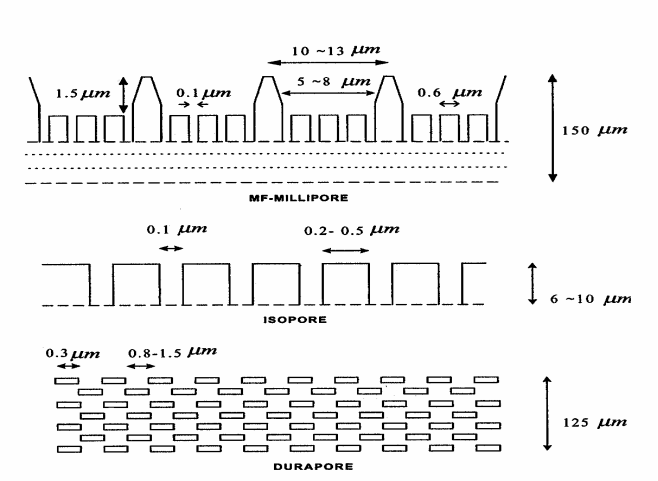

Figure 16 Modelling of pore structures of the three membranes used. Hwang and Lin (2002).

Three blocking mechanism models were reported: a standard blocking, with particles deposited on the surface of the membrane and completely blocking the entrances of the pores, with the MF Millipore membrane; an intermediate blocking, in which the particles are almost the same size as the membrane pores; therefore, the particles may either be deposited at the entrances or migrate inside the pores of the membrane, in the Durapore membrane; and, in the case of the Isopore membrane, a complete blocking, in which the particle size is smaller than the membrane pore size thus most of the particles migrate inside the membrane pores causing irreversible fouling. For all the membranes the blocking model translated to cake filtration within 10 minutes.

In their study, Faibish and Cohen (2001) showed that a permeability decline of less than 2 per cent after cleaning was achieved for a polyvinylpyrrolidone (PVP) modified zirconia based ultrafiltration membrane. A permeability decline of 17 per cent was observed for the non-modified zirconia based ultrafiltration membrane. Nevertheless, it is worth noticing that the clean membrane permeability of the PVP modified zirconia based membrane was 48% less than the native non-modified clean membrane (Table 5).

Table 5. Hydraulic permeability (k_t) of membranes. Faibish and Cohen (2001).

Component	**k_t (10^{-16} m^2) clean membrane**	**k_t (10^{-16} m^2) after filtration and cleaning**	**Reduction %**
(a)			
4% (by vol.) isobutanol	7.39	7.38	< 1
0.002 M octanoic acid	7.39	7.27	2
0.5 M sodium octanoate (>GMC)	7.39	6.12	17
0.3 M sodium octanoate (>GMC)	7.08	5.62	21
Microemulsion	4.40	3.47	26
(b)			
0.5 M sodium octanoate (>GMC)	3.40	3.39	< 1
0.5 M sodium octanoate (>GMC)	3.39	3.37	< 1
(c)			
Native membrane	7.00	5.80	17
Modified membrane	3.39	3.33	< 2

The reduction associated with the modified membrane may suggest that the modification process resulted in the formation of a cake layer on the membrane surface, thus a better control of the irreversible fouling was achieved.

The PVP modified membrane improved the rejection of an oil and its microemulsion by 100 and 20 per cent, respectively Faibish and Cohen (2001). The authors attributed the improvement in the rejection rate to a repairing or narrowing effect of the polymer grafting process on the defects or “pin-holes” of the zirconia based membrane.

2.4.8 Intermittent effects on membrane fouling

In their study, Chua *et al*. (2002) examined the possibility of controlling fouling in an MBR caused by a temporary permeate flux increase by increasing the aeration rate. They concluded that membrane fouling can be eliminated when the permeate flux was reduced back to the sub critical rate. Moreover, the researchers concluded that the intermittent permeation technique was effective in reducing the fouling in an MBR operating above the critical flux rate.

2.4.9 Reversible and irreversible fouling

There is some disagreement between researchers on the definition of reversible and irreversible fouling. Some researchers consider limiting the definitions of membrane fouling to irreversible and reversible fouling as somewhat simplistic (Chang *et al*., 2002). Nevertheless, in general researchers consider irreversible fouling as that which cannot be removed with physical cleaning but can be removed by chemical cleaning (Ye et al., 2005; Judd and Jefferson, 2003; Abrahamse *et al*., 2008). In this work, the following definitions of reversible and irreversible fouling were adopted: any fouling that can be removed without chemical cleaning is considered

reversible and fouling removed by chemical cleaning is considered irreversible fouling.

2.5 Membrane cleaning methods

There is several different membrane cleaning methods in common use, such as forward flush, backward flush and air flush.

2.5.1 Physical cleaning

2.5.1.1 Forward flush

When a forward flush is applied, membranes are flushed with feed water or permeate in the forward direction. The feed water or permeate flows through the system more rapidly than during the production phase. Due to of the more rapid flow and the resulting turbulence, particles that are absorbed onto the membrane are released and discharged. The particles that are absorbed into membrane pores are not released. These particles can only be removed through backward flushing. When a forward flush is applied to a membrane, the barrier that is responsible for dead end management is opened. At the same time the membrane is temporarily performing crossflow filtration, without the production of permeate.
The purpose of a forward flush is the removal of an accumulated layer of contaminants on the membrane through the creation of turbulence. A high hydraulic pressure gradient is in order during a forward flush.

2.5.1.2 Backward flush

Backward flush is a reversed flow process. Permeate is flushed from the permeate side of the system under pressure to the retentate side, applying twice the flux that is used during filtration. When the flux has not been sufficiently restored after back flushing, a chemical cleaning process can be applied.

When backward flush is applied the pores of a membrane are flushed inside out. The pressure on the permeate side of the membrane is higher than the pressure within the membranes, causing the pores to be cleaned. A backward flush is executed under a pressure that is about 2.5 times greater than the production.

Permeate is always used for a backward flush, because the permeate chamber must always be free of contamination. A consequence of a backward flush is a decrease in the recovery of the process. A backward flush therefore must take the smallest possible amount of time and consume as little permeate as possible. However, the flush must be maintained long enough to fully flush the volume of a module at least once.

In their study, Zhong *et al. (2007)* used different sizes and concentrations of micro sized alumina particles for physical cleaning of a fouled microfiltration ceramic membrane. The authors reported a very good cleaning result with different sizes of alumina particles, especially with the 25 µm particles (Figure 17). The cleaning efficiency with the alumina particles increased with increasing alumina particle concentration (Figure 18).

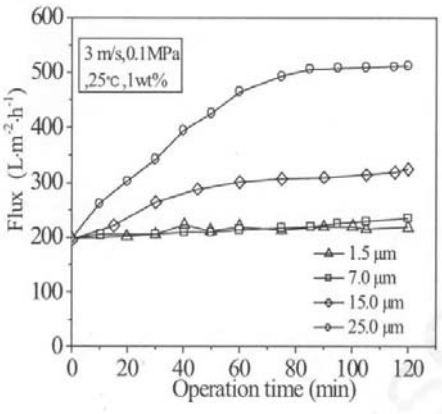

Figure 17. Effect of alumina particle size on recovery of flux. Zhong *et al.* (2007).

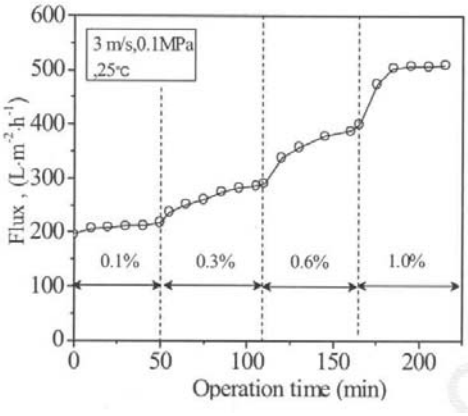

Figure 18. Effect of alumina concentration on recovery of flux. Zhong *et al.* (2007).

The authors further reported that a particle cleaning combined with an acid cleaning restored the membrane flux fully (Figures 19 and 20).

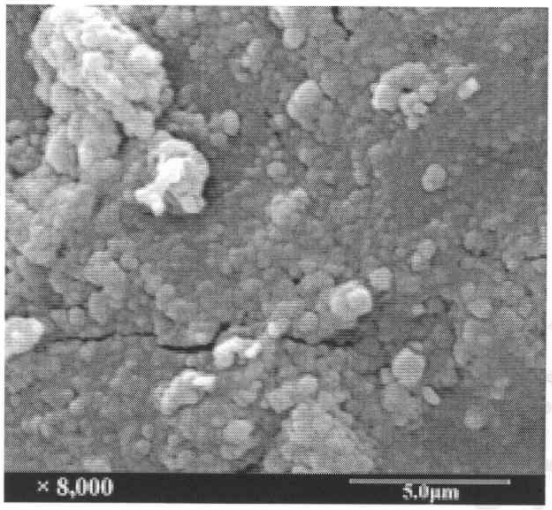

Figure 19. SEM micrograph of fouled membrane. Zhong *et al.* (2007).

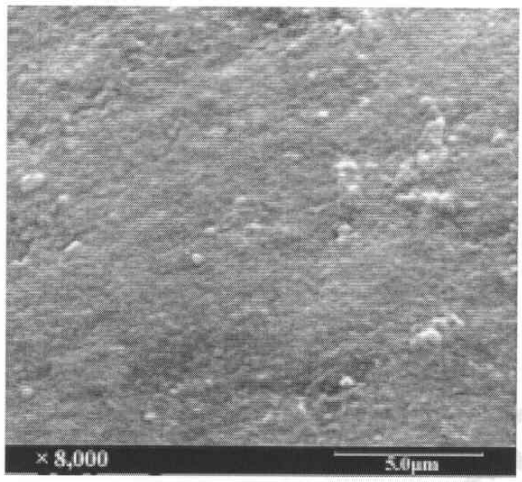

Figure 20. SEM micrograph of membrane after cleaning. Zhong *et al.* (2007).

2.5.2 Chemical cleaning processes

When the above mentioned cleaning methods are not effective to restore the flux to an acceptable level, chemical cleaning of the membranes is necessary. During a chemical cleaning process, membranes are soaked with a solution of chlorine bleach, hydrochloric acid or hydrogen peroxide. First the solution soaks into the membranes for several minutes and after that a forward flush or backward flush is applied, causing the contaminants to be rinsed out.

During chemical cleaning, chemicals such as hydrogen chloride (HCl) and nitric acid (HNO_3), or disinfection agents, such as hydrogen peroxide (H_2O_2) are added to the permeate during backward flush. As soon as the entire module is filled with permeate, the chemicals need to soak in. After the cleaning chemicals have fully soaked in, the module is flushed and, finally, put back into production thus insuring the removal of all the cleaning chemicals used.

Cleaning methods are often combined. For example, one can use a backward flush for the removal of pore fouling, followed by a forward flush or air flush. The cleaning method or strategy that is used is dependent on many factors. In practice, the most suitable method is determined by trial and error (practical tests).

In their study, Zhong *et al. (2007)* started a chemical cleaning procedure to clean a microfiltration membrane by rinsing the filtration system with deionised water, followed by circulating a 1% (v/v) sodium hydroxide solution, then circulating a 1% (v/v) nitric acid solution, both at temperature of 80 °C, for several hours while keeping the permeate line open (Figure 21).

The filtration system was finally rinsed with deionised water. Furthermore, Zhong *et al.* (2007).took advantage of the high thermal stability of the ceramic membrane to remove organic foulants by baking the fouled ceramic membrane for one hour at a temperature of 500 °C. The Zhong *et al.* (2007). reported that EPS analysis showed no organic matter in the cake layer and membrane pores after the baking procedure. Moreover, Zhong *et al.* (2007). reported an increase in the pure water flux from 230 L/(m^2 h) to 247 L/(m^2 h) for the fouling membrane after the high temperature baking procedure. The researchers hypothesised that the high temperature was responsible for removing all organic matter by volatilisation (Zhong *et al.* 2007).

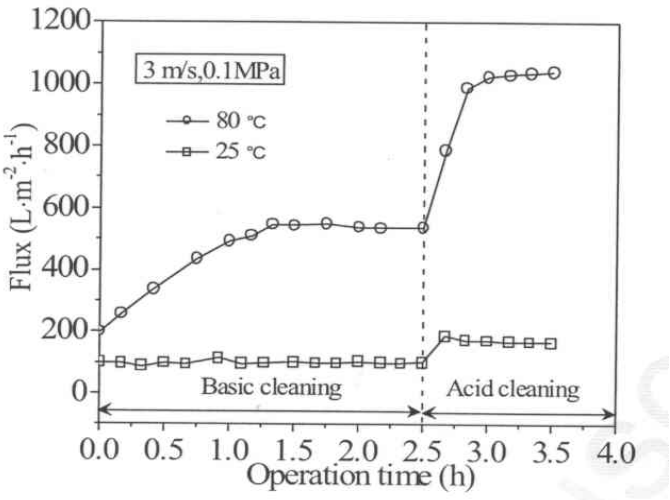

Figure 21. Variation of flux with cleaning time. Zhong *et al.* (2007).

2.5.3 Biofilm removal

A biofilm is a layer of micro organisms contained in a matrix (a slime layer), which forms on surfaces in contact with water. Incorporation of pathogens in biofilms can protect the pathogens from concentrations of biocides that would otherwise kill or inhibit those organisms if freely suspended in water.
Biofilms provide a safe haven for organisms like *Listeria*, *E. coli* and *Legionella* where they can reproduce to levels where contamination of products passing through that water becomes inevitable. Chlorine dioxide has been proven to remove biofilms from water systems and prevents them from forming when dosed at a continuous low level; Hypochlorite on the other hand has been proven to have little effect on biofilms (Li *et al*., 2005).

2.6 Crossflow membrane filtration modelling

In membrane ultrafiltration, the flux is usually distinguished as being in one of two regimes: a non steady state, in which flux declines with time, and a steady state where the flux is constant (Song, 1998).

The rate of initial flux decline and the final steady state flow is dependent on the fouling mechanisms involved and the operating conditions such as trans membrane pressure, flow velocity, shear rate, feed concentration and feed temperature. However, the effects of operating parameters are not very clear even after numerous experimental studies and are sometimes contradictory (Tarleton and Wakeman, 1993).

2.7 Dead end blocking models

The flux reduces with time in a membrane filtration process due to fouling. The three main mechanisms that effect membrane permeate flux are complete blocking, standard blocking and cake formation (Figure 22).

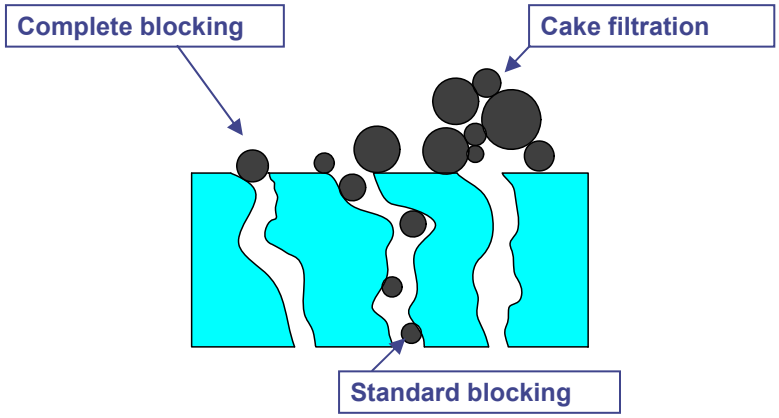

Figure 22. Membrane blocking mechanisms.

In his study, Hermia (1982) started with a dead end filtration equation and adapted it to predict the reduction of permeate flux in crossflow filtration.

For the three different blocking mechanisms, the proposed models for complete blocking, standard blocking, cake and intermediate blocking, respectively, are as follows:

$$-\ln\left(\frac{J}{J_0}\right) = k_b t + E \tag{2.4}$$

$$\frac{t}{V} = \frac{K_b}{2} t + \frac{1}{J_0} \tag{2.5}$$

$$\frac{t}{V} = \frac{K_k}{2} V + \frac{1}{J_0} \tag{2.6}$$

$$\frac{1}{J} = K_i t + \frac{1}{J_0} \tag{2.7}$$

where J and J_0 are the permeate and clean water fluxes respectively, V is permeate volume collected at time t, and K_b, K_k and K_i are constants.

Several models have been developed to predict the flux decline in membrane filtration. A critical factor in most of these models is the particle size. Hermia's

blocking flows are constructed on the basis of the difference between particle size and membrane pore size. Although Hermia's pore blocking and cake formation models were developed for dead end filtration, they can be used to understand the blocking mechanisms for crossflow filtration experiments (Jiraratananon *et al.*, 1998; Mohammadi *et al.*, 2003).

Several researchers have modified Hermia's flow to better suit crossflow filtration configurations (Vela *et al*., 2009; Field *et al*., 1995; Bowen *et al*., 1995). The main consideration in the modified models is that they account for the back diffusion of solutes from the membrane surface to the bulk flow.

2.7.1 Combined blocking mechanisms models

Since the possibility exists for more than one blocking mechanism occurring at the same time, an attempt has been made by some researchers to combine some of the blocking models to give a better description of the experimental data. Bolton *et al.* (2006) formulated five constant pressure combined fouling models as the following:

Cake filtration and complete blocking model:

$$V = \frac{J_o}{K_b} 1 - \left(1 - \exp\left(\frac{-K_b}{K_c {J_o}^2} \left(\sqrt{1 + 2K_c {J_o}^2 t} - 1 \right) \right) \right) \tag{2.8}$$

where the fitted parameters are K_c (s/m^2) and K_b (s^{-1})

Cake filtration and intermediate blocking model:

$$V = \frac{1}{K_i} \ln\left(1 + \frac{K_i}{K_c J_o} \left(\left(1 + 2K_c {J_o}^2 t \right)^{1/2} - 1 \right) \right) \tag{2.9}$$

where the fitted parameters are K_c (s/m^2) and K_i (m^{-1})

Complete blocking and standard blocking model:

$$V = \frac{J_o}{K_b}\left(1 - \exp\left(\frac{-2K_b t}{2 + K_s J_o t}\right)\right) \tag{2.10}$$

where the fitted parameters are K_b (s^{-1}) and K_s (m^{-1})

Intermediate blocking and standard blocking model

$$V = \frac{1}{K_i}\ln\left(1 + \frac{2K_i J_o t}{2 + K_s J_o t}\right) \tag{2.11}$$

where the fitted parameters are K_i (m^{-1}) and K_s (m^{-1})

$$V = \frac{2}{K_s}\left(\beta\cos\left(\frac{2\pi}{3} - \frac{1}{3}\arccos(\alpha)\right) + \frac{1}{3}\right) \tag{2.12}$$

$$\alpha = \frac{8}{27\beta^3} + \frac{4K_s}{3\beta^3 K_c J_o} - \frac{4K_s^2 t}{3\beta^3 K_c},\ \beta = \sqrt{\frac{4}{9} + \frac{4K_s}{3K_c J_o} + \frac{2K_s^2 t}{3K_c}}$$

where the fitted parameters are K_c (s/m^2) and K_s (m^{-1})

Prádanos *et al.* (1996) modified the pore blocking models for crossflow filtration. In the complete blocking model, particles block some of the membrane pores with no superposition of particles and the permeate flux decline with time is given by:

$$\ln J_v = -K_b t + \ln J_{v,0} \tag{2.13}$$

where K_b is the complete blocking kinetic constant (s^{-1})

In the intermediate blocking model, particles can settle on top of other particles that are already blocking membrane pores or they can block open membrane pores by themselves. The flux decline with time is given by:

$$J_v = \frac{J_{v,0}}{1 + K_i t} \tag{2.14}$$

where K_i is the intermediate blocking kinetic constant (s^{-1})

The standard blocking model accounts for the possibility that particles arriving at the membrane surface are smaller than the pore diameter and can deposit on the internal pore walls, thus reducing the pore volume. The flux decline with time is given by:

$$J_v = \frac{J_{v,0}}{(1 + K_s t)^2} \tag{2.15}$$

where K_s is the standard blocking kinetic constant (s^{-1})

Finally, the cake filtration model assumes that particles arriving at the membrane surface are deposited on top of other particles and there is no room for contact with the membrane area. The flux decline with time is given by:

$$J_v = \frac{J_{v,0}}{\sqrt{1 + K_c t}} \tag{2.16}$$

where K_c is the cake filtration kinetic constant (s^{-1})

In complex mixtures such as wastewater, the particle size distribution is very wide, thus the use of a single blocking mechanism for calculating flux decline is an unrealistic approach.

2.7.2 Concentration Polarisation Theory

In a membrane crossflow filtration process, particles with sizes larger than the membrane pore size are rejected by the membrane. During this process the particles rejected by the membrane accumulate near the membrane surface.

The concentration of the rejected particles near the membrane surface becomes higher than the concentration of the particles in the bulk, thus creating what is called the concentration polarisation layer.

In their research, Song and Elimelech (1995) proposed a new method for predicting the formation of a concentration polarisation layer and calculating permeate flux. The researchers proposed a new dimensionless number, called the filtration number, N_F; this number can be calculated using Equation 2.17:

$$N_F = \frac{4\pi a_p^3 \Delta P}{3kT} \tag{2.17}$$

where:

a_p is the particle size

ΔP is the transmembrane pressure

K is the Boltzmann constant

T is the absolute temperature

The filtration number represents the ratio of the energy required to move the particle from the membrane surface back to the bulk solution to the thermal energy of the particle. The researchers reported a critical value for the filtration number. When the value of the filtration number is less than the critical value, a polarisation layer will exist over the membrane surface (Figure 23). Conversely, if the filtration number value is higher than the critical value, a cake layer is formed between the concentration polarisation layer and the membrane surface (Figure 24).

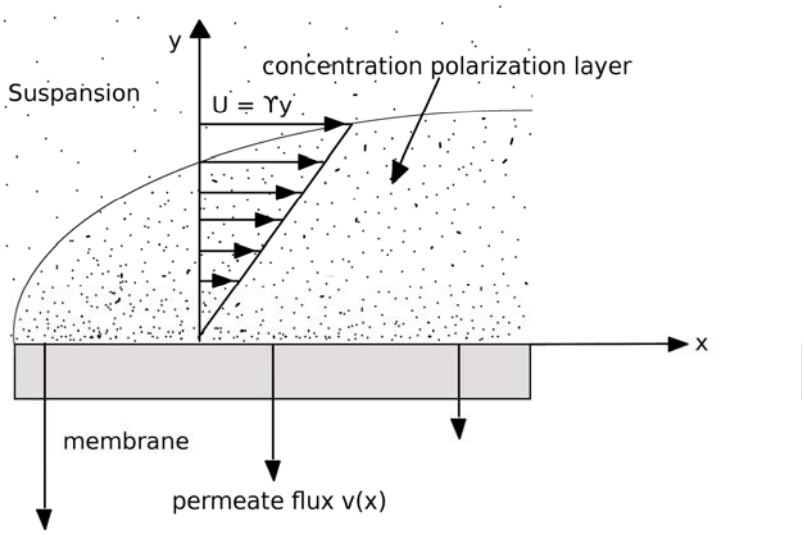

Figure 23. Concentration polarisation layer over a membrane surface.

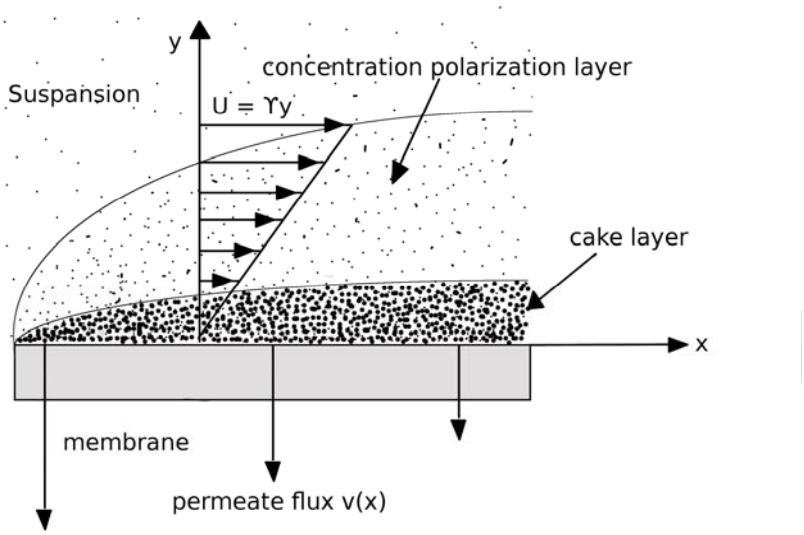

Figure 24. Cake layer between CP layer and membrane surface.

3.0 Equipment and Experimental Methods

In this chapter the artificial wastewater composition and mixing procedure, the filtration apparatus design and filter element, the dead end stirred cell filtration apparatus and samples analyses procedures are described.

3.1 Artificial wastewater composition

In this study, an artificial wastewater was used. Real wastewater is a complex unstable mixture with continuously changing living micro-organisms making it unsuitable for controlled experiments. The need for stable artificial wastewater was widely recgdnized by different researchers (Sanin and Vesilind, 1999; Örmeci and Vesilind, 2000; Nguyen *et al.*, 2008). The artificial wastewater composition was as described by Lu *et al* (2001); furthermore, sodium alginate was added to simulate the effect of soluble microbial products (SMP); see Table 6.

Table 6. Artificial wastewater compositions Lu *et al* (2000).

Substance	**Concentration, mg/L**	**wt %**
Na alginate	100	9.90
Peptone	180	17.82
Meat extract	180	17.82
Urea	30	2.97
NH_4Cl	70	6.93
$(NH_4)_2CO_3$	160	15.84
NaCl	20	1.98
K_2HPO_4	90	8.91
$CaCl_2{\cdot}2H_2O$	35	3.47
KCl	110	10.89
$MgCl_2{\cdot}6H_2O$	35	3.47

The main components in the wastewater which it was believed would have the most effect on membrane fouling are alginate, peptone, meat extract and $CaCl_2 \cdot 2H_2O$. Throughout this study, the concentration of these compounds was varied to examine their effects on the membrane fouling rate.

3.2 Artificial wastewater preparation procedure

For each experiment, the amount of each component in the artificial wastewater was measured using a four decimal sensitive balance. The correct weight for each component was then dispersed into a 2 L beaker filed with ultra pure water from a Millipore reverse osmosis purification system. Once all components were added and stirred, the suspension was transferred to the filtration apparatus feed tank where fresh ultra pure water was added to obtain a total volume of around 20 litres in the feed tank.

3.3 Artificial wastewater characterisation

The artificial wastewater in this study was characterised with respect to particle size distribution, solids concentration, density, viscosity, shear rate and Zeta potential.

The particle size distribution of the artificial wastewater was characterised using a Malvern MS20 Mastersizer. The particle size measurement was done to characterise the particle size distribution of the artificial wastewater for each experiment, to ensure that all compounds in the artificial wastewater feed were adequately dispersed, and that no major changes in the particle size distribution occurred in all the experiments with the same component concentrations.

3.3.1 The Malvern Mastersizer

The Malvern Mastersizer works on the principle of the laser diffractometer, where the laser light from the instrument is scattered by the particles in the suspension depending on their size and light scattering characteristics. The scattered light is focused onto an array of sensors. The data from the sensors are processed by a computer that calculates the particle size distribution. The lens and focal length for the instrument should be selected according to the particle sizes in the suspension and the presentation factor was chosen in accordance with the Mastersizer instruction manual.

3.3.2 Zeta potential measurement

The Zeta potential for each artificial wastewater mixture was measured using a Malvern Zetamaster. The Zeta potential measurement gave an indication of the tendency of the compounds in the artificial wastewater to agglomerate at a certain pH, and was used to ensure the similarity of the artificial wastewaters used in all the experiments.

The Malven Zetamaster measures the speed at which charged particles move through an electrical field via a laser light and a light sensor. The Zetamaster relates the speed to the particle surface charge, thus calculating the Zeta potential of the particles.

The Malven Zetamaster is computer controlled and equipped with an auto titrator filled with hydrochloric acid and sodium hydroxide. After specifying the range of pH at which to test the solution, the auto titrator changes the artificial wastewater solution pH according to a chosen range and measures the Zeta potential at different pH values. The pH and corresponding Zeta potential of the artificial wastewater solution are recorded automatically.

3.4 Experimental crossflow filtration apparatus

A diagram of the crossflow filtration apparatus is shown in (Figure 25). The artificial wastewater mixture was loaded into the 20 L stainless steel feed tank. The artificial wastewater was feed to the membrane filter element by a constant flow centrifugal pump. The pump was a 0.5 HP Lowara CKM70/3 rated at 2,850 rpm. The pump was capable of delivering maximum pressure of 5 bars. The pressures at the membrane module inlet as well as the membrane outlet were both measured by two Farnell MM10013 pressure transducers.

The temperature of the wastewater feed to the membrane module was monitored by thermocouples. The computer controlled the temperature of the wastewater via a hot water jacket surrounding the wastewater feed tank.

The membrane module inlet and outlet pressures, feed tank temperature, and membrane module inlet wastewater feed temperature were automatically recorded by a data logging system. The permeate flux was measured manually. The crossflow filtration apparatus could be operated in a constant concentration mode by returning the permeate back to the feed tank or concentration mode by removing the permeate from the filtration system.

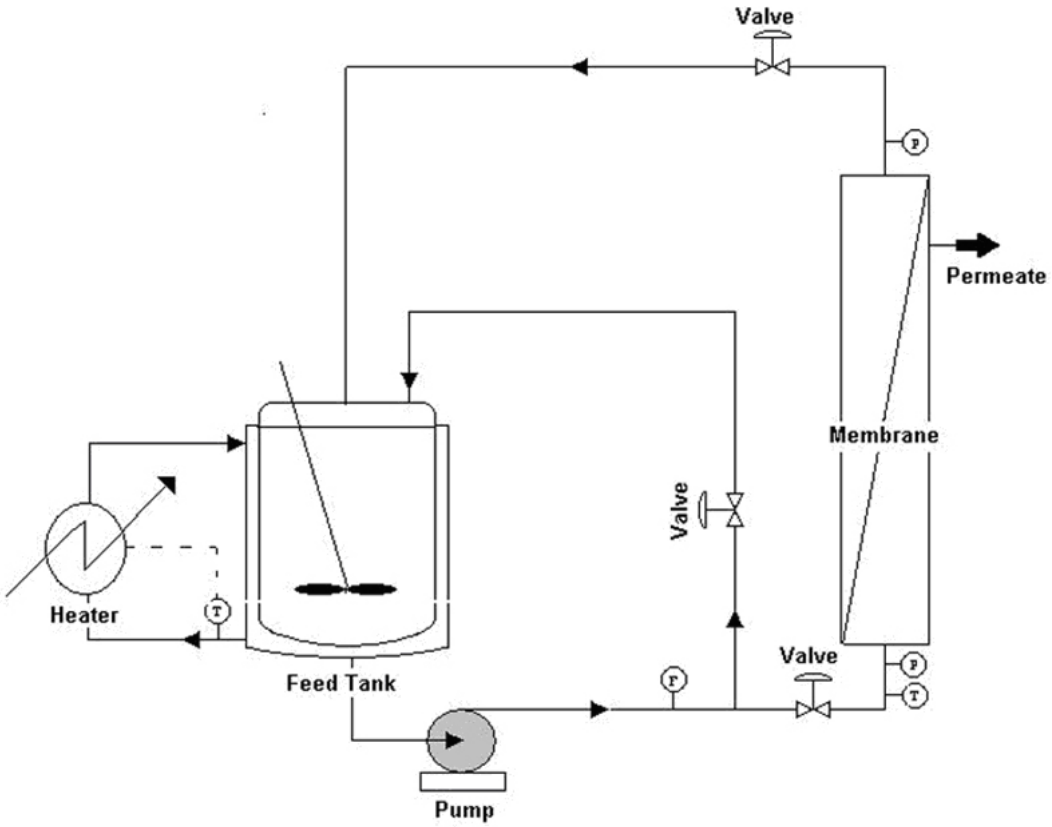

Figure 25. Crossflow filtration apparatus.

3.5 Apparatus control

The major equipment in the crossflow filtration apparatus were controlled via a computer program written in Visual Basic. The computer program controlled the following:

1. The apparatus main pump
2. The feed tank mixer
3. The heating elements
4. The heating water loop pump.

Moreover, the computer program recorded the following:

1. Membrane module inlet and outlet pressures

2. Feed tank temperature
3. Membrane module wastewater feed inlet temperature.

3.5.1 Membrane filter element

In this research, two Atech ceramic membrane elements were used for the artificial wastewater filtration experiments. A 1 m long α-Al_2O_3 microfiltration membrane with a pore size of 0.2 μm and two 1 m long TiO_2 ultrafiltration membrane elements with pore sizes of 20 and 5 kDa were used in this study. All the membranes were single channel tubular ceramic membranes with an outer diameter of 10 mm and a 6 mm internal diameter. Each ceramic membrane filter was installed in a stainless steel housing and sealed by rubber O-rings at each end. The module (housing and membrane element) was mounted vertically in the filtration apparatus and secured by flanges at both ends and sealed with plastic gaskets.

3.5.2 Filtration apparatus piping and fittings

The apparatus pipework, fitting, ball valves, feed tank and built in water jacket were all of stainless steel. A 20 mm terylene mesh reinforced PVC tubing was used to return the retentate to the feed tank. The filter permeate was returned to the feed tank via a polypropylene tube when operating in constant concentration mode.

3.5.3 Filtration apparatus temperature control

Water in an insulated storage tank was heated by 3 kW heating elements. This hot water was then pumped around the wastewater feed tank hot water jacket. The wastewater feed temperature was measured by RS PT100 thermocouples. The temperature of the wastewater was maintained at a user

defined set point by turning the heating elements on or off as required by the computer control program.

3.6 Experimental procedures

3.6.1 Wastewater mixture filtration experiments

3.6.1.1 Factorial design of the experiments

The ultrafiltration experiments were designed using a full two level factorial design statistical method described in Appendix D. Four factors, sodium alginate, peptone, meat extract and calcium chloride, were selected for study at high and low concentrations to determine their effects on the wastewater filtration process (Table 7).

Table 7 Four factor, two level designs.

factor	**High (mg/L)**	**Low (mg/L)**
Sodium alginate	150	50
Peptone	270	90
Meat extract	270	90
$CaCl_2 \cdot 2H_2O$	60	20

Sixteen experiments plus the central experiment (Table 8) were required to investigate all the possible combinations of the high and low concentrations of the four factors under investigation.

In all sixteen experiments and the central experiment, the effects of the changes in the factor (component) levels (concentrations) on a measured response (Y) such as flux, COD, TOC and membrane resistance were

recorded. The results were analysed as a set of equations (Equation 3.1) that was solved for the factors effect βs.

Table 8 Full factorial, two level experimental design runs.

Experiment	Peptone (mg/L)	Meat Extract (mg/L)	Sodium Alginate (mg/L)	$CaCl_2$ $2H_2O$ (mg/L)
F1	90	270	150	20
F2	270	270	150	20
F3	270	90	50	20
F4	90	270	150	60
F5	270	90	150	20
F6	270	90	150	60
F7	90	90	150	20
F8	90	270	50	20
F9	270	270	50	60
F10	270	270	150	60
F11	90	90	50	20
F12	90	90	150	60
F13	270	270	50	20
F14	90	90	50	60
F15	270	90	50	60
F16	90	270	50	60

$$Y = \beta_0 + \beta_1 X_1 + \beta_2 X_2 + \beta_3 X_3 + \beta_4 X_4 + \beta_{12} X_1 X_2 + \beta_{13} X_1 X_3 + \beta_{14} X_1 X_4 + \beta_{23} X_2 X_3 + \beta_{24} X_2 X_4 + \beta_{34} X_3 X_4 + \beta_{123} X_1 X_2 X_3 + \beta_{124} X_1 X_2 X_4 + \beta_{134} X_1 X_3 X_4 + \beta_{234} X_2 X_3 X_4 + \beta_{1234} X_1 X_2 X_3 X_4 \quad (3.1)$$

where:

X_1 = Peptone concentration (mg/L)

X_2 = Meat extract concentration (mg/L)

X_3 = Sodium alginate concentration (mg/L)

X_4 = Calcium chloride concentration (mg/L)

3.6.1.2 Measurement of clean water flux

The clean membrane flux measurement was carried out after installing the new membrane using ultra pure water to establish the membrane resistance (R_m). The flux of the new membrane was taken at different pure water temperatures, flow rates and trans membrane pressures.

The clean water flux was measured before the start of every wastewater filtration experiment to record any change to the membrane resistance.

3.6.1.3 Measurement of experimental flux

The following procedures were followed for all experimental runs.

Start of Experiment; Clean water flux measurement:

1. The feed tank was filled with twenty litres of clean ultra pure water.
2. The heater set point temperature was set to 40 °C and the water was heated to this temperature.
3. The pump was started and the permeate side valve was opened.
4. Three flux measurements were taken.
5. The pump was stopped and the feed tank drain valve was opened to empty the feed tank.

Artificial wastewater preparation and wastewater filtration experiment:

1. The artificial wastewater chemical components were measured using a sensitive balance.
2. The components were dissolved in 10 litres of ultra pure water in a bucket.
3. The artificial wastewater was mixed for 60 minutes using a mixer.
4. The artificial wastewater was loaded into the filtration apparatus feed tank and diluted with 10 litres of ultra pure water to obtain a total volume of 20 litres of artificial wastewater in the feed tank.
5. The filtration apparatus mixer was started.
6. The temperature set point was set to 40 °C and the heaters were turned on in the apparatus computer control programme.
7. The pump was turned on and the artificial wastewater was circulated in the filtration apparatus with the permeate side valve closed for about 10 minutes.
8. The permeate side valve was opened and permeate was recycled to the feed tank.
9. The permeate flux was measured by collecting samples at pre determined time intervals. Permeate volume was measured using a measuring cylinder and a stopwatch to record the time for each sample.
10. Permeate sample volume and time were manually recorded throughout the duration of the experiment and the permeate samples were returned to the feed tank after the measurements, except for samples at 5, 30, 80, 120 and 180 minutes, for which 8 mL samples were taken for laboratory analysis.

End of Experiment:

1. The pump was stopped.
2. The drain valve was opened to empty the feed tank.

End of Experiment; Clean water flux measurement:

1. The feed tank was filled with twenty litres of clean ultra pure water.
2. The heater set point temperature was set to 40 °C and the water was heated to this temperature.

3. The pump was started and the permeate side valve was opened.
4. Three flux measurements were taken.
5. The pump was stopped and the feed tank drain valve was opened to empty the feed tank.

Apparatus cleaning after wastewater experiments:

1. The cleaning solution was filled into the feed tank.
2. The heater set point was set to 50 °C.
3. The pump was started and the cleaning solution was circulated through the filtration apparatus for 60 to 90 minutes.
4. The pump was stopped and the cleaning solution was kept in the filtration apparatus for 10 minutes before it was drained via the drain valve.
5. The filtration apparatus was flushed with tap water twice for 5 and 15 minutes each.
6. Finally, the feed tank was filled with ultra pure water and the pump was started to circulate the water through the membrane for 30 minutes.
7. The pump was stopped and the inlet valve to the membrane housing was closed to keep the membrane wet.
8. The computer was shut down and the main power to the filtration apparatus was turned off.

3.6.1.4 Total Organic Carbon (TOC) and Inorganic Carbon (IC) Measurement

The ThermoEuroglas Total Organic Carbon analyser, TOC 1200, uses a non dispersive infrared detector (NDIR) to measure the amount of CO_2 produced by a sample oxidised in the high temperature furnace and relates the amount of CO_2 to the concentration of total carbon in the sample.

The liquid sample is injected into a boat that introduces the sample to the analyser high temperature furnace, set at 1000 °C. The sample is flushed with argon during the boat movement to the furnace so volatile components will

enter the furnace. The sample is oxidised with oxygen gas. The oxidation products are led through a copper oxide scrubber then though the inorganic carbon scrubber, after which the oxidation products pass through a Perma pure dryer. The oxidation product gases pass through a particle filter before finally flowing into the NDIR detector, which measures the concentration of CO_2. The area of the signal measured by the NDIR detector is used to calculate the TOC concentration.

In the TOC 1200 analyser, a sample can be introduced at either of two places: boat injection, to measure the total carbon, TC, or IC scrubber injection for inorganic carbon, IC, measurement.

Total organic carbon (TOC) and inorganic carbon (IC) concentrations were determined as follows:

1. TC measurement via boat injection
2. IC measurement via IC scrubber injection
3. TOC Calculated as TC – IC = TOC

The ThermoEuroglas Total Organic Carbon analyser, TOC 1200 was calibrated with known standards to establish a calibration curve for analysing the filtration experiment samples (Figures 26 and 27).

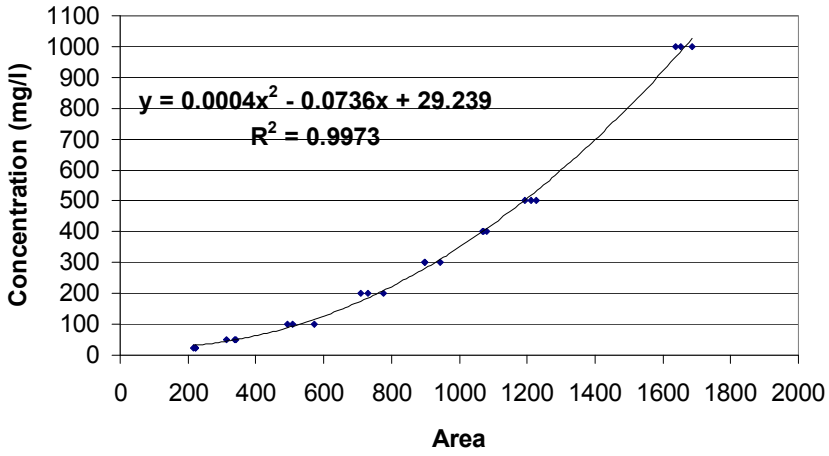

Figure 26. Total carbon calibration for the TOC 1200 Analyser.

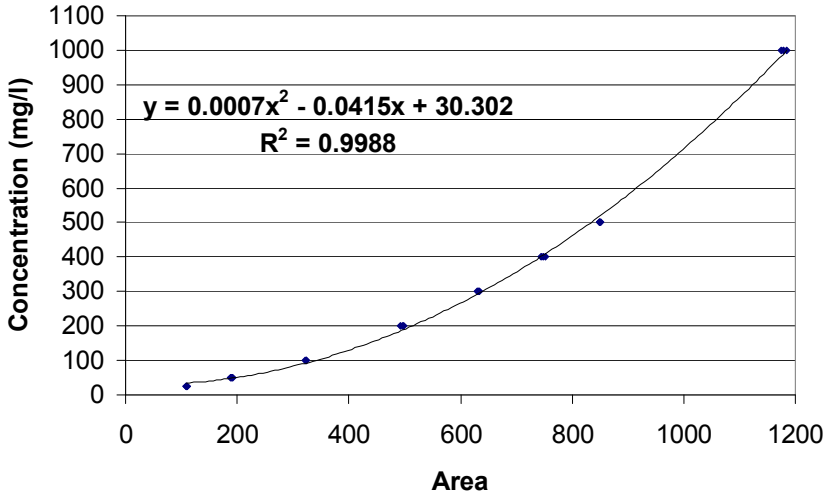

Figure 27. Inorganic carbon calibration for the TOC 1200 Analyser.

3.6.1.5 Chemical Oxygen Demand (COD) measurement

Ready to use Palintest reagent tubes with sulphuric acid and potassium dichromate in the presence of a silver sulphate catalyst were used to oxidise the water sample by digestion. The reduction in the amount of potassium dichromate is proportional to the COD in milligrams of oxygen consumed per litre of sample (Palintest Photometer Instruction Manual, 2007).

The amount of Cr^{3+} formed from the reduction of potassium dichromate was used to indirectly measure the COD of the water sample according to:

$$C_nH_aO_bN_c + dCr_2O_7^{2-} + (8d + c)H^+ \rightarrow nCO_2 + \frac{a + 8d - 3c}{2}H_2O + cNH_4^+ + 2dCr^{3+}$$

where: $d = \frac{2n}{3} + \frac{a}{6} - \frac{b}{3} - \frac{c}{2}$

3.6.1.6 Phosphate measurement

An optical method was used to determine the concentration of phosphate in the artificial wastewater feed and permeate samples. Palintest® Photometer 7100 and Phosphate HR reagent tablets were supplied by Palintest, Ltd. The test is based on the vanadomolybdate method in which the intensity of yellow colour of the phosphovanadomolybdate produced by the reaction of

phosphates with ammonium molybdate in the presence of ammonium vanadate is proportional to the concentration of phosphate (Palintest Potometer 7100 Instructions Manual 2007).

Test Procedure:

1. A test tube is filled with 10 mL of the water sample.
2. One tablet of Phosphate HR reagent is added, crushed and mixed to dissolve.
3. The sample is allowed to stand for 10 minutes to allow full colour development.
4. The test tube is inserted into the photometer tube holder.
5. The Phot 29 automatic wavelength programme is selected.
6. The photometer reading is displayed as mg/L PO_4.

3.7 Bicomponent dead end stirred cell filtration experiments

3.7.1 Sodium alginate and calcium chloride dihydrate solution preparation

A 1000 mg/L solution of sodium alginate was prepared by dissolving 0.5 gram of brown algae alginic acid sodium salt (Fluka Chemie AG) in 500 mL of Millipore Milli Q system purified water.

A 1000 mg/L solution of calcium chloride dihydrate was prepared by dissolving 0.5 grams of calcium chloride dihydrate (Fisher Scientific, USA) in 500 mL Millipore Milli-Q system purified water.

Solutions with different concentrations of sodium alginate and calcium chloride dihydrate were prepared by combining the appropriate volumes of both solutions and diluting to 100 mL with Milli-Q purified water.

The Sodium alginate calcium mixture preparation procedures were as follows.

Sodium alginate and calcium stock solution preparation:

1. Prepare 500 mL of 1000 mg/L sodium alginate solution:
    a. Dissolve 0.5 grams of sodium alginate powder in 500 mL of deionised water.
    b. Mix and stir for two hours

2. Prepare 500 mL of 1000 mg/L Ca^{++} solution:
    a. Dissolve 0.5 grams of calcium chloride in 500 mL deionised water.
    b. Mix and stir for two hours

Preparation of different sodium alginate-calcium solutions:

1. For a 300 mg/L sodium alginate /100 mg/L calcium solution:
    a. Mix 30 mL of the 1,000 mg/L sodium alginate solution with 10 mL of the 1,000 mg/L calcium chloride solution.
    b. Dilute to 100 mL with deionised water
    c. Stir for 30 min

2. For a 300 mg/L sodium alginate /80 mg/L calcium solution:
    a. Mix 30 mL of the 1,000 mg/L sodium alginate solution with 8 mL of the 1,000 mg/L calcium chloride solution.
    b. Dilute to 100 mL with deionised water
    c. Stir for 30 min.

3. For a 300 mg/L sodium alginate / 60 mg/L calcium solution:
    a. Mix 30 mL of the 1,000 mg/L sodium alginate solution with 6 mL of the 1,000 mg/L calcium chloride solution.
    b. Dilute to 100 mL with deionised water
    c. Stir for 30 min.

4. For a 300 mg/L sodium alginate / 40 mg/L calcium solution:

a. Mix 30 mL of the 1,000 mg/L sodium alginate solution with 4 mL of the 1,000 mg/L calcium chloride solution.
b. Dilute to 100 mL with deionised water
c. Stir for 30 min.

5. For a 300 mg/L sodium alginate / 20 mg/L calcium solution:
    a. Mix 30 mL of the 1,000 mg/L sodium alginate solution with 2 mL of the 1,000 mg/L calcium chloride solution.
    b. Dilute to 100 mL with deionised water
    c. Stir for 30 min

Table 9. Sodium alginate and calcium chloride solutions.

Solution concentration (mg/L)	**$CaCl_2$ solution (mL)**	**Alginate (mL)**	**Purified water (mL)**
[Alg.] = 300, [CaCl2] = 20	2	30	68
[Alg.] = 300, [CaCl2] = 40	4	30	66
[Alg.] = 300, [CaCl2] = 60	6	30	64
[Alg.] = 300, [CaCl2] = 80	8	30	62
[Alg.] = 300, [CaCl2] = 100	10	30	60

3.7.2 Meat extract and calcium chloride dihydrate solution preparation:

A 1000 mg/L solution of meat extract was prepared by dissolving 0.5 gram of meat extract (Oxoid, Ltd., England) in 500 mL Millipore Milli-Q system purified water.

A 1000 mg/L solution of calcium chloride dihydrate was prepared by dissolving 0.5 grams of calcium chloride dihydrate (Fisher Scientific, USA) in 500 mL Millipore Milli-Q system purified water.

Solutions with different concentrations of meat extract and calcium chloride dihydrate were prepared by combining the appropriate volumes of both solutions and diluting to 100 mL with Milli-Q purified water.

The meat extract-calcium mixture preparation procedure was as follows.
Meat extract and calcium stock solution preparation:

1. Prepare 500 mL solution of 1,000 mg/L meat extract:
    a. Dissolve 0.5 grams of meat extract powder in 500 mL deionised water.
    b. Mix and stir for two hours.

2. Prepare 500 mL solution of 1,000 mg/L Ca^{++}:
    a. Dissolve 0.5 grams of calcium chloride in 500 mL deionised water.
    b. Mix and stir for two hours.

Preparing different meat extract-calcium solutions:

1. For a 300 mg/L meat extract / 100 mg/L calcium solution:
    a. Mix 30 mL of the 1,000 mg/L meat extract solution with 10 mL of the 1,000 mg/L calcium chloride solution.
    b. Dilute to 100 mL with deionised water
    c. Stir for 30 min

2. For a 300 mg/L meat extract / 80 mg/L calcium solution:
    a. Mix 30 mL of the 1,000 mg/L meat extract solution with 8 mL of the 1,000 mg/L calcium chloride solution.
    b. Dilute to 100 mL with deionised water
    c. Stir for 30 min

3. For a 300 mg/L meat extract / 60 mg/L calcium solution:
    a. Mix 30 mL of the 1,000 mg/L meat extract solution with 6 mL of the 1,000 mg/L calcium chloride solution
    b. Dilute to 100 mL with deionised water

c. Stir for 30 min.

4. For a 300 mg/L meat extract / 40 mg/L calcium solution:
    a. Mix 30 mL of the 1,000 mg/L meat extract solution with 4 mL of the 1,000 mg/L calcium chloride solution.
    b. Dilute to 100 mL with deionised water
    c. Stir for 30 min

5. For a 300 mg/L meat extract / 20 mg/L calcium solution:
    a. Mix 30 mL of the 1,000 mg/L meat extract solution with 2 mL of the 1,000 mg/L calcium chloride solution.
    b. Dilute to 100 mL with deionised water
    c. Stir for 30 min

Table 10. Meat extract and calcium chloride solutions.

Solution concentration (mg/L)	**$CaCl_2$ solution (mL)**	**Meat Ex. (mL)**	**Purified water (mL)**
[Meat Ex.] = 300, [CaCl2] = 20	2	30	68
[Meat Ex.] = 300, [CaCl2] = 40	4	30	66
[Meat Ex.] = 300, [CaCl2] = 60	6	30	64
[Meat Ex.] = 300, [CaCl2] = 80	8	30	62
[Meat Ex.] = 300, [CaCl2] = 100	10	30	60

3.7.3 Stirred cell filtration experiments

A 50 mL Millipore stirred cell with a 47 mm ultrafiltration membrane disc filter was used to filter the sodium alginate and calcium chloride solutions and the meat extract and calcium chloride solutions.

For the sodium alginate and calcium chloride experiments, a 47 mm polyethersulfone ultrafiltration membrane with an NMWL cut-off of 10,000 Daltons (Millipore Corporation, USA) was used to filter the solution. For the meat extract and calcium chloride experiments, an OMEGA 47 mm polyethersulfone ultrafiltration membrane with a MWCO of 1,000 Daltons (Pall

Life Sciences, USA) was used to filter the solutions. Both disc membranes had an effective filtration area of 17.3 cm^2.

3.7.4 Membrane preparation

The membranes were washed by soaking for 24 hours in Milli-Q system purified water. Membranes were rinsed upon installation by passing 50 mL of purified water through the stirred cell to remove any impurities and additives used during the manufacturing process, as recommended by the manufacturer.

3.7.5 Stirred cell ultrafiltration experiment

The stirred cell was loaded with 50 mL of the solution to be filtered, a nitrogen gas line was connected to the stirred cell and the two way valve was opened. The pressure in the stirred cell was monitored by a pressure gauge and controlled using a model 8286 pressure regulator (Porter Instrument Co., USA). All filtrations were conducted using a TMP pressure of 1.25 bars and room temperature (Figure 28).

Figure 28. Stirred cell ultrafiltration

3.7.6 Calcium cation concentration analysis

Atomic absorption spectroscopy was used to measure free calcium cation concentration in the solution. A Varian atomic absorption spectrophotometer (model SpectrAA 200; Varian Australia Pty., Ltd.) was used (Figure 29). Elemental metals absorb UV when they are in an excited state. Although atoms exist in a stable state called the ground state in normal conditions, atoms can be transformed to higher excited state by some processes such as the addition of thermal energy.

Figure 29. Atomic absorption spectrophotometer.

In the atomic absorption spectroscopy instrument, a nebuliser aspirates the sample into a flame. The flame provides calcium atoms with the thermal energy needed to be transferred to an excited state. Upon making that transition calcium atoms absorb some of the light of the beam (Figure 30).

The lamp generates a beam of light specific for the metal analysed. In the case of calcium the light beam wavelength is 442.7 nm (Varian Australia Pty., Ltd. SpectrAA 200 Manual, 1989). The light beam travels through the flame to the detector where some of the light is absorbed by the excited calcium

atoms. The reduction of light is recorded by the detector. The instrument compares the reduction in the light intensity to the reduction obtained by a known concentration in a standard calibration curve and calculates the sample calcium concentration.

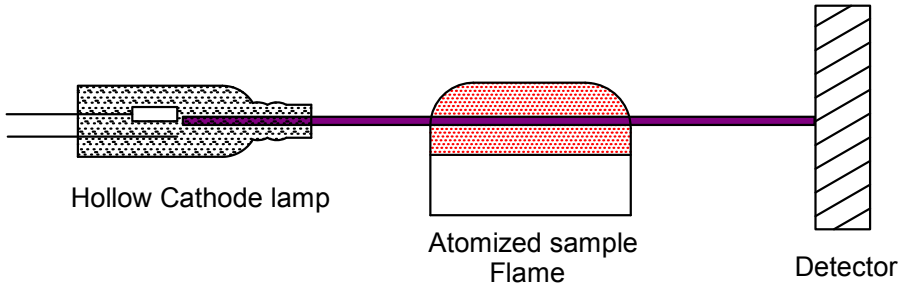

Figure 30. Simplified atomic absorption spectroscopy apparatus schematic.

3.8 Bicomponent mixture cross-flow filtration experiments

3.8.1 Factorial design of the experiments

A full two level factorial design setup was used for the bicomponent ultrafiltration experiments. The two level factorial design statistical method was described in Appendix D.

Two bicomponent mixtures were tested with five experiments run for each mixture at different concentrations. Sodium alginate-calcium mixture and meat extract-calcium mixtures were selected for study at high and low concentration to determine their single and interaction effects on the fouling of the ultrafiltration membrane (Table 11).

Table 11. High and low concentrations for the two level design factors.

factor	High (mg/L)	Low (mg/L)
Sodium alginate	150	50
Meat extract	270	90
$CaCl_2 \cdot 2H_2O$	60	20

Four experiments plus the central experiment were required to investigate all the possible combinations of the high and low concentrations for the two bicomponent mixtures under investigation (Tables 12 and 13).

Table 12. Sodium alginate-calcium mixture full factorial, two level experimental design runs.

Experiment	**Sodium alginate (mg/L)**	**$CaCl_2 \cdot 2H_2O$ (mg/L)**
1	100	40
2	50	20
3	150	20
4	50	60
5	150	60

Table 13. Meat extract-calcium mixture full factorial, two level experimental design runs.

Experiment	**Meat extract (mg/L)**	**$CaCl_2 \cdot 2H_2O$ (mg/L)**
1	180	40
2	90	20
3	270	20
4	90	60
5	270	60

4.0 Results and Discussion

In this chapter the result of the microfiltration scoping experiments, the 20 and 5 kD ultrafiltration experiments are described in detail. The flux results of the filtration experiments as will as the samples analysis results are examined in detail to determine the effect of changing the artificial wastewater components concentration.

4.1 Wastewater mixture microfiltration scoping experiments

4.1.1 Filtration flux

The reduction in the flux with time (Figure 31) suggests that one of the pore blocking mechanisms affected the filtration process. The quality of the permeate COD did not change throughout the filtration experiments which indicated that the feed particles size is smaller than the membrane pore size thus allowing the artificial wastewater components to flow to the permeate side.

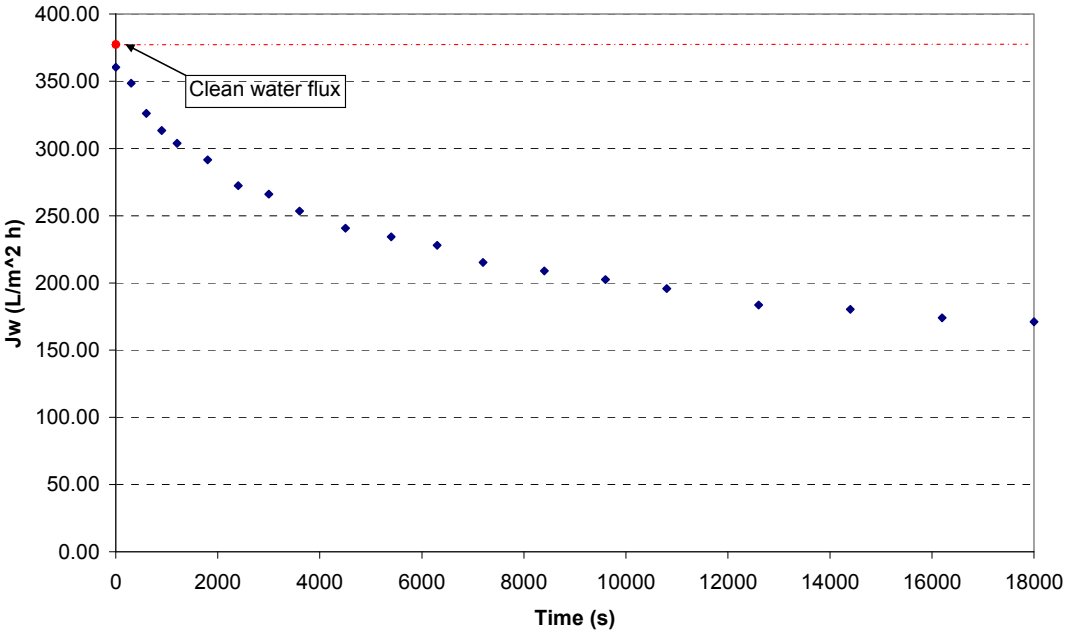

Figure 31. Flux vs. time for a microfiltration experiment.

4.1.2 COD and TOC analyses

The microfiltration experiment result clearly shows that the artificial wastewater component particle sizes were much smaller than the microfilter membrane pore size. The COD analysis of the feed and permeate samples (Table 14) show the same values indicating that no separation was achieved by the 0.2 μm microfiltration membrane.

A smaller pore size membrane was selected to examine the effect of the different size components on the membrane fouling therefore, ultrafiltration membranes with pore size of 20 and 5 kilo Dalton were selected to carry on the rest of the artificial wastewater filtration experiments.

Table 14. COD analysis results for microfiltration wastewater experiment.

Sample	Time (min)	COD (ppm)
Feed	-	340 ± 20
1	5	350 ± 10
2	15	360 ± 10
3	30	350 ±10
4	50	360 ± 00
5	75	350 ±10
6	105	330 ± 10
7	140	340 ± 00
8	180	330 ± 10
9	240	340 ± 20
10	300	330 ± 20
End feed	-	310 ± 10

4.2 Artificial wastewater mixture 20 kD ultrafiltration experiments

4.2.1 Flux analysis

The flux decline for experiments F4, F10 and F12, of 78, 78 and 77 per cent, respectively, was the highest among the artificial wastewater filtration

experiments performed. In these experiments, the calcium concentration was at the high level 60 ppm (Table 8). On the other hand, the flux decline for experiments F7, F1 and F2 which were conducted with a low calcium concentration level of 20 ppm had the lowest flux decline recorded, 61, 63 and 63 per cent respectively. This behaviour supports the hypothesis of the bridging effect of calcium on proteins and polysaccharides proposed by Katsoufidou *et al.* (2007).

Table 15. Initial and final permeate flux and membrane resistance for 20 kD membrane artificial wastewater experiments.

Experiment	J_{cw} (L/m^2 h)	J_{ss} (L/m^2 h)	R_{cw} (1/m)	R_{ss} (1/m)
F0	1,443	376	4.00E+11	1.56E+12
F1	1,274	475	5.36E+11	1.33E+12
F2	1,198	447	4.98E+11	1.36E+12
F3	1,656	551	3.54E+11	1.08E+12
F4	1,697	373	3.43E+11	1.58E+12
F5	1,515	482	3.82E+11	1.25E+12
F6	1,644	444	3.50E+11	1.44E+12
F7	1,166	452	4.92E+11	1.31E+12
F8	1,783	463	3.52E+11	1.30E+12
F9	1,601	418	3.58E+11	1.40E+12
F10	1,499	335	3.51E+11	1.59E+12
F11	1,601	427	3.50E+11	1.35E+12
F12	1,317	304	3.61E+11	1.82E+12
F13	1,440	385	4.04E+11	1.52E+12
F14	1,508	411	3.82E+11	1.41E+12
F15	1,498	440	3.80E+11	1.30E+12
F16	1,621	402	3.58E+11	1.48E+12

Although experiments F1 and F2 had higher alginate, peptone and meat extract concentrations than experiments F14 and F15, the reduction in normalised flux was less compared to experiments F14 and F15 in which the calcium concentrations were higher even though the concentration of alginate, peptone and meat extract were low (Table 20).

The concentration of calcium had more effect on the flux reduction than the change in concentration of the other factors.

4.2.2 TOC analyses

The highest feed total carbon (TC) concentration used was in the artificial wastewater mixture for experiment numbers F2, F10 and F13, in which all the factors (components) were at high level, except for F13, in which alginate level was low. The wastewater feed used in experiments F11 and F14, where meat extract, peptone and alginate were all at low concentration, registered the lowest concentration of TC. Further, F7 gave a low TC feed result where the alginate concentration level was high, which indicate that the major source of TC were meat extract and peptone (Table 16).

The highest reduction of TC concentration was obtained in experiments F7, F12 and F14. The lowest separation for total carbon was noted in experiments F9, F13 and F15, in which either meat extract or alginate or both were at low concentration in the wastewater feed (Table 16).

Table 16. Total carbon analysis results for 20 kD membrane artificial wastewater experiments.

Experiment	Feed (ppm)	Permeate sample # 1	Permeate sample# 4	Permeate sample # 6	ΔTC (%)
F0	127±0	95.5±0.7	95.1±0.9	95.3±0.8	25
F1	N/A	N/A	N/A	N/A	N/A
F2	302.5±3.1	235.4±6.5	243.3±6.2	225.6±8.8	25
F3	215.0±117	171.6±7.3	164.8±14.5	161.5±9.9	25
F4	241.3±1.9	166.7±8.6	161.5±4.4	169.6±2.4	30
F5	267.6±9.7	170.5±4.0	164.5±9.9	178.3±5.7	33
F6	245.0±15.6	181.7±3.0	179.8±11.7	169.6±0.5	31
F7	151.0±1.8	97.2±1.3	92.2±5.9	98.5±0.8	35
F8	199.6±2.1	163.4±3.3	167.0±1.3	167.5±3.8	16
F9	285.1±3.0	254.1±2.2	253.1±10.9	250.5±1.1	12
F10	331.4±2.0	258.4±5.0	250.2±10.5	258.6±5.9	22
F11	136.7±6.6	105.2±2.4	99.2±1.7	99.5±0.9	27
F12	205.8±1.7	110.5±0.2	108.4±3.0	108.0±0.5	48
F13	302.5±10.1	269.5±10.3	264.2±0.2	266.6±5.0	12
F14	173.6±12.3	118.1±6.5	113.8±1.8	114.3±3.6	34
F15	246.5±6.1	213.6±10.3	213.5±17.5	222.6±5.0	10
F16	275.8±10.3	218.3±12.4	201.1±4.2	221.2±1.6	21

The reduction of inorganic carbon by the membrane separation was the lowest of all the parameters measured in this study, indicating that the major concentration of inorganic carbon in the artificial wastewater existed as CO_3^- ions formed by the disassociation of ammonium carbonate (NH_4 $2CO_3$), which is too small to be separated by the ultrafiltration membrane.

Table 17. Inorganic carbon analysis results for 20 kD membrane artificial wastewater experiments.

Experiment	Feed (ppm)	Permeate sample # 1	Permeate sample # 4	Permeate sample # 6
F0	28.80±0	26.7±0.1	26.7±0.1	26.5±0.1
F1	46.1±1.4	48.7±3.7	51.7±1.0	50.2±1.7
F2	46.4±3.1	48.3±1.1	45.5±0.6	42.8±1.1
F3	45.8±2.2	45.4±2.3	44.4±0.5	44.7±2.4
F4	47.7±1.2	49.1±0.2	52.0±5.3	48.6±2.8
F5	48.5±2.2	48.1±0.1	45.8±1.0	49.1±2.8
F6	48.6±0.9	45.8±4.1	49.9±6.4	45.7±0.3
F7	46.3±0.6	44.6±0.1	44.2±0.1	44.9±1.0
F8	46.7±0.0	44.6±0.1	45.8±0.4	43.0±0.5
F9	46.5±0.7	46.1±0.8	46.4±0.1	47.8±0.8
F10	48.0±0.9	46.3±0.2	45.8±0.1	48.8±1.7
F11	48.4±0.0	45.4±0.0	41.9±2.7	46.5±0.2
F12	49.9±0.5	47.6±0.9	48.9±0.2	45.3±0.7
F13	49.5±1.8	48.3±0.6	49.6±1.0	48.1±0.6
F14	52.7±0.4	46.5±4.5	52.6±1.9	46.0±0.5
F15	53.3±1.2	51.9±1.5	51.6±1.4	45.7±0.1
F16	50.5±6.4	52.3±0.7	58.7±4.6	57.1±1.0

4.2.3 COD analyses

The highest chemical oxygen demand for the artificial wastewater feed was used in the feed for experiments F1 and F7, in which all factors (components) except for calcium were at the high level (concentration) (Table 18). Furthermore, the highest COD reduction by the filtration process was achieved in experiments F7 and F12, at 39% and 53%, respectively. In experiments F7 and F12, the alginate was at high concentration. Moreover, the COD reduction in experiments F9, F13, F14 and F16 was very low at

14%, 17%, 18% and 15%, respectively. The alginate concentration was at a low level in the experiments where low COD reduction in the permeate was observed. The large size of the alginate molecules may be responsible for fouling the membrane and reducing the organic concentration on the permeate side.

Table 18. Chemical oxygen demand (COD) analysis results for 20 kD membrane artificial wastewater experiments.

Experiment	Feed (ppm)	Permeate sample # 1	Permeate sample # 4	Permeate sample # 6
F0	460 ± 10	333 ± 6	357 ± 21	360 ± 10
F1	467 ± 6	290 ± 0	303 ± 6	297 ± 6
F2	693 ± 6	510 ± 0	523 ± 6	540 ± 10
F3	447 ± 6	380 ± 0	377 ± 6	360 ± 10
F4	493 ± 6	317 ± 6	337 ± 6	343 ± 6
F5	543 ± 6	357 ± 6	380 ± 0	377 ± 6
F6	513 ± 6	363 ± 6	380 ± 0	373 ± 6
F7	323 ± 6	210 ± 10	203 ± 6	197 ± 6
F8	453 ± 6	363 ± 6	350 ± 0	347 ± 6
F9	673 ± 6	577 ± 6	567 ± 12	577 ± 6
F10	703 ± 6	540 ± 0	523 ± 6	510 ± 0
F11	267 ± 6	203 ± 6	207 ± 6	187 ± 6
F12	250 ± 0	117 ± 6	117 ± 6	117 ± 6
F13	627 ± 6	517 ± 12	517 ± 6	523 ± 6
F14	233 ± 6	170 ± 0	173 ± 6	190 ± 0
F15	450 ± 0	370 ± 0	360 ± 0	363 ± 6
F16	373 ± 6	300 ± 0	317 ± 6	317 ± 6

4.2.4 Phosphate analyses

The highest concentration of phosphate was observed in experiments F0, F1 and F2, in which the meat extract was at high concentration level (Table 19). The lowest value of phosphate concentration was in experiments F3, F5 and F7, in which the concentration of meat extract and were both at low levels. It is worth noting that although experiment F4 has a low concentration of peptone and a high concentration of alginate the concentration of phosphate in the permeate was low, perhaps due to the high concentration of calcium. The bridging effect of calcium may have caused an increase in the size of the proteins due to aggregation, thus increasing their rejection by the membrane.

Table 19. Phosphate analysis results for 20 kD membrane artificial wastewater experiments.

Experiment	Feed (ppm)	Permeate sample # 1	Permeate sample # 4	Permeate sample # 6
F0	105.7±3.4	88.2±0.5	87.7±0.2	85.8±0.4
F1	103.7±3.0	86.4±0.5	86.6±0.4	83.4±0.5
F2	106.7±1.2	83.7±1.7	79.0±1.6	85.9±0.4
F3	57.5±2.8	43.5±0.4	40.6±0.1	37.2±0.0
F4	77.1±1.9	46.3±0.2	46.3±0.2	45.0±0.5
F5	45.4±0.5	43.8±0.3	22.5±0.2	20.8±0.2
F6	101.8±0.4	68.7±1.4	62.2±0.2	64.6±0.3
F7	58.3±1.2	44.5±0.3	41.3±0.2	42.9±0.2
F8	72.8±1.2	67.0±0.3	67.5±0.3	65.8±0.3
F9	95.6±1.3	91.5±1.3	87.9±0.7	84.1±0.4
F10	91.8±0.8	78.1±1.2	73.1±0.9	70.3±0.4
F11	61.8±0.0	42.1±0.2	39.3±1.4	40.2±2.4
F12	90.4±5.4	62.5±0.7	55.2±0.2	70.7±0.9
F13	98.3±2.3	84.1±1.8	75.1±1.9	87.5±0.3
F14	59.9±0.3	45.1±0.2	41.3±0.1	41.8±0.4
F15	89.1±1.3	68.4±0.3	70.5±0.3	74.6±0.4
F16	87.6±2.1	73.3±0.2	71.2±0.3	67.3±0.6

Table 20. Results of 20 kD ultrafiltration experiments component concentration in (mg/L) responses in reduction percentage from feed.

Run	Peptone (ppm)	Meat extract (ppm)	Alginate (ppm)	$CaCl_2$ (ppm)	Δflux (%)	ΔCOD (%)	ΔTC (%)		ΔPO^{4-} (%)
F0	180	180	100	40	74	22	25		19
F1	90	270	150	20	63	36	N/A		20
F2	270	270	150	20	63	22	25		19
F3	270	90	50	20	67	19	25		35
F4	90	270	150	60	78	30	30		42
F5	270	90	150	20	68	31	33		54
F6	270	90	150	60	73	27	31		37
F7	90	90	150	20	61	39	35		26
F8	90	270	50	20	74	23	16		10
F9	270	270	50	60	74	14	12		12
F10	270	270	150	60	78	27	22		23
F11	90	90	50	20	73	30	27		35
F12	90	90	150	60	77	53	48		22
F13	270	270	50	20	73	17	12		11
F14	90	90	50	60	73	18	34		30
F15	270	90	50	60	71	19	10		16
F16	90	270	50	60	75	15	20		23

4.3 Artificial wastewater mixture 5 kD ultrafiltration experiments

4.3.1 Flux analysis

The highest flux reductions were observed in experiments F2, F4 and F15, while the lowest flux reductions were in experiments F3, F5, F8 and F11, all of which had low concentration levels of calcium and alginate, except for experiment F5, where the alginate concentration level was high (Table 21).

Table 21. Initial and final permeate flux and membrane resistance for 5 kD membrane artificial wastewater experiments.

Experiment	J_{cw} (L/m^2 h)	J_{ss} (L/m^2 h)	R_{cw} (1/m)	R_{ss} (1/m)
F0	1,329	380	4.44E+11	1.61E+12
F1	1,456	386	3.94E+11	1.55E+12
F2	1,455	367	3.92E+11	1.62E+12
F3	1,371	471	4.27E+11	1.26E+12
F4	1,520	361	3.86E+11	1.62E+12
F5	1,384	443	4.19E+11	1.36E+12
F6	1,392	399	4.16E+11	1.51E+12
F7	1,470	430	3.85E+11	1.40E+12
F8	1,234	443	4.77E+11	1.36E+12
F9	1,323	392	4.46E+11	1.53E+12
F10	1,423	379	4.02E+11	1.66E+12
F11	1,454	465	3.94E+11	1.29E+12
F12	1,287	392	4.50E+11	1.43E+12
F13	1,340	341	4.27E+11	1.71E+12
F14	1,456	380	3.97E+11	1.53E+12
F15	1,739	424	3.34E+11	1.43E+12
F16	1,365	383	4.13E+11	1.56E+12

4.3.2 TOC analyses

The highest feed TC concentration was obtained in experiments F2, F9 and F10; these experiments had high levels meat extract and peptone concentrations. Experiments F7 and F12 gave the highest reduction in TC concentrations in the permeate; in both experiments, meat extract and

peptone concentrations were low and alginate concentration was high. Due to the fact that the major TC concentration was from alginate in experiments F12 and F7, with high alginate concentration and low meat extract and peptone concentration, the rejection of the large alginate molecules by the 5 kD membrane led to a higher reduction of TC in the permeate (Table 22).

The major source of inorganic carbon in the artificial wastewater mixture was ammonium carbonate ($NH_4 \cdot 2CO_3$), and there was no major reduction in the concentration of inorganic carbon in the permeate (Table 23).

Table 22. Total carbon analysis results for 5 kD membrane artificial wastewater experiments.

Experiment	Feed (ppm)	Permeate sample # 1	Permeate sample # 4	Permeate sample # 6
F0	253.9±2.1	174.2±5.9	179.9±3.3	173.9±3.2
F1	253.8±4.1	193.7±5.9	179.4±0.4	180.6±1.3
F2	352.2±6.4	258.2±11.2	277.9±1.9	275.9±1.2
F3	215.9±0.4	201.0±3.2	188.8±8.8	185.3±0.5
F4	298.7±1.3	216.4±10.7	198.3±0.4	211.1±2.9
F5	267.8±23.5	195.2±9.9	178.7±1.8	180.3±3.8
F6	273.0±6.6	191.3±8.6	190.3±6.1	173.8±0.9
F7	209.1±1.0	140.1±4.0	119.8±2.3	122.8±3.2
F8	205.5±1.9	170.0±4.2	158.7±0.1	166.7±4.7
F9	316.7±17.5	266.8±12.0	271.6±11.0	270.3±14.4
F10	360.4±5.3	267.2±1.0	273.7±1.0	273.1±0.2
F11	163.9±2.6	129.7±5.9	120.1±2.5	119.4±1.0
F12	181.0±6.2	106.5±3.0	110.7±4.9	103.4±0.9
F13	312.4±6.9	241.8±2.9	234.9±1.9	241.2±5.4
F14	136.4±5.5	106.7±2.2	98.2±1.8	94.5±1.3
F15	288.5±3.1	238.3±4.1	226.5±1.0	226.0±4.8
F16	251.8±1.9	197.5±2.0	201.1±1.1	201.3±5.9

Table 23. Inorganic carbon analysis results for 5 kD membrane artificial wastewater experiments.

Experiment	Feed (ppm)	Permeate sample # 1	Permeate sample # 4	Permeate sample # 6
F0	53.9±1.3	50.2±0.2	51.4±1.2	48.1±1.0
F1	55.9±2.2	47.7±0.5	35.9±1.8	49.5±0.1
F2	48.5±2.3	45.5±9.1	45.3±0.9	46.6±1.4
F3	62.3±1.7	55.1±3.3	50.2±1.3	51.4±0.7
F4	53.7±1.8	53.7±0.7	46.9±6.0	46.5±6.2
F5	53.1±4.7	51.4±1.8	42.5±0.7	46.2±1.0
F6	58.8±3.0	54.4±1.4	50.9±8.1	52.1±3.5
F7	50.2±2.1	49.8±0.9	45.9±7.2	44.1±2.4
F8	51.5±0.4	48.3±3.0	46.2±1.2	46.0±1.4
F9	55.0±1.9	53.7±2.0	53.5±0.4	46.3±2.3
F10	59.3±1.6	51.5±1.9	55.4±2.6	47.9±2.9
F11	51.6±0.8	48.5±7.9	49.1±3.8	46.1±5.6
F12	47.4±0.5	46.3±3.2	44.8±1.5	45.0±0.4
F13	50.9±2.3	46.8±0.4	46.8±1.4	45.0±0.6
F14	57.2±3.0	54.2±4.1	50.1±1.2	48.2±0.5
F15	54.8±0.2	52.4±7.0	53.9±6.0	50.1±2.8
F16	53.9±0.4	50.2±0.3	51.4±1.3	48.1±0.0

4.3.3 COD analyses

Among the experiments with high concentrations of meat extract, peptone and alginate (F2, F9, F10 and F13), the highest COD concentration reductions were obtained in the experiments with high alginate concentration and low meat extract and peptone concentration due to the rejection of alginate by the membrane (Table 24).

Table 24. Chemical oxygen demand (COD) analysis results for 5 kD membrane artificial wastewater experiments.

Experiment	Feed (ppm)	Permeate sample # 1	Permeate sample # 6
F0	450 ± 0	357 ± 6	360 ± 0
F1	433 ± 6	297 ± 6	293 ± 6
F2	677 ± 6	513 ± 6	510 ± 0
F3	413 ± 6	347 ± 15	353 ± 6
F4	460 ± 0	310 ± 0	330 ± 0
F5	477 ± 6	317 ± 6	337 ± 6
F6	470 ± 0	293 ± 6	330 ± 10
F7	303 ± 6	N/A	170 ± 0
F8	380 ± 10	317 ± 6	333 ± 6
F9	620 ± 10	543 ± 6	520 ± 0
F10	587 ± 6	430 ± 10	433 ± 12
F11	210 ± 0	163 ± 6	173 ± 6
F12	277 ± 10	167 ± 6	187 ± 12
F13	660 ± 0	N/A	520 ± 0
F14	207 ± 6	157 ± 6	163 ± 6
F15	470 ± 0	N/A	363 ± 6
F16	420 ± 10	350 ± 10	370 ± 10

4.3.4 Phosphate analyses

The highest reduction of phosphate in the permeate, at 37%, was found in both experiments F7 and F12; alginate concentration in the feed wastewater was also at the same high concentration level of 150 ppm in both experiments. The lowest phosphate reduction was found in experiments F9, F13 and F16, at 17%, 15% and 7%, respectively. In all these experiments, the concentration level of alginate was low, at 50 ppm. The rejection of alginate by the 5 kD membrane for experiments with high alginate concentration (making it the major source of phosphate) resulted in a greater fractional reduction of phosphate concentration in the permeate (Table 25).

Table 25. Phosphate analysis results for 5 kD membrane artificial wastewater experiments.

Experiment	Feed (ppm)	Permeate sample # 1	Permeate sample # 6
F0	81.7±0.2	61.2±0.7	65.8±0.4
F1	84.9±1.6	57.3±0.5	66.0±0.2
F2	74.5±0.9	52.3±0.1	47.7±1.5
F3	84.3±0.5	61.7±0.7	68.2±0.1
F4	94.3±3.1	68.4±0.2	67.6±1.0
F5	93.5±1.7	66.8±0.4	68.4±0.3
F6	97.2±0.8	65.9±0.3	68.4±0.3
F7	62.9±1.4	42.8±0.2	39.6±1.3
F8	68.6±0.7	60.4±0.1	68.6±0.4
F9	60.0±0.4	47.7±0.2	49.7±1.1
F10	80.3±4.7	54.1±0.2	52.8±0.7
F11	65.2±1.2	48.8±0.6	43.8±1.5
F12	68.4±0.6	44.1±0.4	43.1±1.2
F13	96.8±0.9	88.9±1.7	82.1±0.6
F14	57.1±1.3	45.7±0.1	40.5±0.3
F15	86.1±1.1	69.8±0.7	70.0±1.2
F16	81.0±1.5	69.5±1.5	75.1±0.9

Table 26. Results of 5 kD ultrafiltration experiments: component concentration responses as percentage reductions from the feed.

Run	Peptone (ppm)	Meat extract (ppm)	Alginate (ppm)	$CaCl_2$ (ppm)	Δflux (%)	ΔCOD (%)	ΔTC (%)	ΔPO^{4-} (%)
F0	180	180	100	40	71	20	32	19
F1	90	270	150	20	73	32	29	22
F2	270	270	150	20	75	25	22	36
F3	270	90	50	20	66	15	14	19
F4	90	270	150	60	76	28	29	28
F5	270	90	150	20	68	29	33	27
F6	270	90	150	60	71	30	36	30
F7	90	90	150	20	71	44	41	37
F8	90	270	50	20	64	12	19	0
F9	270	270	50	60	70	16	15	17
F10	270	270	150	60	73	26	24	34
F11	90	90	50	20	68	18	27	33
F12	90	90	150	60	70	32	43	37
F13	270	270	50	20	75	21	23	15
F14	90	90	50	60	74	21	31	29
F15	270	90	50	60	76	23	22	19
F16	90	270	50	60	72	12	20	7

4.3.5 Particles size, pH and Zeta potential measurements

The artificial wastewater particles size, pH and zeta potential were measured. Although both pH and zeta potential have not changed noticeable for all the factorial experiments, the particle size of artificial wastewater did change with different artificial wastewater experiments. The change in the particle size indicates an effect of changing calcium cations concentration which promotes aggregation of alginate and meat extract (Table 27).

Table 27 Artificial wastewater Particles size, pH and Zeta potenrial

Experiment	Zeta (mV)	pH	Size (μm)
F0	-33.1	8.31	N/A
F1	-35.3	8.36	N/A
F2	-37.5	8.34	7.62
F3	-40.5	8.37	N/A
F4	-25.7	8.26	N/A
F5	-40.1	8.3	7.35
F6	-30.5	8.19	9.98
F7	-39.6	8.46	6.53
F8	-35.5	8.46	9.97
F9	-30.5	8.3	5.62
F10	-31.4	8.31	5.03
F11	-41.2	8.34	5.25
F12	-23.1	8	4.41
F13	-33.4	8.3	6.78
F14	-30.4	8.38	12.3
F15	-29.7	8.31	7.62
F16	-25	8.35	6.87

4.4 Effects of wastewater component concentrations on membrane fouling factorial design analysis

The membrane resistance increase was calculated by dividing the membrane resistance at steady state flux, R_{ss}, by the clean membrane resistance calculated using the pure water flux measurement, R_{cw}.

$$\% \text{ Membrane resistance increase} = \frac{R_{ss}}{R_{cw}} \cdot 100 \qquad (4.1)$$

4.4.1 Component main effects for 20 kD ultrafiltration membrane wastewater experiments

4.4.1.1 Effect of changing the calcium chloride concentration on membrane fouling

Each two experiments with the same concentrations of all other artificial wastewater components and high or low calcium concentration (Table 28) were compared by their percentages of membrane fouling (Figure 32).

Table 28. Equivalent wastewater experiments with different calcium concentration levels.

Peptone (ppm)	Meat extract (ppm)	Sodium alginate (ppm)	Experiments	
			High level Calcium 60 ppm	Low level Calcium 20 ppm
90	270	150	F4	F1
270	270	150	F10	F2
270	90	50	F15	F3
270	90	150	F6	F5
90	90	150	F12	F7
90	270	50	F16	F8
90	90	50	F14	F11
270	270	50	F9	F13

The change in calcium concentration had a great effect on the membrane fouling. Experimental runs with high calcium levels resulted in a large increase in membrane fouling, of about 45 per cent on average, compared to experiments conducted with low calcium concentrations (Figure 33). Among all the components in the artificial wastewater, changes in the calcium level had the highest and clearest effect on membrane fouling.

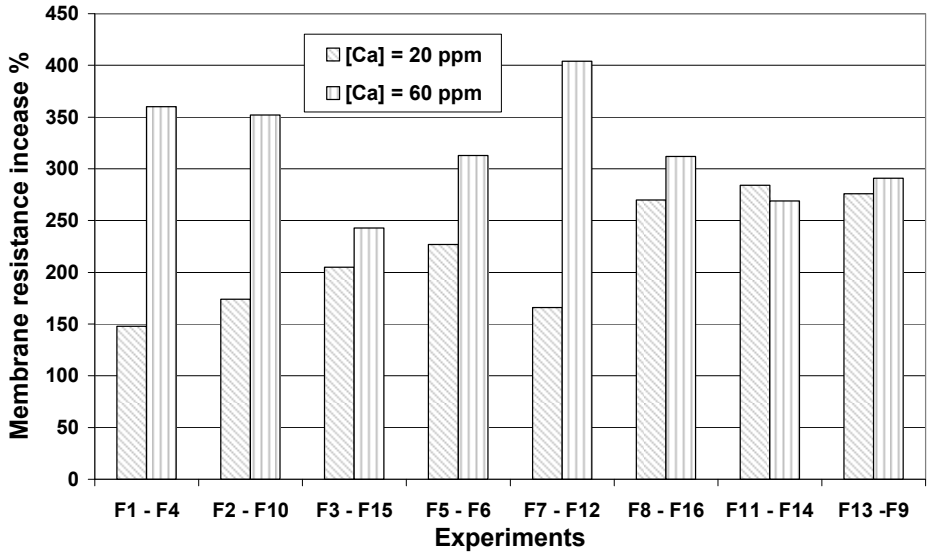

Figure 32. Equivalent wastewater experiments with high and low calcium concentrations; membrane fouling results.

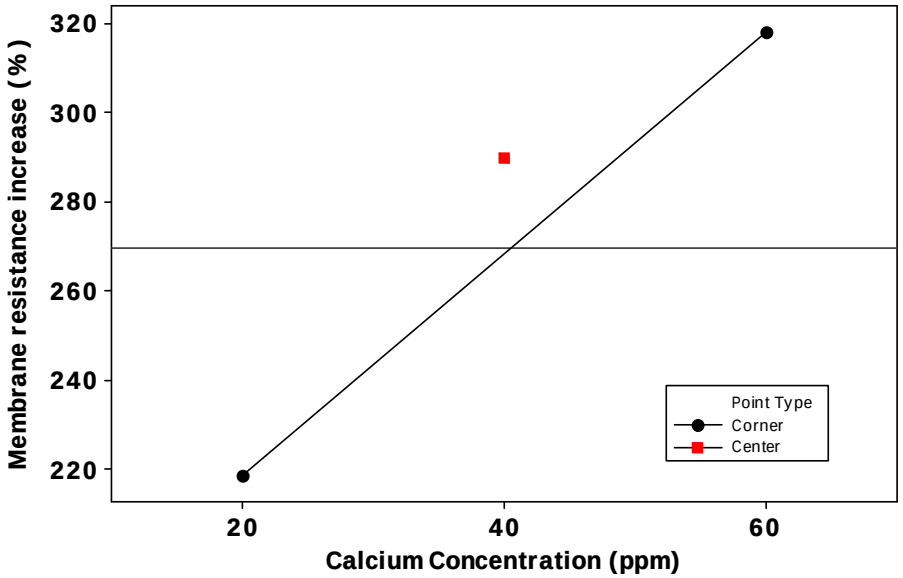

Figure 33. Average membrane resistance increase for experiments with high and low calcium concentrations.

4.4.1.2 Effect of changing the sodium alginate concentration on membrane fouling

Each two experiments with the same concentrations of all other artificial wastewater components and high or low sodium alginate concentration (Table 29) were compared by their percentages of membrane fouling (Figure 34).

Table 29. Equivalent wastewater experiments with different sodium alginate concentration levels.

Peptone (ppm)	Meat extract (ppm)	Calcium (ppm)	Experiments	
			High level Alginate 150 ppm	Low level Alginate 50 ppm
270	90	20	F5	F3
90	270	20	F1	F8
270	270	60	F10	F9
90	90	20	F7	F11
270	270	20	F2	F13
90	90	60	F12	F14
270	90	60	F6	F15
90	270	60	F4	F16

The fouling behaviour of sodium alginate was similar to that of meat extract. Changes in the concentration level of alginate did not result in noticeable changes in the membrane fouling (Figure 35). A high level of alginate gave more fouling than was observed in experiments with low alginate concentrations; however, it was a very small increase.

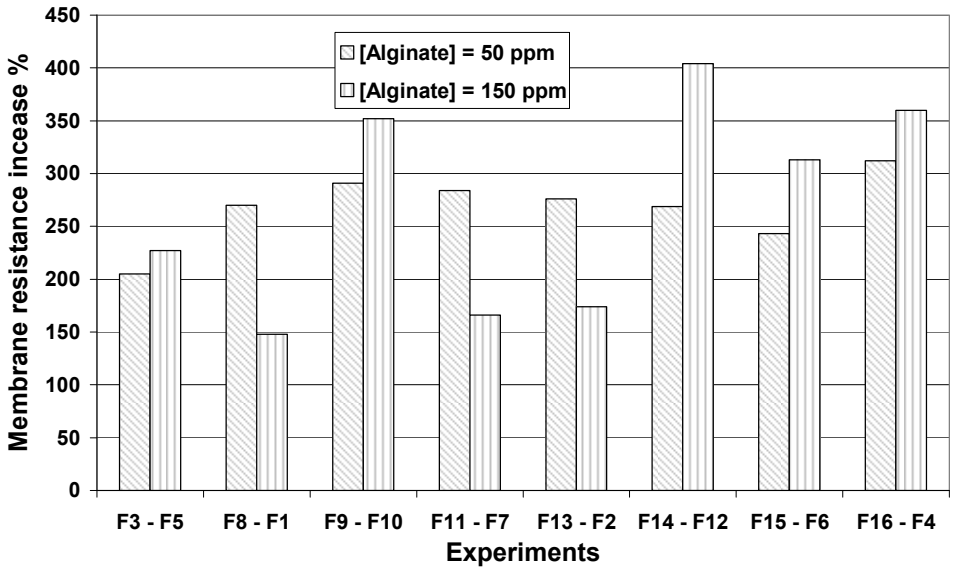

Figure 34. Equivalent wastewater experiments with high and low alginate concentrations; membrane fouling results.

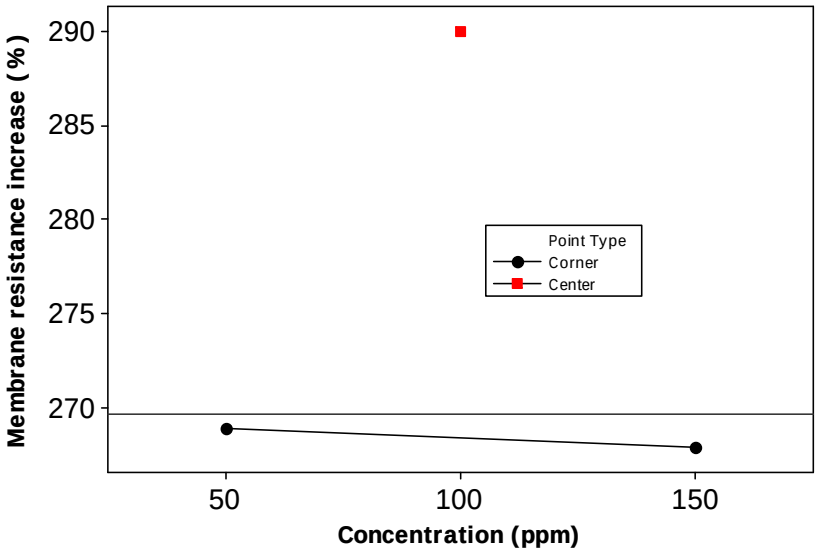

Figure 35. Average membrane resistance increase for experiments with high and low alginate concentrations.

4.4.1.3 Effect of changing the meat extract concentration on membrane fouling

Each two experiments with the same concentrations of all other artificial wastewater components and high or low meat extract concentrations (Table 30) were compared by their percentages of membrane fouling (Figure 36).

Changes in the concentration level of meat extract did not result in noticeable changes in the membrane fouling. While, on average, high levels of meat extract gave more fouling than was observed in experiments with low meat extract concentrations, it was a very small increase (Figure 37).

Table 30. Equivalent wastewater experiments with different meat extract concentration levels.

Peptone (ppm)	Sodium alginate (ppm)	Calcium (ppm)	Experiments	
			High level Meat extract 270 ppm	Low level Meat extract 90 ppm
270	50	20	F13	F3
270	150	20	F2	F5
270	150	60	F10	F6
90	150	20	F1	F7
90	50	20	F8	F11
90	150	60	F4	F12
90	50	60	F16	F14
270	50	60	F9	F15

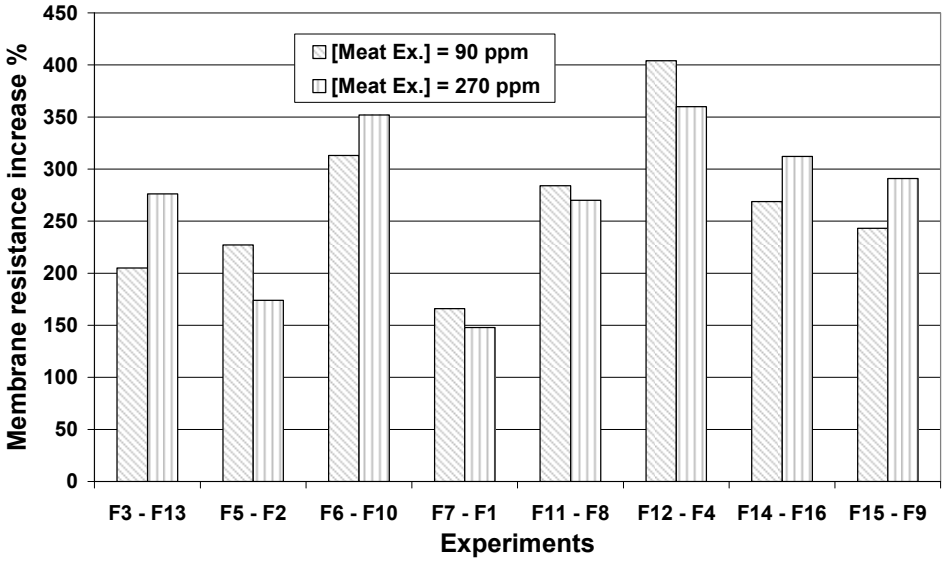

Figure 36. Equivalent wastewater experiments with high and low meat extract concentrations; membrane fouling results.

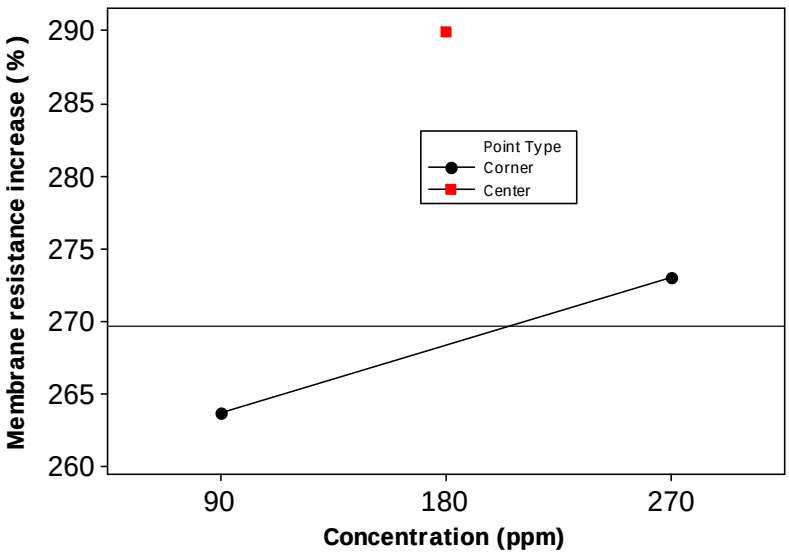

Figure 37. Average membrane resistance increase for experiments with high and low meat extract concentrations.

4.4.1.4 Effect of changing the peptone concentration on membrane fouling

Each two experiments with the same concentrations of all other artificial wastewater components and high or low peptone concentrations (Table 31) were compared by their percentages of membrane fouling (Figure 38).

Table 31. Equivalent wastewater experiments with different peptone concentration levels.

Meat extract (ppm)	Sodium alginate (ppm)	Calcium (ppm)	Experiments	
			High level Calcium 60 ppm	Low level Calcium 20 ppm
270	150	20	F2	F1
270	150	60	F10	F4
90	150	20	F6	F7
270	50	20	F13	F8
90	50	20	F3	F11
90	150	60	F6	F12
90	50	60	F15	F14
270	50	60	F9	F16

There was a small effect of different concentration levels of peptone on the membrane fouling. Experiments with low levels of peptone resulted in slightly more fouling, about 17%, compared with experiments with high concentrations of peptone (Figure 39).

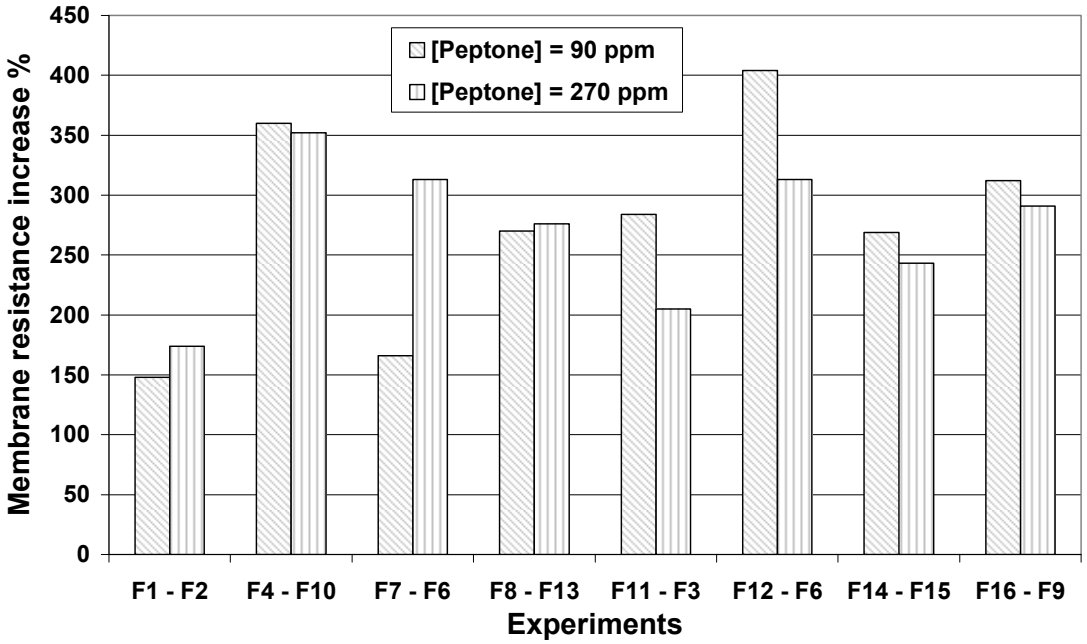

Figure 38. Equivalent wastewater experiments with high and low peptone concentrations; membrane fouling results.

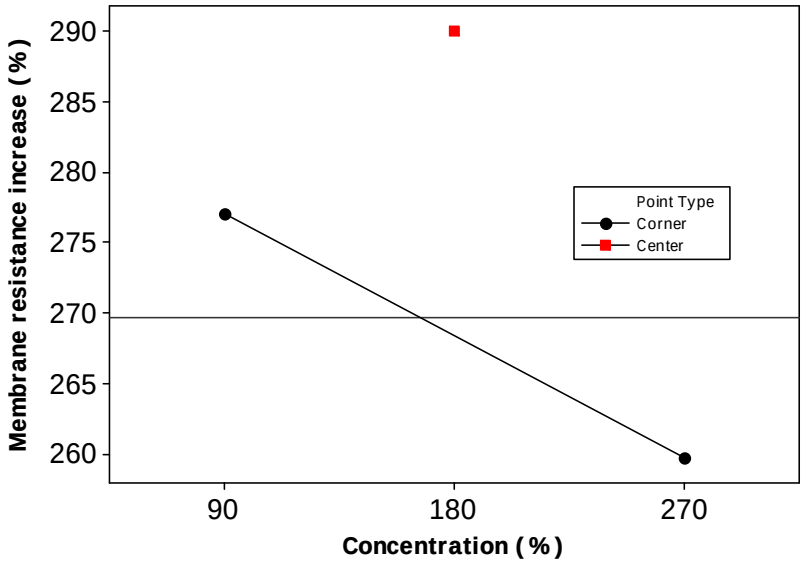

Figure 39. Average membrane resistance increase for experiments with high and low peptone concentrations.

4.4.2 Component main effects for 5 kDa ultrafiltration membrane wastewater experiments

4.4.2.1 Effect of changing the calcium chloride concentration on membrane fouling

Each two experiments with the same concentrations of all other artificial wastewater components and high or low calcium concentrations (Table 28) were compared by their percentages of membrane fouling (Figure 40).

The changes in calcium concentration showed the greatest effect on membrane fouling among all the four components examined in this study for the 5 kDa ultrafiltration membrane. A high concentration of calcium fouled the membrane to a greater extent than a low level (Figure 41).

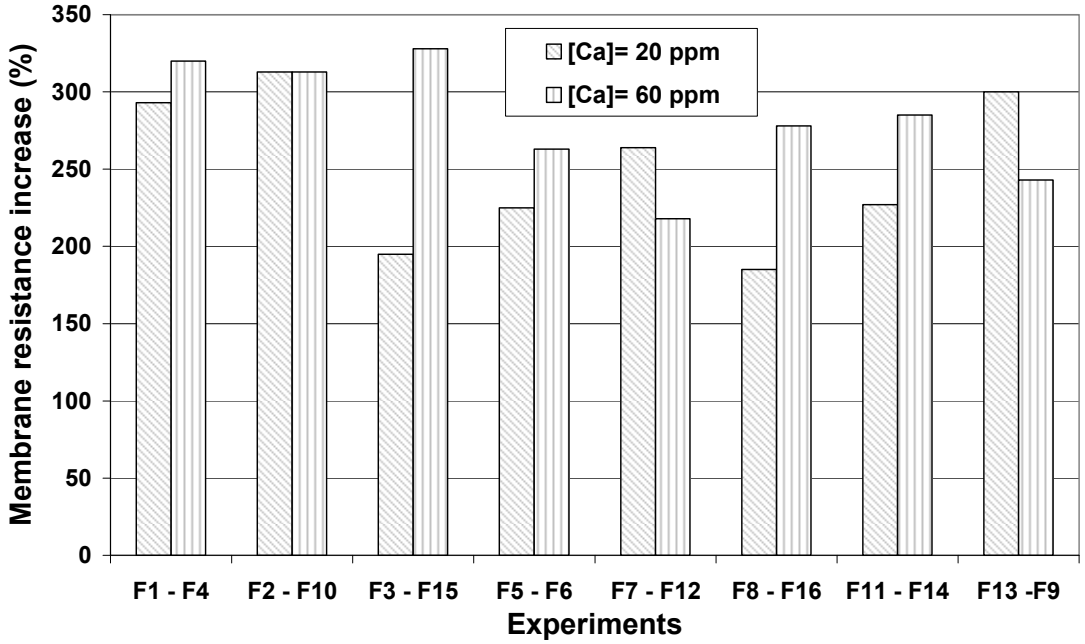

Figure 40. Equivalent wastewater experiments with high and low calcium concentrations; membrane fouling results.

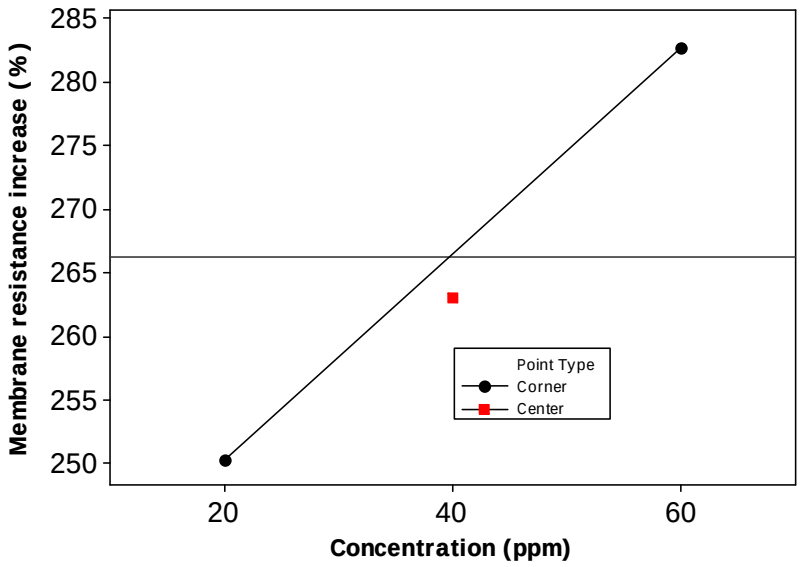

Figure 41. Average membrane resistance increase for experiments with high and low calcium concentrations.

4.4.2.2 Effect of changing the sodium alginate concentration on membrane fouling

Each two experiments with the same concentrations of all other artificial wastewater components and high or low sodium alginate concentrations (Table 28) were compared by their percentages of membrane fouling (Figure 42).

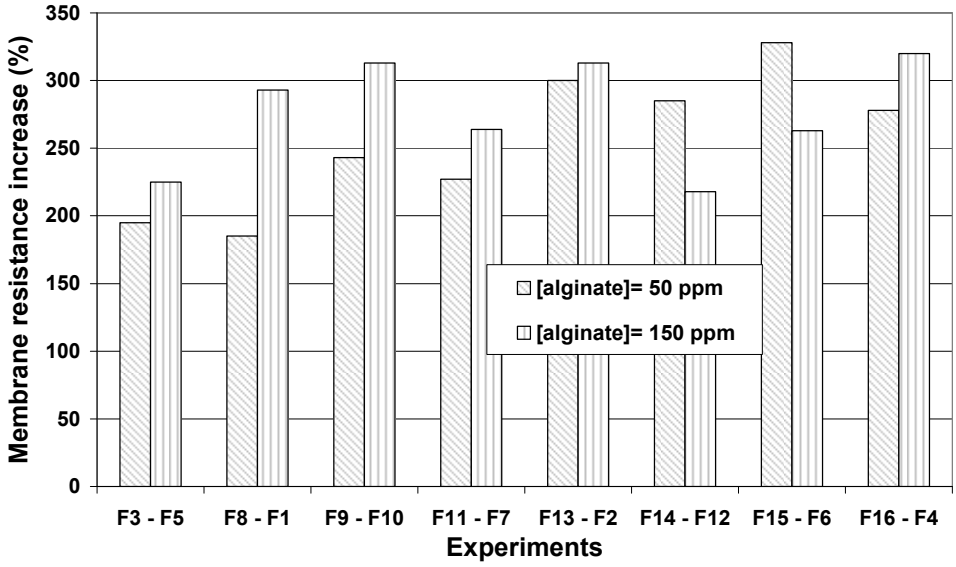

Figure 42. Equivalent wastewater experiments with high and low alginate concentrations; membrane fouling results.

Membrane fouling increased with increasing levels of sodium alginate concentration. It is clear that changes in alginate concentration had an effect on the membrane fouling level; however, it was not as strong as the effect of meat extract or calcium concentration levels (Figure 43).

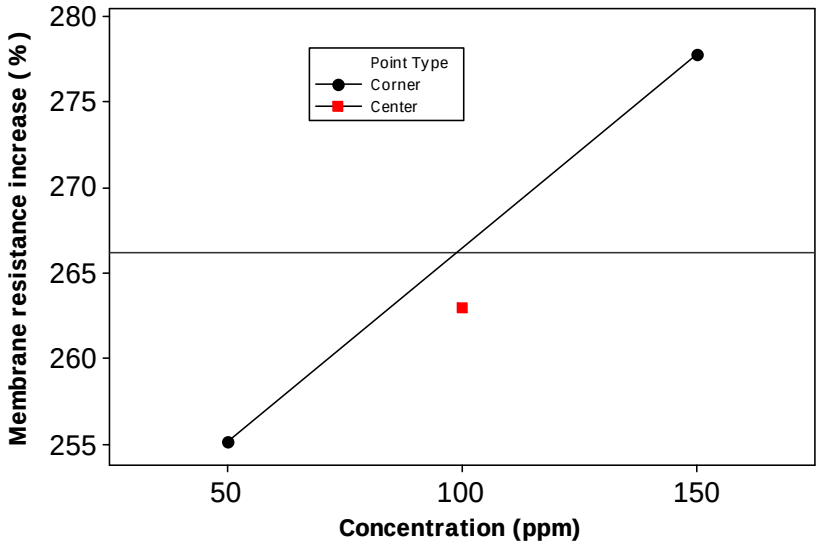

Figure 43. Average membrane resistance increase for experiments with high and low alginate concentrations.

4.4.2.3 Effect of changing the meat extract concentration on membrane fouling

Each two experiments with the same concentrations of all other artificial wastewater components and high or low meat extract concentrations (Table 30) were compared by their percentage of membrane fouling (Figure 44).

Changes in meat extract concentration had a great effect on membrane fouling. Experiments with high meat extract concentrations resulted in higher membrane fouling than experiments with low levels (Figure 45).

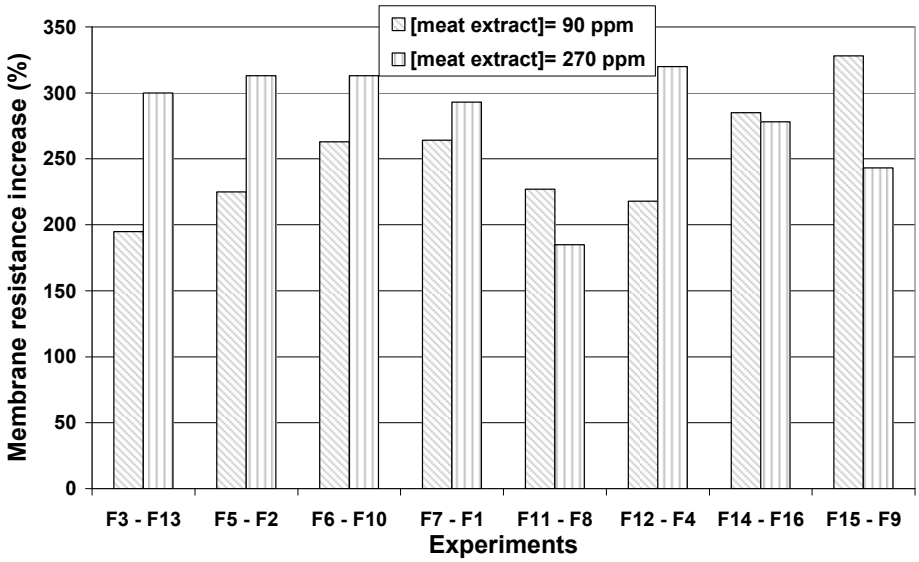

Figure 44. Equivalent wastewater experiments with high and low meat extract concentrations; membrane fouling results.

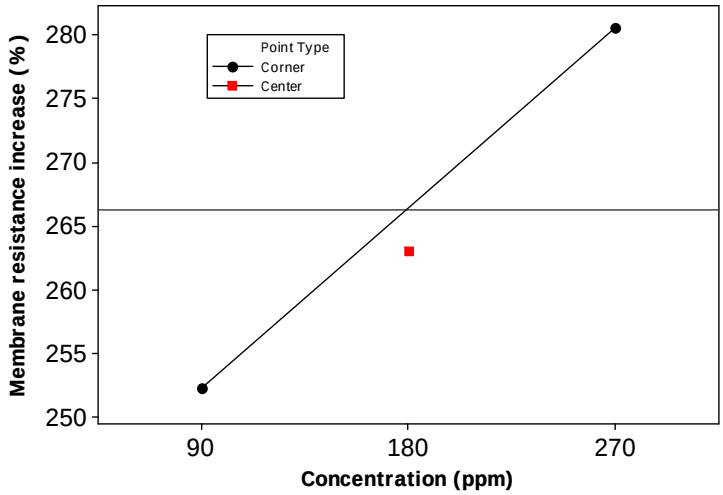

Figure 45. Average membrane resistance increase for experiments with high and low meat extract concentrations.

4.4.2.4 Effect of changing the peptone concentration on membrane fouling

Each two experiments with the same concentrations of all other artificial wastewater components and high or low peptone concentrations (Table 31) were compared by their percentage of membrane fouling (Figure 46).

The changes in peptone concentration affected the membrane fouling. High concentration levels of peptone resulted in higher membrane fouling. Nevertheless, the effect of the different concentration levels of peptone on membrane fouling was less than the effects of the meat extract, sodium alginate and calcium on the fouling of the membrane (Figure 47).

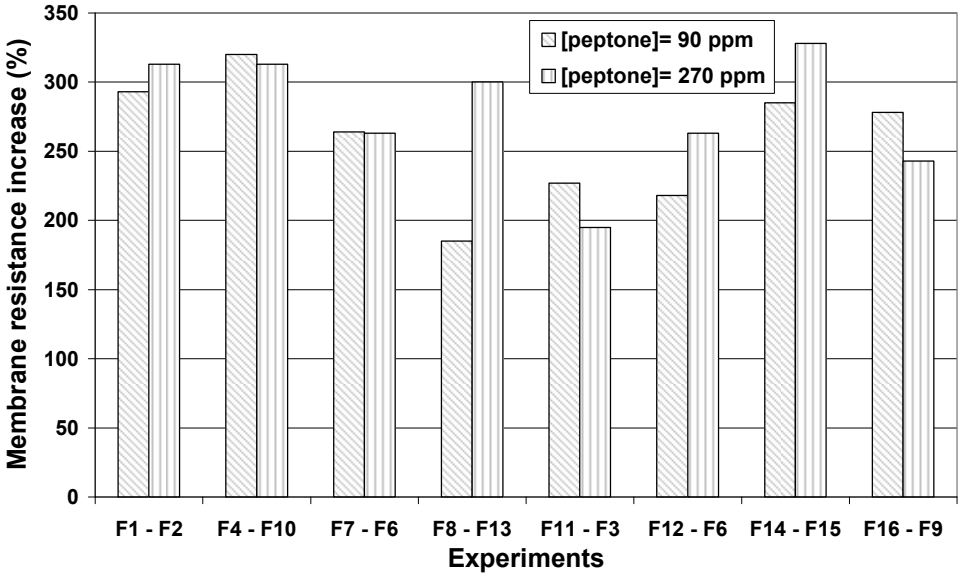

Figure 46. Equivalent wastewater experiments with high and low peptone concentrations; membrane fouling results.

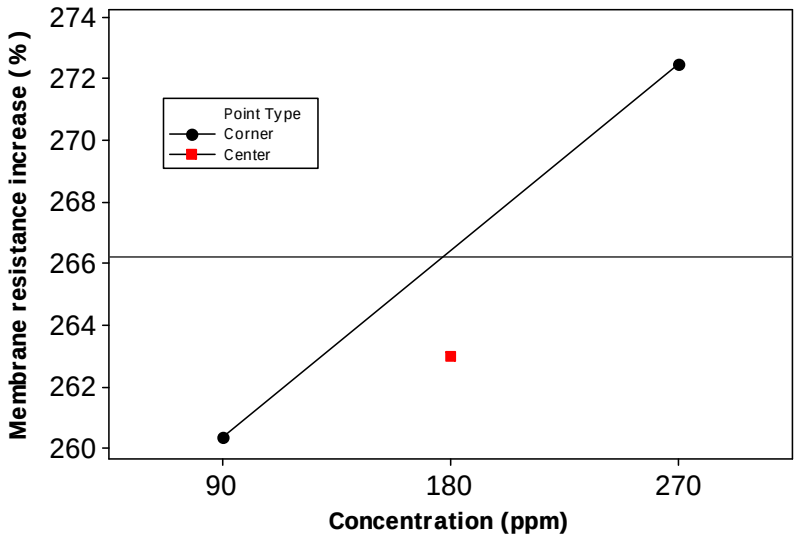

Figure 47. Average membrane resistance increase for experiments with high and low peptone concentrations.

4.4.3 Component interaction effects for 20 kDa ultrafiltration membrane wastewater experiments

4.4.3.1 Calcium chloride interactions with other main wastewater components

In general, increasing the calcium concentration increased the membrane fouling at the same concentration level for all the other components considered in this study. Nevertheless, the interaction between calcium and each other individual component was different. In the cases of high and low concentrations of peptone (Figure 48) and meat extract at low calcium concentration (Figure 49). The membrane fouling was almost the same for the high and the low concentration of both components; moreover, there was an increase in membrane fouling at the high concentration level of calcium. Although there was not a large difference between high and low concentrations of peptone and meat extract at the high calcium concentration.

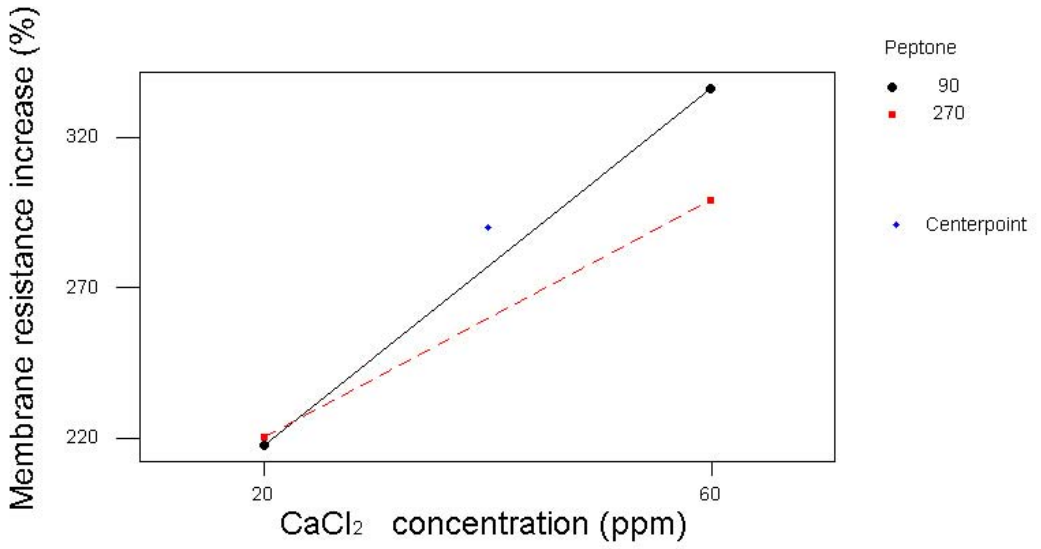

Figure 48. Calcium-peptone interaction effect on 20 kD ultramembrane fouling.

In contrast, a clear change in the membrane fouling was seen for experiments with high sodium alginate concentrations (Figure 50). At high alginate concentrations, the high calcium concentration level nearly doubled the

membrane fouling. Furthermore, at low alginate concentrations, the change in calcium concentration level had a very minor effect on membrane fouling.

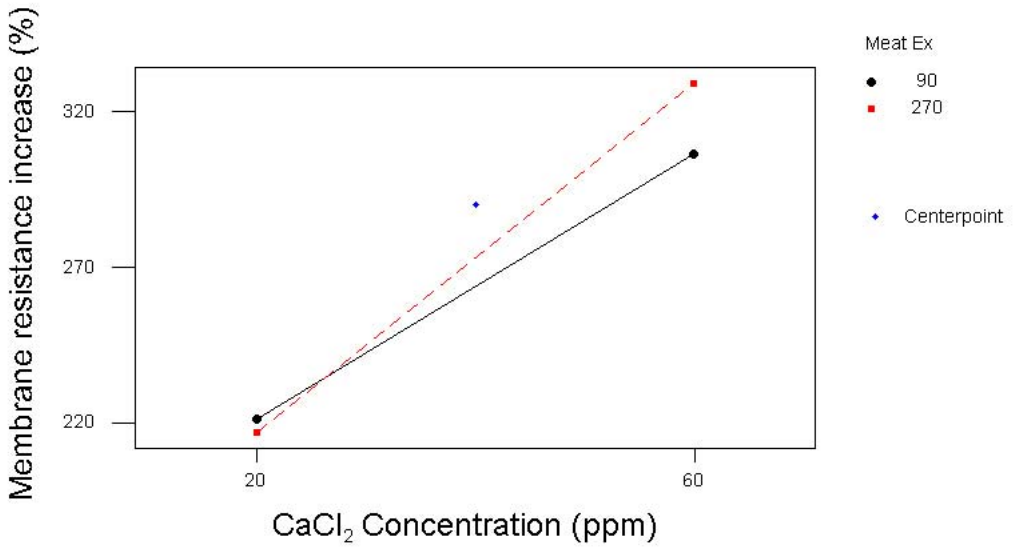

Figure 49. Calcium-meat extract interaction effect on 20 kD ultramembrane fouling.

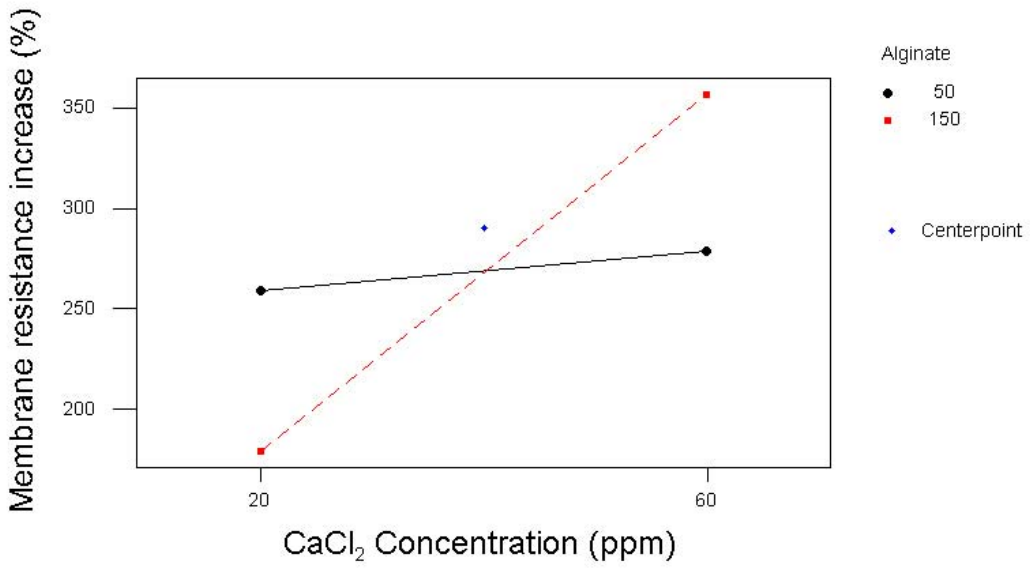

Figure 50. Calcium-alginate interaction effect on 20 kD ultramembrane fouling.

4.4.3.2 Sodium alginate interaction with other main wastewater components

At high alginate concentrations, membrane fouling was the same at both high and low peptone concentrations (Figure 51). Furthermore, the change in membrane fouling was very small (around 15%) at different peptone and alginate concentrations, indicating a minor or no interaction between peptone and sodium alginate.

There was a low interaction between alginate and meat extract (Figure 52). At high meat extract concentrations, the membrane fouling was reduced by about 27% with increased alginate concentration. However, the opposite was true for low meat extract concentration; here, membrane fouling increased by 27% with increased alginate concentration.

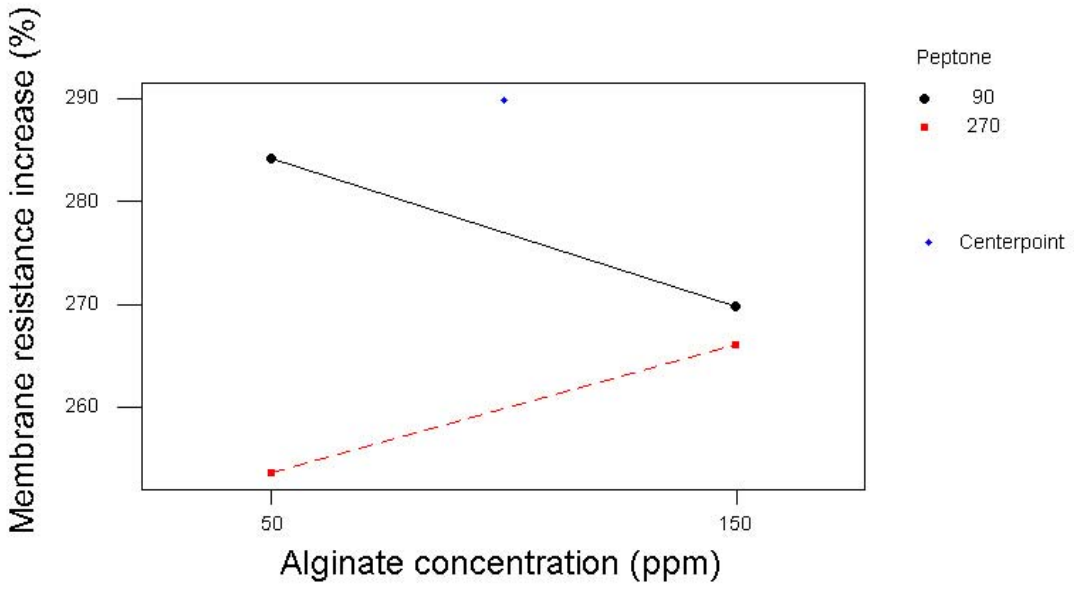

Figure 51. Alginate-peptone interaction effect on 20 kD ultramembrane fouling.

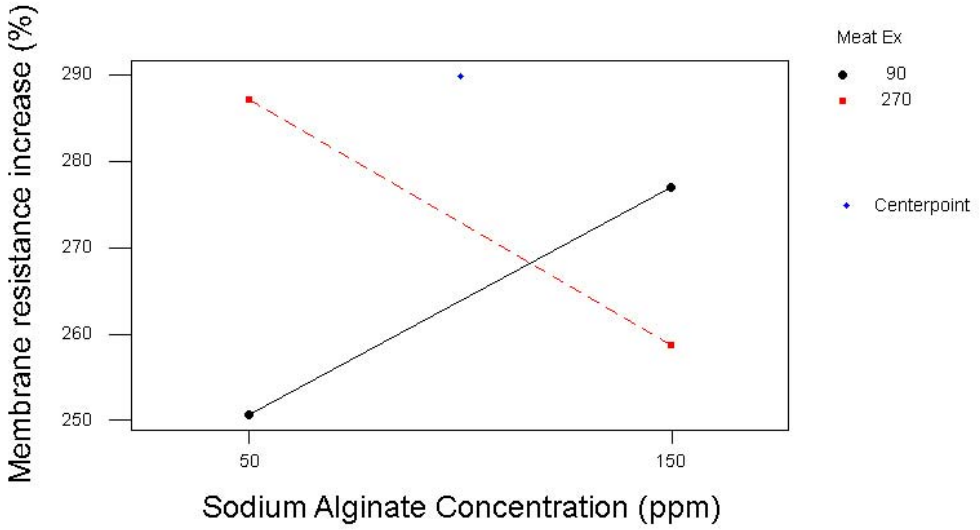

Figure 52. Alginate-meat extract interaction effect on 20 kD ultramembrane fouling.

4.4.3.3 Meat extract interaction with other main wastewater components

There was almost no interaction effect on membrane fouling observed with the change in meat extract concentration at the low peptone level (Figure 53).

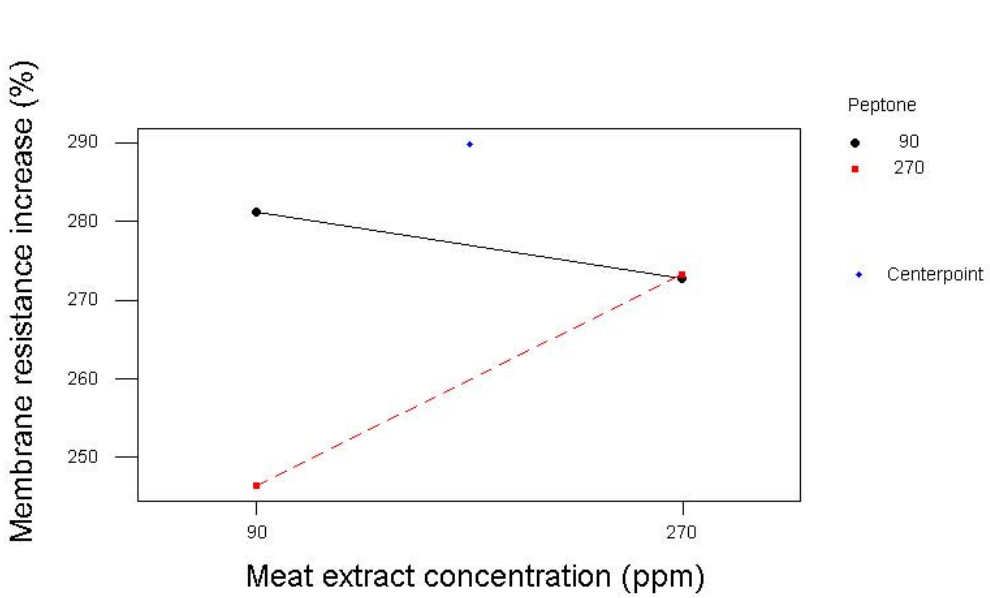

Figure 53. Meat extract-peptone interaction effect on 20 kD ultramembrane fouling.

Different peptone concentrations did not yield noticeable changes in membrane fouling at the high level of meat extract. At the low meat extract level, experiments performed with low peptone concentration increased the membrane fouling more (33% on average) than experiments conducted with the high peptone level.

4.4.4 Component interaction effects for 5 kDa ultrafiltration membrane wastewater experiments

4.4.4.1 Peptone interaction with other main wastewater components

The interaction of peptone with the other three components in this study was almost the same. Generally, higher membrane fouling was seen with higher peptone and meat extract, sodium alginate and calcium concentration levels (Figures 54, 55 and 56, respectively). At low meat extract concentration and at high alginate concentration the fouling of the membrane was the same for high and low peptone levels.

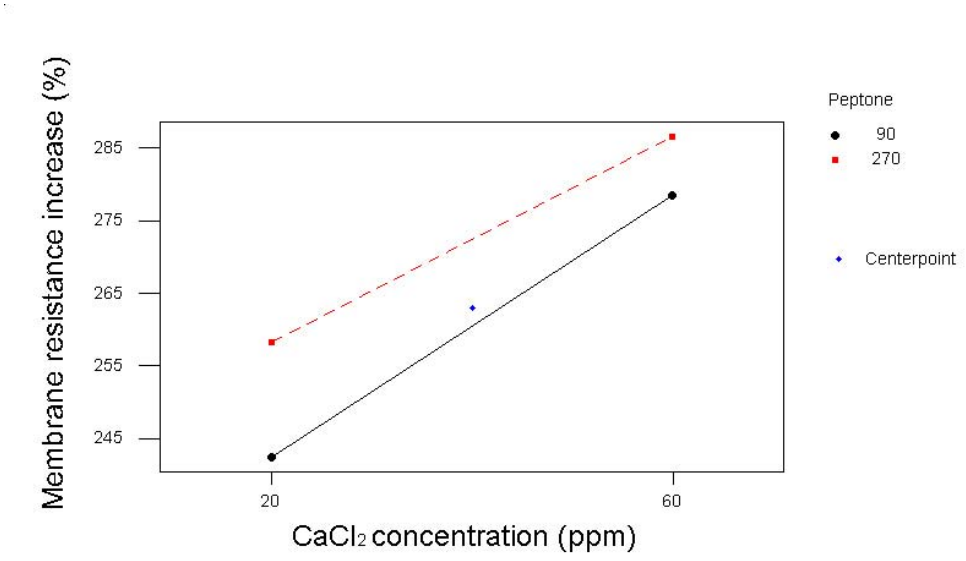

Figure 54. Calcium-peptone interaction effect on 5 kD ultramembrane fouling.

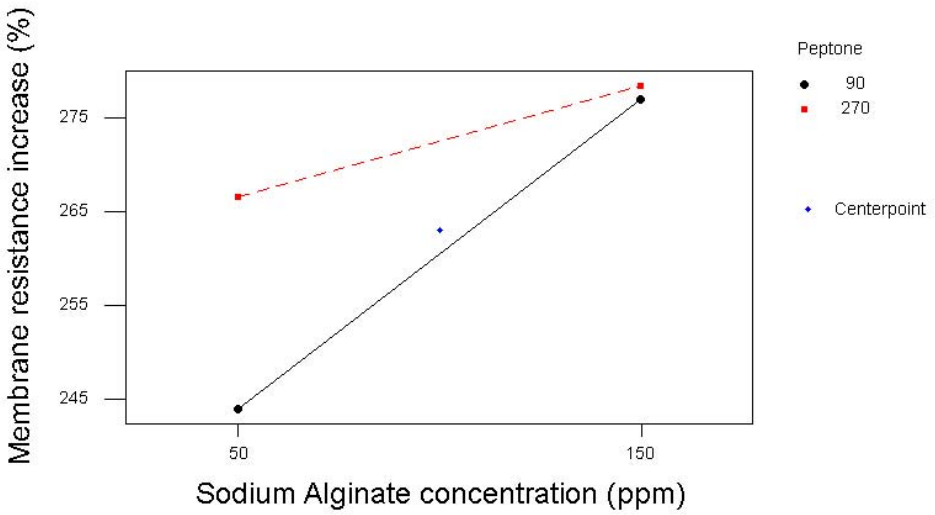

Figure 55. Alginate-peptone interaction effect on 5 kD ultramembrane fouling.

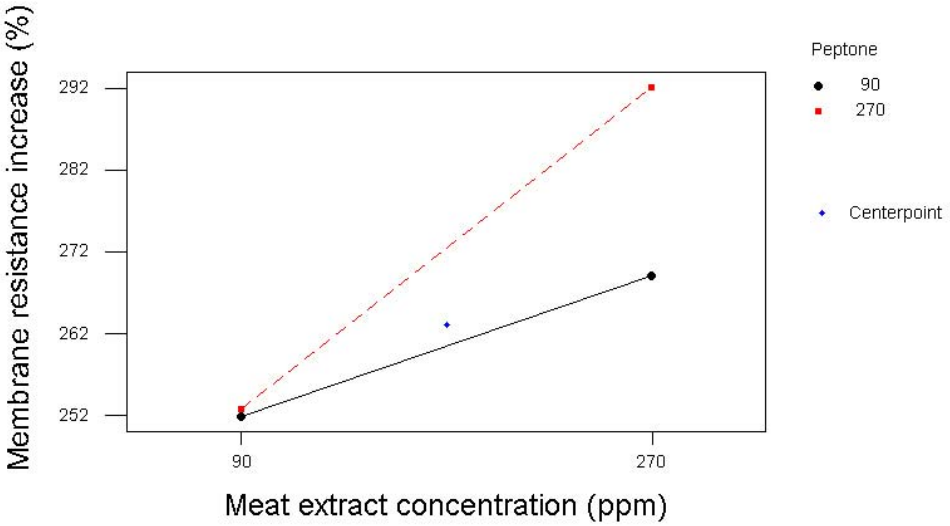

Figure 56. Meat extract-peptone interaction effect on 5 kD ultramembrane fouling.

4.4.4.2 Sodium alginate interaction with other main wastewater components

The interaction between sodium alginate and calcium is very interesting. A large difference in membrane fouling level can be seen between experiments with high and low alginate concentrations when the calcium concentration is

low (Figure 57). However, at high calcium concentration no effect of different alginate concentration on membrane fouling level can be seen.

No noticeable interaction effect on membrane fouling was observed between meat extract and alginate at low alginate levels (Figure 58). Nevertheless, at high alginate concentrations, high meat extract concentration increased the membrane fouling by around 60% on average over experiments conducted with the low meat extract level.

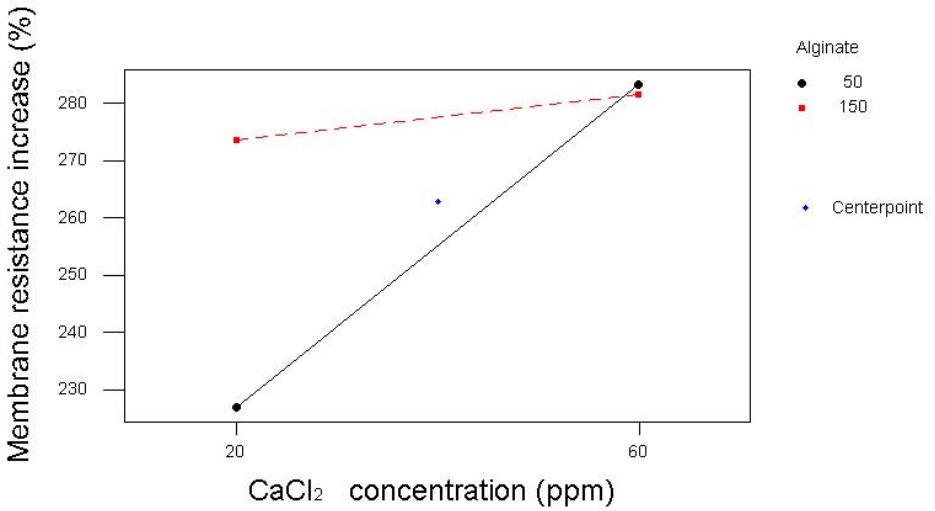

Figure 57. Alginate-calcium interaction effect on 5 kD ultramembrane fouling.

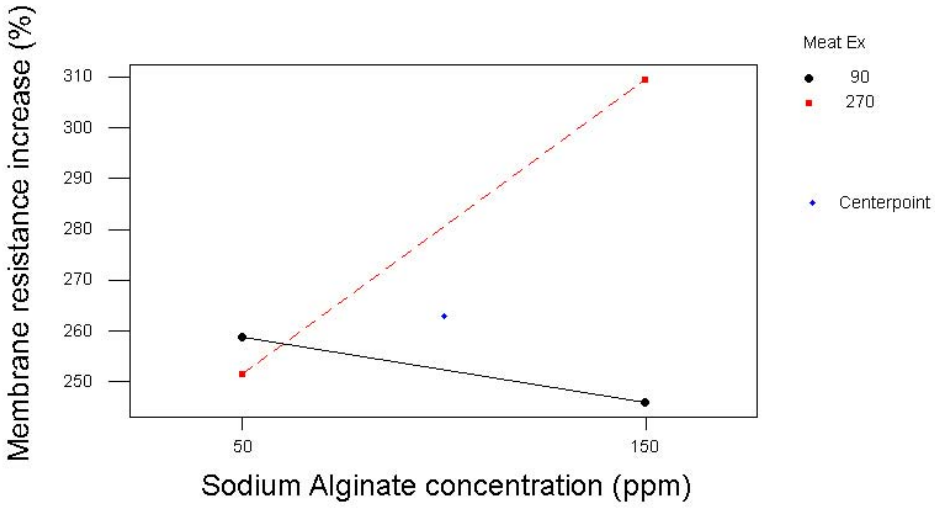

Figure 58. Alginate-meat extract interaction effect on 5 kD ultramembrane fouling.

4.4.4.3 Meat extract interaction with other main wastewater components

In case of the meat extract and calcium interaction, higher fouling of the membrane was observed with high meat extract concentration than with low meat extract concentration at the same calcium concentration (Figure 59). However, the membrane fouling difference was less for both high and low meat extract levels at high calcium concentration. Furthermore, the membrane fouling level for experiments with high meat extract concentrations and low calcium concentrations were the same as in experiments with high meat extract concentrations and high calcium concentrations.

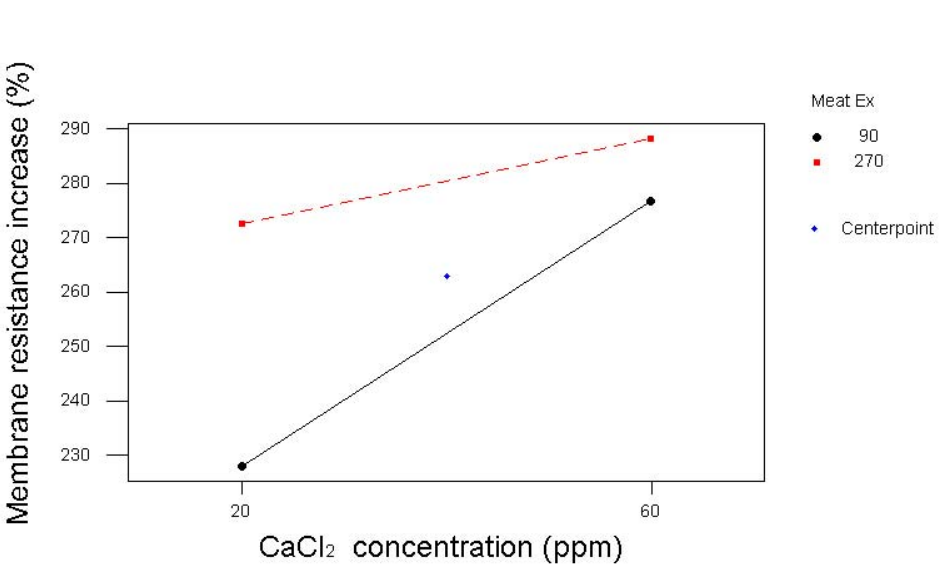

Figure 59. Meat extract-calcium interaction effect on 5 kD ultramembrane fouling.

4.5 Effect of artificial wastewater components on fouling reversibility

4.5.1 Dead end stirred cell ultrafiltration experiments

Sodium alginate solutions at a concentration of 300 mg/L with different Ca^{++} concentrations (5, 10, 15, 20 and 25 mg/L) were filtered in the stirred cell ultrafiltration unit using a 10000 Dalton MWCO disc membrane and the filtrate solution was analysed for free Ca^{++} concentration. Comparing the concentration of the Ca^{++} in the filtrate to the initial feed concentration, Figure 61 shows that almost all the calcium cations were absorbed by the alginate in the 20, 40, and 60 mg/L calcium chloride dihydrate solutions used in experiments 1, 2 and 3, respectively (Figure 60). For the 80 and 100 mg/L $CaCl_2 \cdot 2H_2O$ solutions, 12% and 14%, respectively, of the initial Ca^{++} cations passed through the membrane into the filtrate solution.

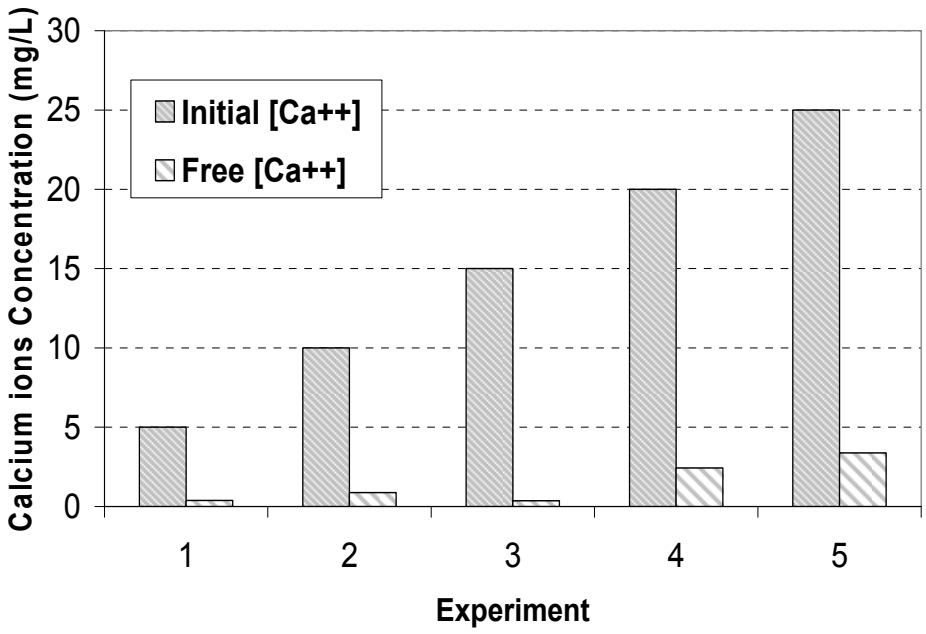

Figure 60. Initial concentration of calcium ions in the sodium alginate-calcium solution and remaining free calcium ions in the filtrate.

Five solutions containing meat extract at a concentration of 300 mg/L and different Ca^{++} concentrations (4.94, 9.87, 14.81, 19.74 and 24.68 mg/L) were

filtered in the stirred cell ultrafiltration unit using a 1000 Dalton disc membrane filter. The filtrates were analysed for Ca^{++} concentration using atomic absorption spectroscopy.

Unlike in the alginate case, there was no complete absorption of calcium cations by the meat extract. On average, 50% of the total feed calcium was absorbed regardless of the different starting concentrations (Figure 61).

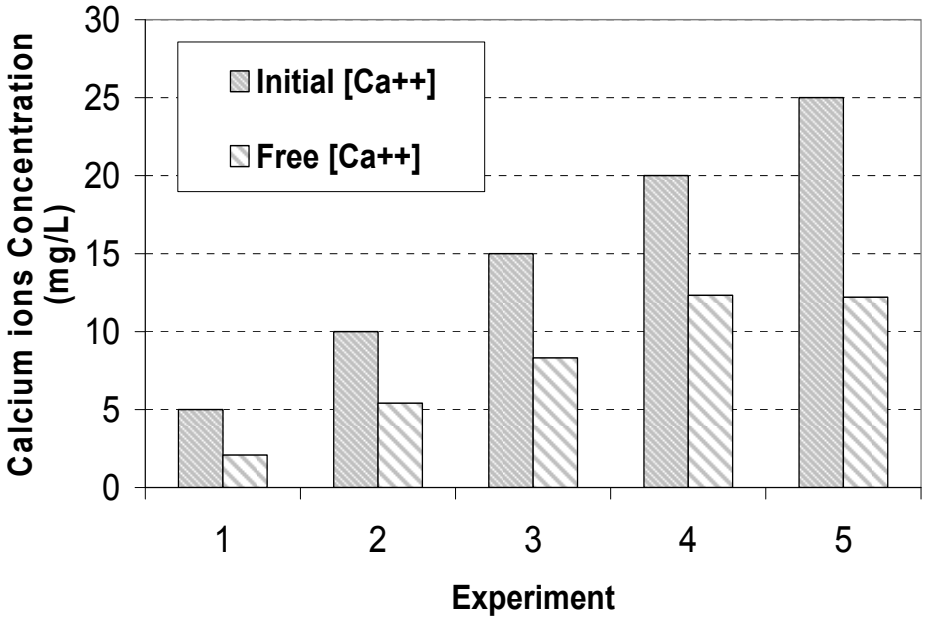

Figure 61. Initial concentration of calcium ions in the meat extract-calcium solution and remaining free calcium ions in the filtrate.

4.5.2 Binary crossflow ultrafiltration experiments

The increase in membrane resistance for the two experiments with high calcium concentrations (15 mg/L) was the highest among all the five experiments performed. In the experiment with the highest resistance increase, alginate was present at a low concentration (50 mg/L), while in the experiment with the second highest resistance increase, alginate was present at a high concentration (150 mg/L; Figure 62). This behaviour supports the postulate of a bridging effect of calcium on proteins and polysaccharides, the

hypothesis proposed by Katsoufidou *et al*. (2007). Furthermore, the calcium to alginate ratio was an important indicator of fouling level. The highest membrane fouling was observed at a high $[Ca^{++}]$/[alginate] ratio of 0.3, while the lowest membrane fouling was observed at the low $[Ca^{++}]$/[alginate] ratio of 0.03. For the remaining three experiments, which registered intermediate membrane fouling levels, the $[Ca^{++}]$/[alginate] ratio was 0.1. The order of solutions from the highest to the lowest fouling in these experiments was 150, 100 and 50 mg/L alginate. It is clear that when the $[Ca^{++}]$/[alginate] ratio was the same, experiments with higher alginate concentration fouled the membrane more.

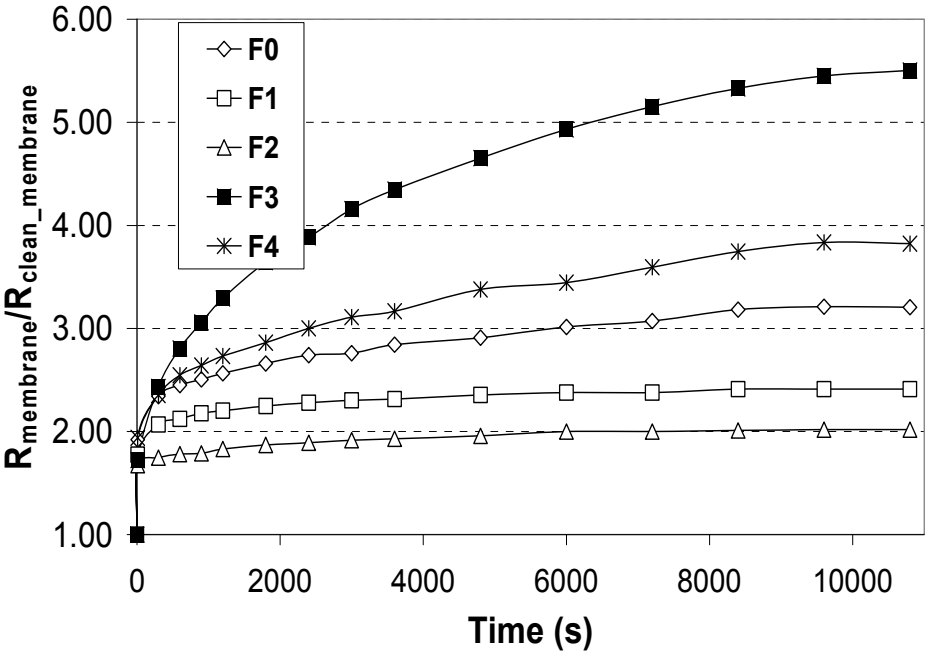

Figure 62. The increase of membrane resistance during alginate–calcium crossflow filtration experiments (F0: [Alginate]=100 ppm, $[Ca^{++}]$=10 ppm; F1: [Alginate]=50 ppm, $[Ca^{++}]$=5 ppm; F2: [Alginate]=150 ppm, $[Ca^{++}]$=5 ppm; F3: [Alginate]=50 ppm, $[Ca^{++}]$=15 ppm; F4: [Alginate]=150 ppm, $[Ca^{++}]$=15 ppm).

In contrast to the alginate-calcium experiments, the $[Ca^{++}]$/[meat extract] ratio was not the key factor in controlling the level of membrane fouling in this experimental set. Experiments with high concentrations of meat extract and Ca^{++} registered the highest increase in membrane resistance. Furthermore, the experiment with low concentrations of both meat extract and Ca^{++} gave the lowest rise in membrane resistance (Figure 63).

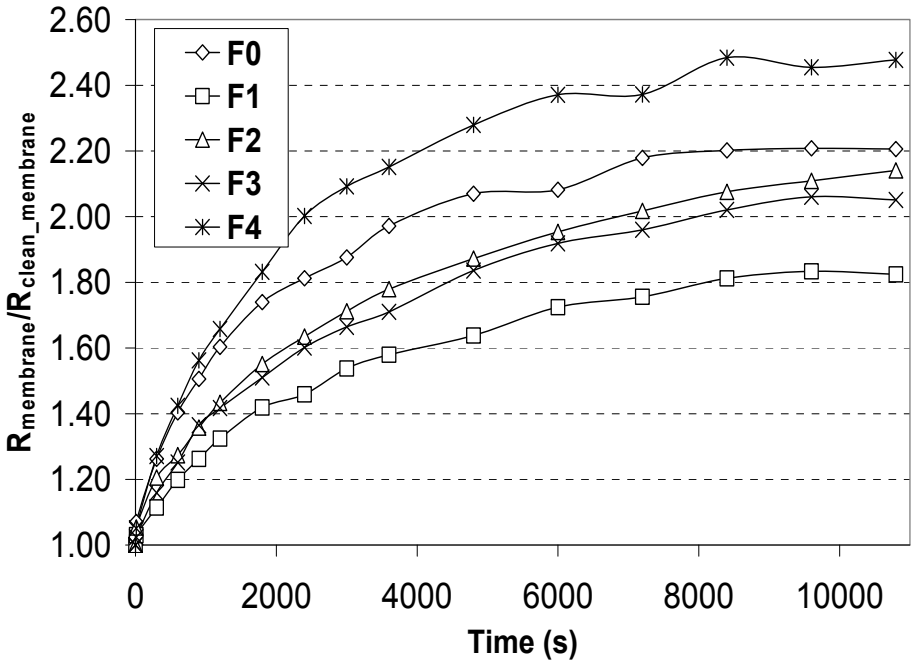

Figure 63. The increase of membrane resistance during meat extract–calcium crossflow filtration experiments (F0: [Meat Ex.]=180 ppm, [Ca^{++}]=10 ppm; F1: [Meat Ex.]=90 ppm, [Ca^{++}]=5 ppm; F2: [Meat Ex.]=270 ppm, [Ca^{++}]=5 ppm; F3: [Meat Ex.]=90 ppm, [Ca^{++}]=15 ppm; F4: [Meat Ex.]=270 ppm, [Ca^{++}]=15 ppm).

Toward the end of each experiment the permeate flux was at steady state. In experiment F2 (Table 32), with the lowest calcium to alginate ratio of 0.03, 35% of the membrane fouling at steady state was due to reversible fouling and 65% was due to irreversible fouling. For the rest of the experiments the reversible fouling was between 5–7% (Figure 64). Very low calcium to alginate ratios resulted in an increased percentage of reversible fouling relative to total membrane fouling. The increase in reversible fouling translates into a lower chemical cleaning requirement and a higher membrane resistance recovery.

Table 32. Alginate-calcium/meat extract-calcium experiments factorial design matrix.

Experiment	Alginate/Meat extract (mg/L)	Calcium (mg/L)
F0	100 / 180	10
F1	50 / 90	5
F2	150 / 270	5
F3	50 / 90	15
F4	150 / 270	15

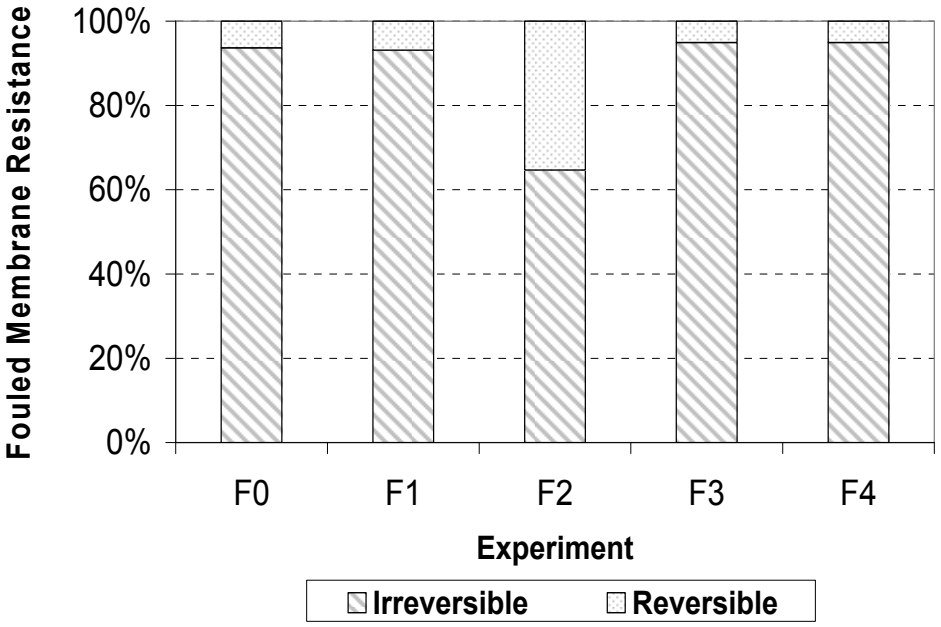

Figure 64. Types of membrane fouling at steady state permeate flux in alginate–calcium crossflow filtration experiments.

In general, for the meat extract and calcium experiments, 28 – 44% of the membrane fouling was reversible fouling (Figure 65). However, there was no clear relationship between the percentage of reversible fouling and either meat extract or calcium concentrations or the meat extract to calcium ratio.

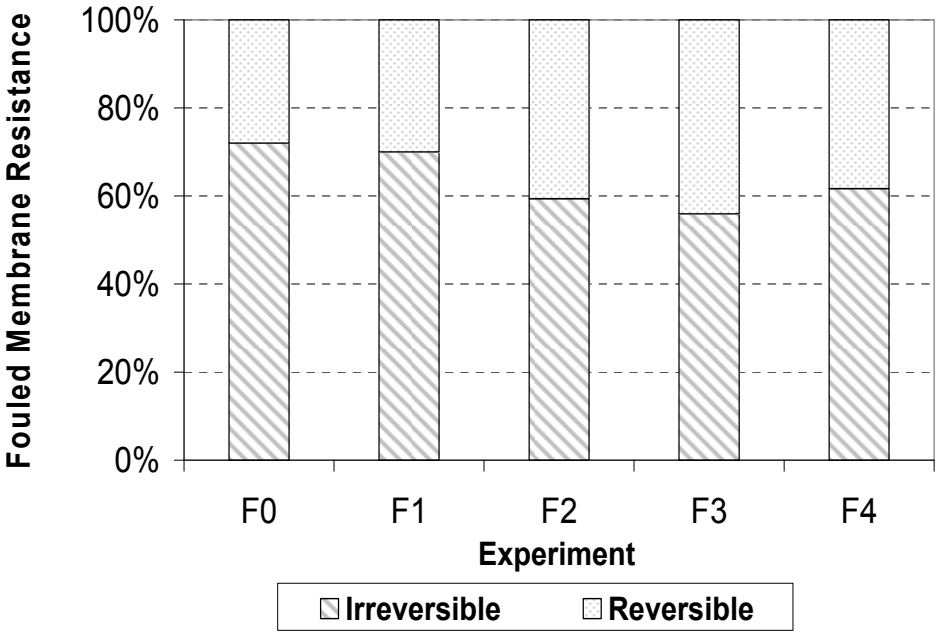

Figure 65. Types of membrane fouling in meat extract crossflow filtration experiments.

The artificial wastewater solution fouled the membrane more on average than fouling by either alginate-calcium or meat extract-calcium solutions (Figure 66). This finding is in agreement with other studies of the fouling behaviour of individual and mixed polysaccharide and protein solutions (Ye *et al.* 2005; Susanto *et al.* 2008). Fouling reversibility for the artificial wastewater was comparable to that of the meat extract-calcium binary solution (Figure 67). When comparing the reversible fouling for the three solutions (34%, 12% and 36% for wastewater, alginate-calcium and meat extract-calcium, respectively), the alginate-calcium solution caused the highest irreversibility among the three solutions (Table 33), which may be due to the “egg-box” structure of the alginate-calcium complex and its deposition on and interaction with the membrane surface.

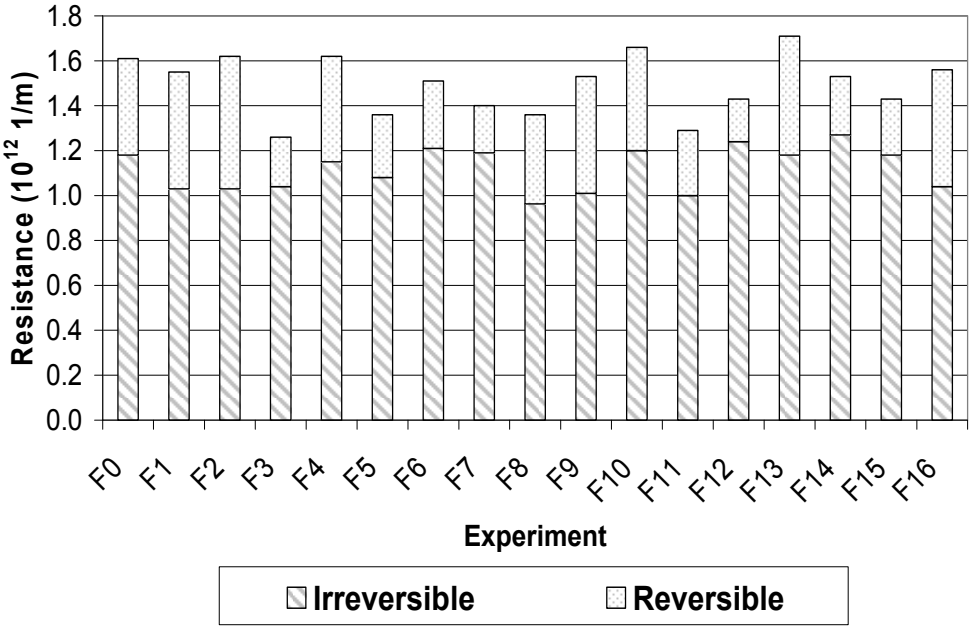

Figure 66. Absolute membrane total resistance increase for artificial wastewater experiments.

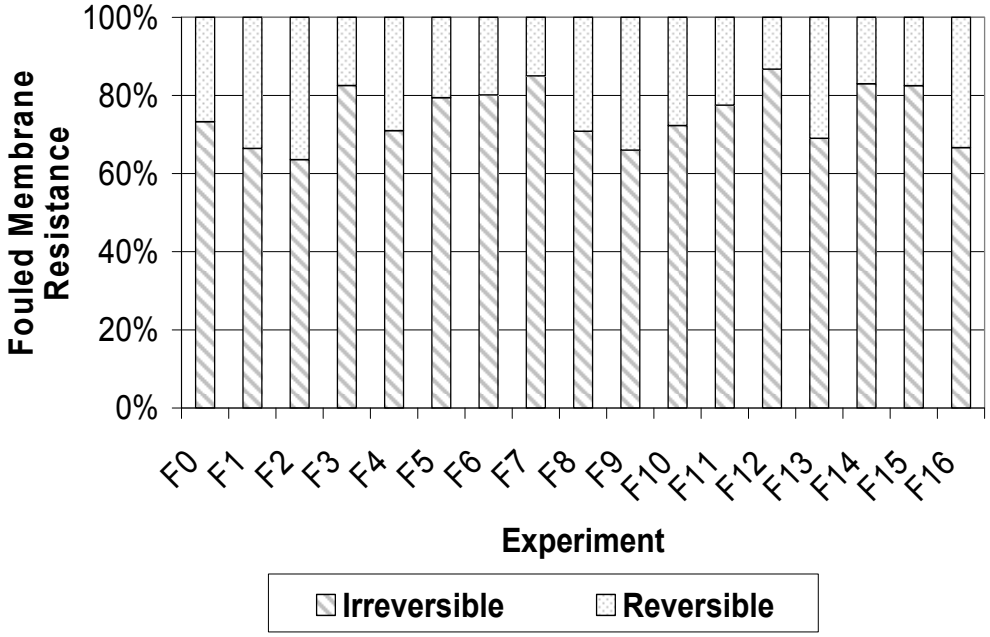

Figure 67. Reversible and irreversible fouling for the artificial wastewater ultrafiltration experiments.

Table 33. Range and average for total and reversible membrane resistance increase for the wastewater, alginate-calcium and meat extract-calcium experiments.

Feed Mixture	Total Membrane Resistance Increase (%)		Reversible Membrane Resistance (%)	
	Range	Average	Range	Average
Artificial Wastewater	185-328	265	13-36	34
Alginate-Calcium	102-452	239	5-35	12
Meat extract-Calcium	83-148	114	28-44	36

4.6 Membrane cleaning

In this study the cleaning solution used to clean the membrane after each artificial wastewater filtration experiments was changed from an industrial cleaning chemical Decon 90 to a cleaning mixture made in the lab from sodium hydroxide, hydrogen peroxide and Decon 90 in different concentrations.

In the early stages of the experiments design (the microfiltration scoping experiments and initial artificial wastewater ultra filtration experiments) the industrial cleaning chemical was used to cleaning the membrane. Nevertheless, the membrane resistance could not be restored to the initial clean membrane resistance even with increasing chemical agent concentration (Figure 68).

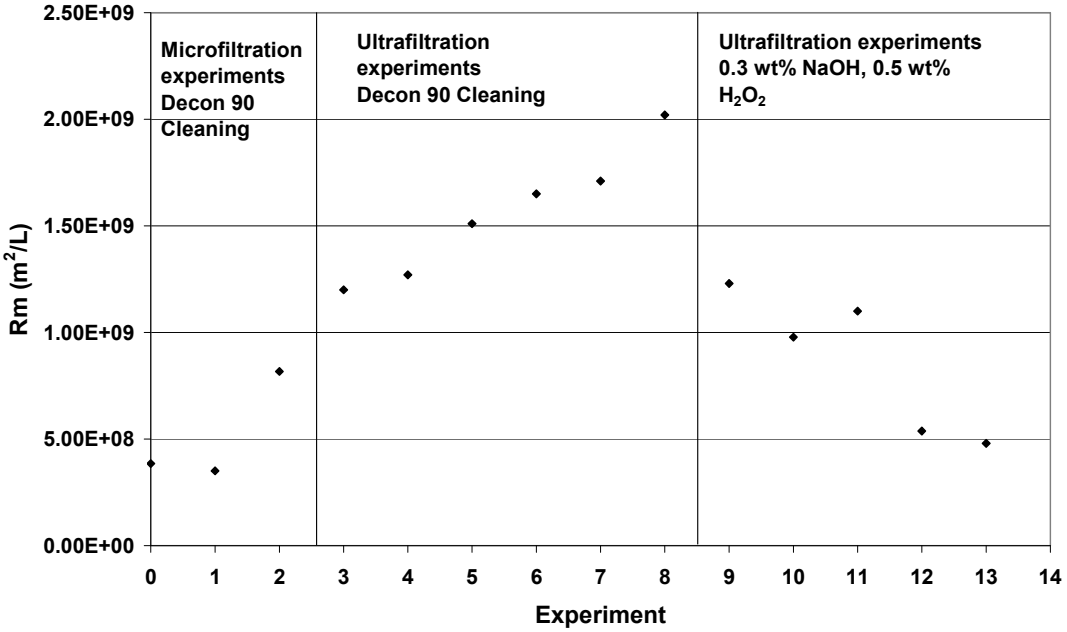

Figure 68 Membrane resistance changes after artificial wastewater filtration in scoping experimental stages for microfiltration and ultrafiltration membranes.

4.6.1 Cleaning recovery for 20 kD artificial wastewater Ultrafiltration experiments

The need to clean the membrane was critical in order to return the membrane resistance to the resistance of the clean membrane after each artificial wastewater filtration experiment. The effect of wastewater components concentration on membrane fouling can only be examined if the starting clean membrane resistance is the same.

In order to effectively clean the membrane cleaning solution was prepared in the lab adapting the chemicals cleaning mixture used by Gan *et al* (1999). A mixture made from 0.1-0.3 wt% NaOH, 0.7-0.1 wt% H_2O_2 and 0-50 ml Decon 90 in Millipore ultrapure water (Table 34).

Table 34 Artificial wastewater 20 kD ultrafiltration membrane cleaning results.

Run	NaOH (g)	H_2O_2 (ml)	Deacon 90 (ml)	Temperature °C	Time (min)	Recovery (%)
F0	60	100	0	50	165.00	114
F1	50	150	50	50	90.00	108
F2	50	150	50	50	90.00	141
F3	50	150	0	50	80.00	103
F4	50	100	0	50	90.00	90
F5	43	150	25	50	90.00	109
F6	40	150	20	50	90.00	74
F7	40	150	20	50	150.00	97
F8	50	150	10	50	105.00	98
F9	50	150	10	50	90.00	102
F10	50	150	10	30	105.00	99
F11	50	100	10	30	90.00	98
F12	50	100	10	40	90.00	89
F13	50	150	10	40	100.00	106
F14	50	100	10	50	120.00	101
F15	50	150	10	50	120.00	106

The effect of the changes in the concentration of the cleaning solution chemical component cleaning temperature and time has been examined. The most noticeable effect is the change of sodium hydroxide concentration in the cleaning mixture. In general increasing the concentration of sodium hydroxide increased fouled membrane recovery (Figure 69).

Gan et al (1999) suggested that hydrolysis of polysaccharides and proteins at high pH played a very important part in the cleaning process, with the chemical reactions being:

Hydrolysis of polysaccharides:

$$\left[C_6H_{10}O_5\right]_n + nH_2O \xrightarrow{OH^-} nC_6H_{12}O_6$$

Hydrolysis of proteins:

$$RNH - C^{=O} - R' + H_2O \xrightarrow{OH^-} RNH_2 + HO - C^{=O} - R'$$

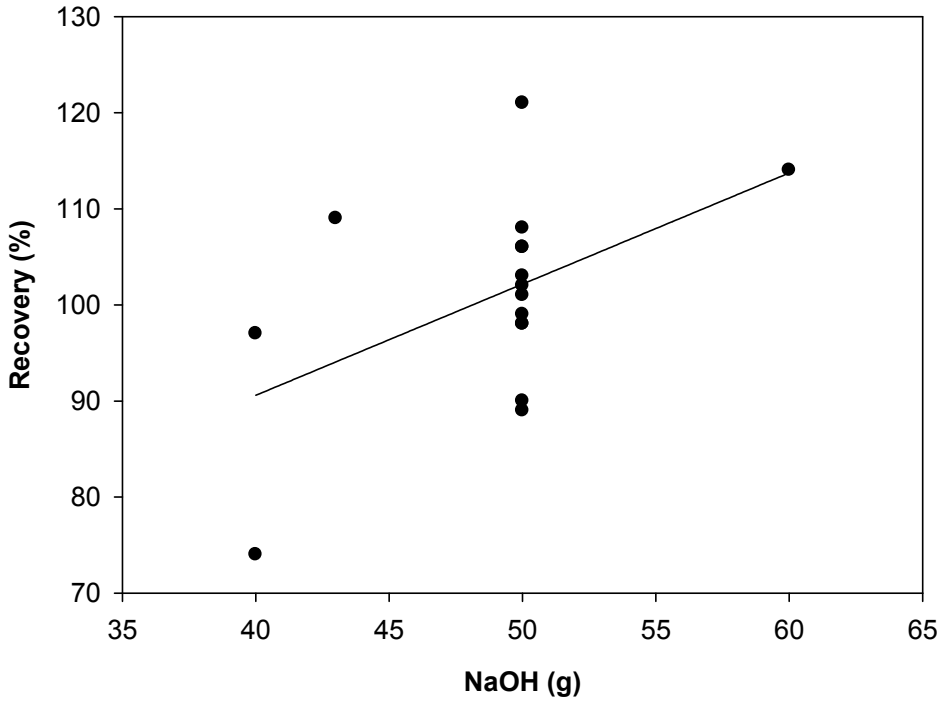

Figure 69 Effect of increasing NaOH concentration on 20 kD membrane recovery (line is for guidance).

The changes in hydrogen peroxide concentration did not have noticeable effect on the 5 kD membrane recovery. The average recovery for experiments cleaned with 100 ml hydrogen peroxide was almost the same as the average recovery for experiments cleaned with 150 ml hydrogen peroxide (
Figure 70).

Increasing the concentration of Decon 90 in the cleaning solution increased the average membrane recovery. On average the recovery obtained for experiments cleaned with 50 ml of Decon 90 was higher than experiments cleaned with lower amount of Decon 90 or no Decon 90 (Figure 71).

Changing the cleaning solution temperature between 30 to 50 °C did not have a strong effect on the membrane average recovery, although, higher

temperature cleaning resulted in better membrane recovery than low temperature cleaning (Figure 72).

Longer cleaning time gave a better membrane recovery on average than shorter cleaning time (Figure 73).

The best membrane cleaning result was obtained with increasing sodium hydroxide and Decon 90 concentration in the cleaning solution. Hydrogen peroxide, temperature, and time did not have a very strong effect on the membrane recovery.

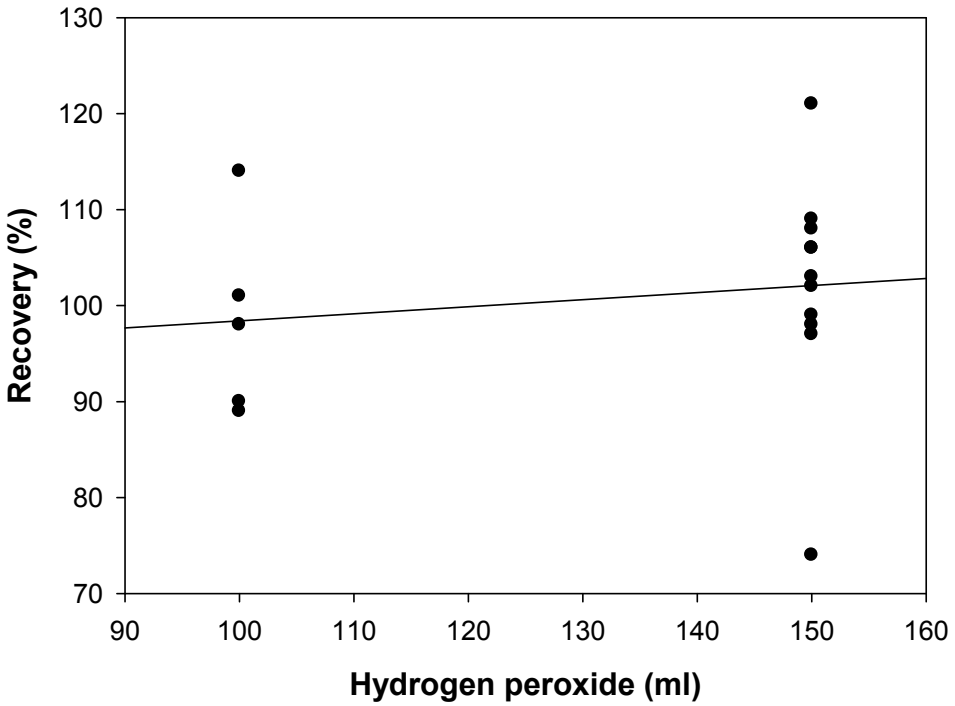

Figure 70 Effect of increasing H_2O_2 concentration on 20 kD membrane recovery (line is for guidance).

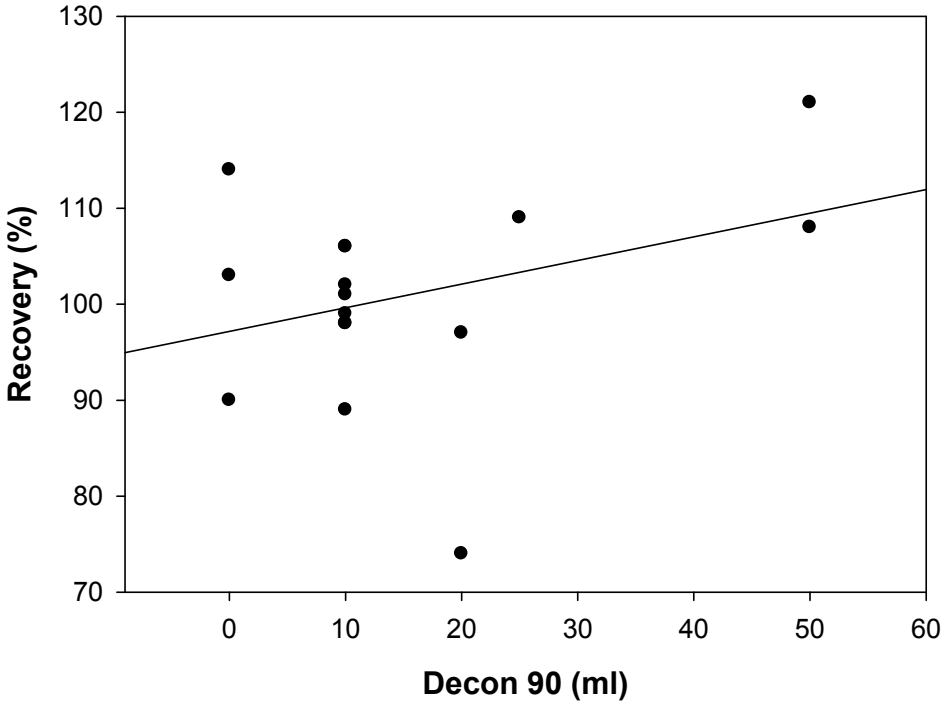

Figure 71 Effect of increasing Decon 90 concentration on 20 kD membrane recovery (line is for guidance).

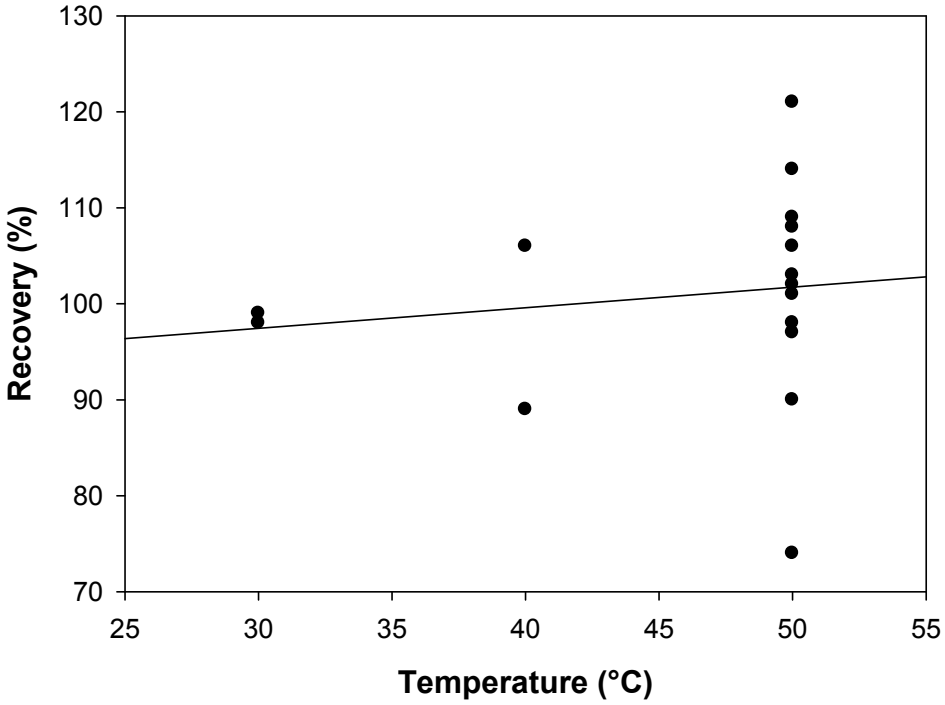

Figure 72 Effect of cleaning mixture temperature on 20 kD membrane recovery (line is for guidance).

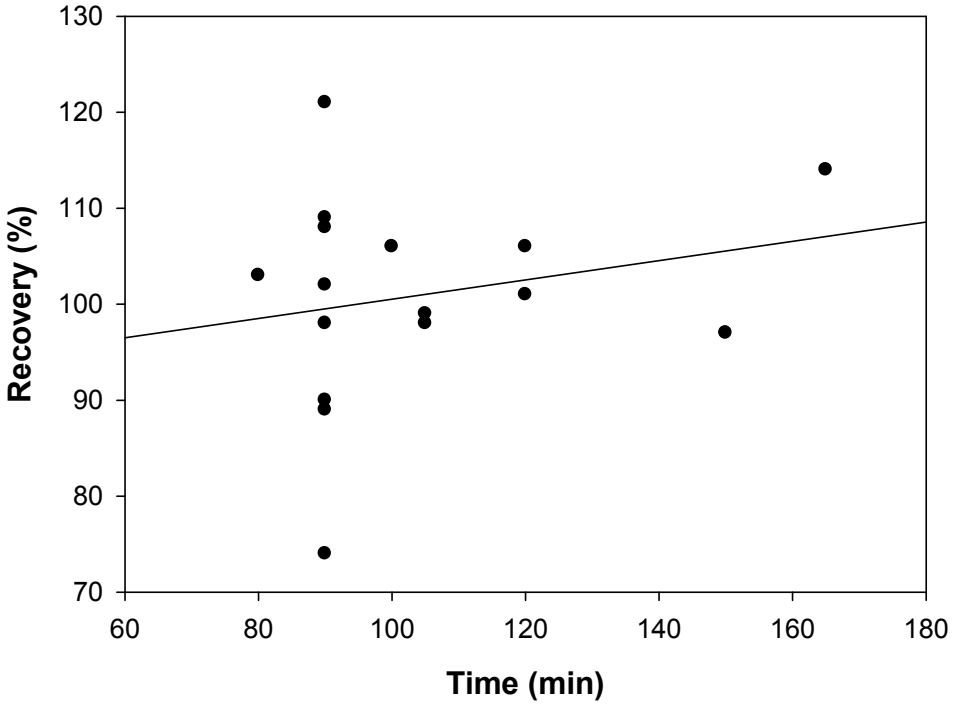

Figure 73 Effect of cleaning time on 20 kD membrane recovery (line is for guidance).

4.6.2 Cleaning recovery for 5 kD artificial wastewater Ultrafiltration experiments

The effect of changing the concentration of the cleaning solution chemicals components such sodium hydroxide and hydrogen peroxide, the cleaning temperature and cleaning time was examined. Decon 90 was not used in the cleaning of the 5 kD membrane (Table 35).

The effect of sodium hydroxide on the 5 kD membrane recovery was not as strong as its effect on the larger pore 20 kD membrane filter (Figure 74). Increasing the concentration of NaOH increased the recovery, however the increase was not as strong as the increase achieved by increasing the hydrogen peroxide (Figure 75), temperature (Figure 76) and time (Figure 77).

Table 35 Artificial wastewater 5 kD ultrafiltration membrane cleaning results.

Experiment	NaOH (g)	H_2O_2 (ml)	Decon 90 (ml)	Temperature (°C)	Time (min)	Recovery (%)
F0	20	20	0	45	120	104
F1	20	20	0	45	120	98
F2	20	20	0	45	110	95
F3	20	20	0	45	120	103
F4	15	15	0	45	90	98
F5	20	20	0	45	120	93
F6	20	20	0	40	105	99
F7	15	0	0	45	90	90
F8	25	50	0	50	120	107
F9	25	25	0	45	120	100
F10	20	20	0	45	120	103
F11	15	15	0	45	100	118
F12	20	20	0	50	120	103
F13	20	0.0	0	45	90	108
F14	20	0.0	0	45	90	83
F15	15	0.0	0	40	60	87

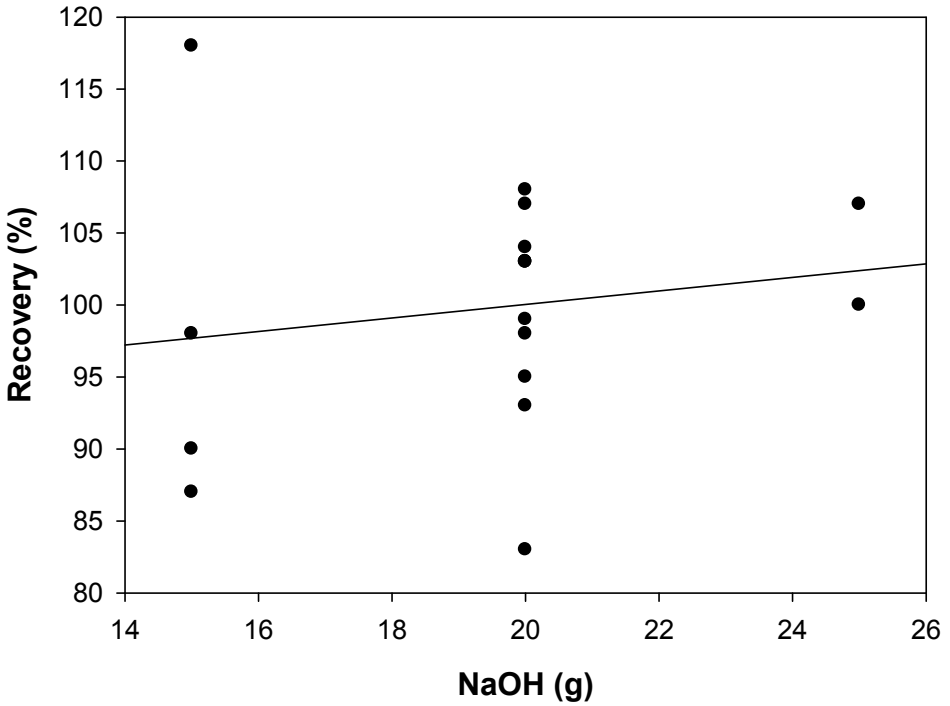

Figure 74 Effect of sodium hydroxide concentration on 5 kD membrane recovery.

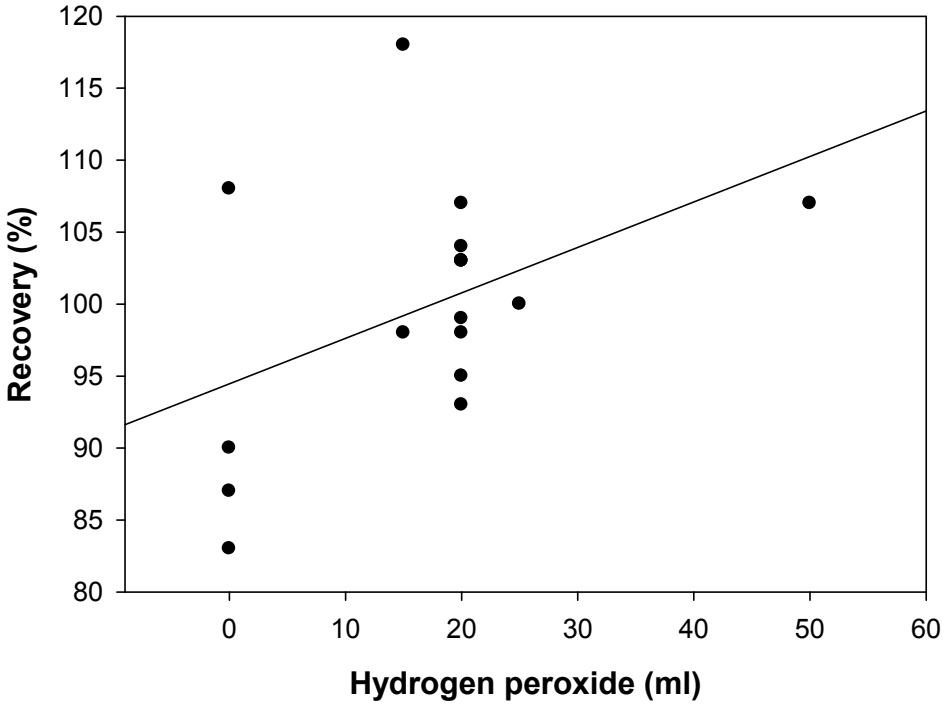

Figure 75 Effect of increasing H_2O_2 concentration on 5 kD membrane recovery.

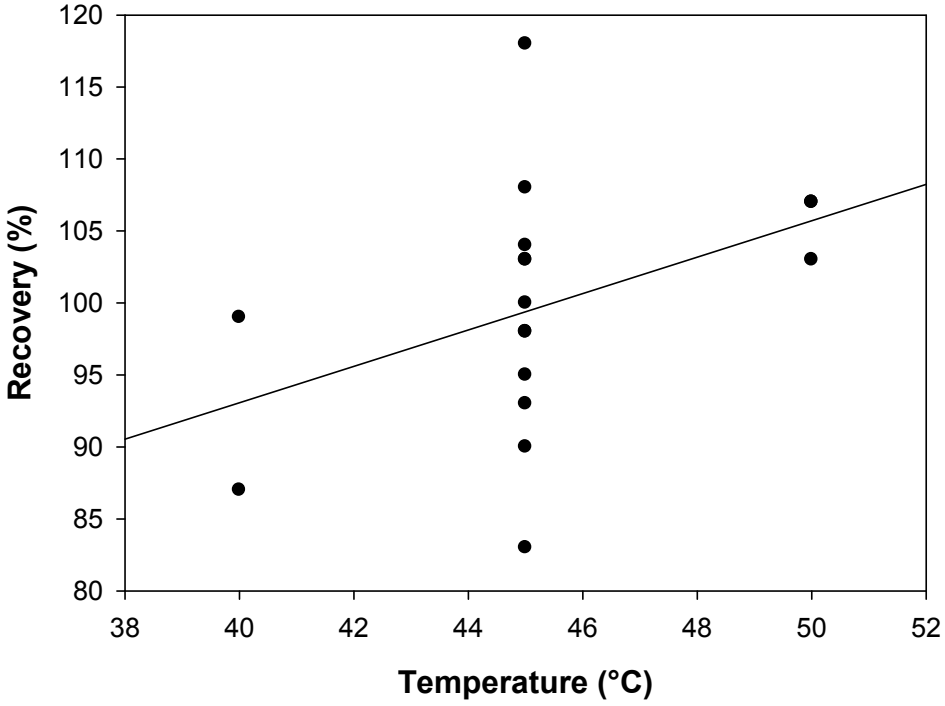

Figure 76 Effect of cleaning mixture temperature on 5 kD membrane recovery.

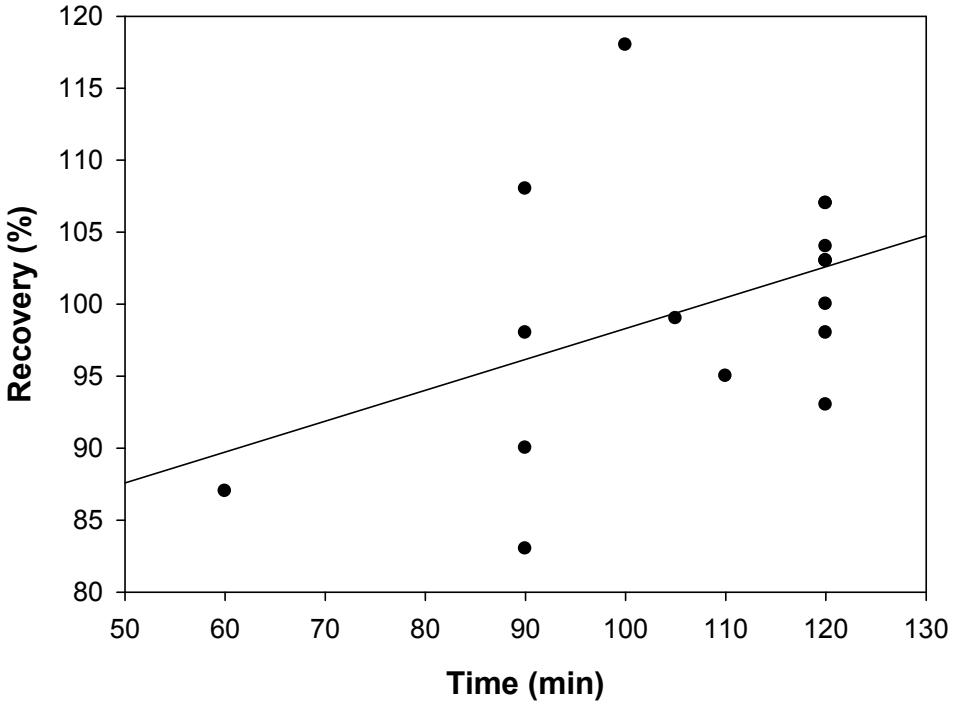

Figure 77 Effect of cleaning time on 5 kD membrane recovery.

5.0 MODELLING OF ULTRAFILTRATION DATA

5.1 Pore blocking model fitting of crossflow filtration experiments

In their work, Vela *et al* (2009) adapted Hermia's dead end filtration blocking models for crossflow filtration (Table 36) by accounting for foulant removal mechanisms. Vela *et al*. (2009) produced a modified general differential equation 5.1.

$$-\frac{dJ_p}{dt} = K_{CF}\left(J_p - J_{pss}\right)\cdot J_p^{2-n} \qquad (5.1)$$

where J_p and J_{pss} are the initial flux and steady state flux, respectively, K_{CF} is a constant depending on membrane blocked area per unit of permeate flux, permeate dynamic viscosity, TMP and membrane resistance. The value of the parameter *n* depends on the blocking mechanism as follows: cake filtration blocking (*n* = 0), intermediate (*n* = 1), complete blocking (*n* = 2) and standard blocking (*n* = 3/2).

Filtration experiment data for the meat extract-calcium binary mixture using the 5 kD membrane were fitted to the four blocking models using a Matlab® program routine (Appendix C). Further, data fitting was preformed using SigmaPlot® software package. The predictions of the fitted blocking models were compared to the experimental filtration data for the central experiment F1 and are presented in Figures 79 through 82.

The predictive accuracy of the model fitting was examined by comparing the coefficients of determination, R^2, for all the experiments (Table 37).

Apart from the standard blocking model, where the fitting accuracy was low, with an average R^2 value of 0.6436, all other blocking models had a high R^2 value. The highest R^2 value, and thus the best fitting model, was for the

intermediate blocking model with an average R^2 value of 0.9914. The complete blocking model and the cake filtration model were the second and third best fitting models, with R^2 values of 0.9769 and 0.9152, respectively (Table 37).

Table 36. Crossflow membrane filtration blocking model Vela *et al*. (2009).

Blocking model	n	Equation	constant
Complete	2	$J_p = J_{pss} + \left(J_o - J_{pss}\right)\cdot e^{-K_C J_o t}$	K_C
Intermediate	1	$J_p = \frac{J_o J_{pss} e^{K_i J_{pss} t}}{J_{pss} + J_o\left(e^{K_i J_{pss} t} - 1\right)}$	K_i
Standard	3/2	$J_p = \frac{J_o}{\left(1 + J_o^{1/2} K_s t\right)^2}$	K_s
Cake filtration	0	$t = \frac{1}{K_{gl} J_{pss}^2} \ln\left[\begin{array}{l}\left(\frac{J_p}{J_o}\frac{J_o - J_{pss}}{J_p - J_{pss}}\right) \\ - J_{pss}\left(\frac{1}{J_p} - \frac{1}{J_o}\right)\end{array}\right]$	K_{gl}

5.1.1 Blocking models fitting meat extract-calcium binary mixture filtration experiments

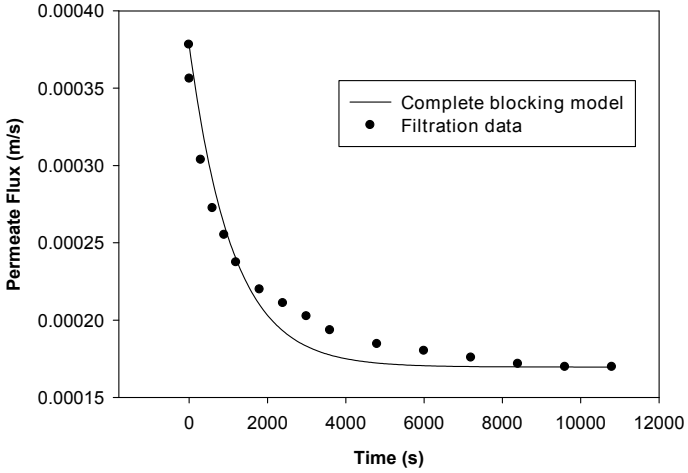

Figure 78. Complete blocking model fitting for F1 meat extract-calcium binary mixture 5 kD membrane filtration experiments.

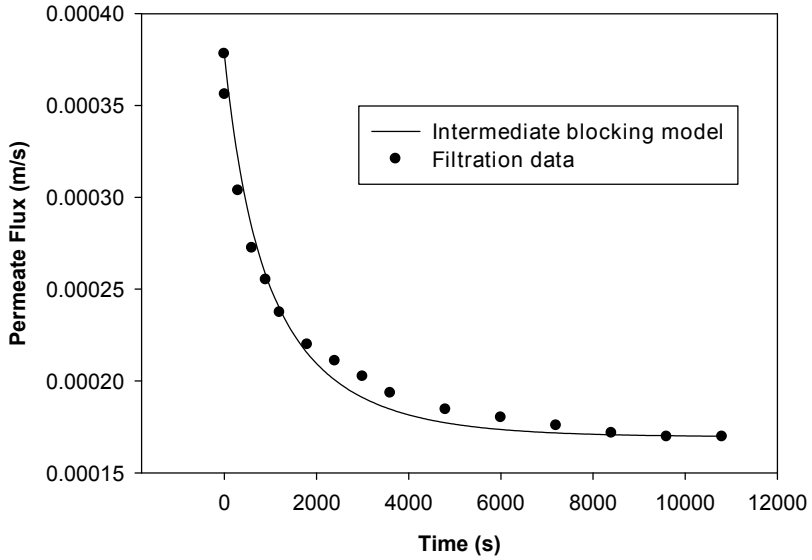

Figure 79. Intermediate blocking model fitting for F1 meat extract-calcium binary mixture 5 kD membrane filtration experiments.

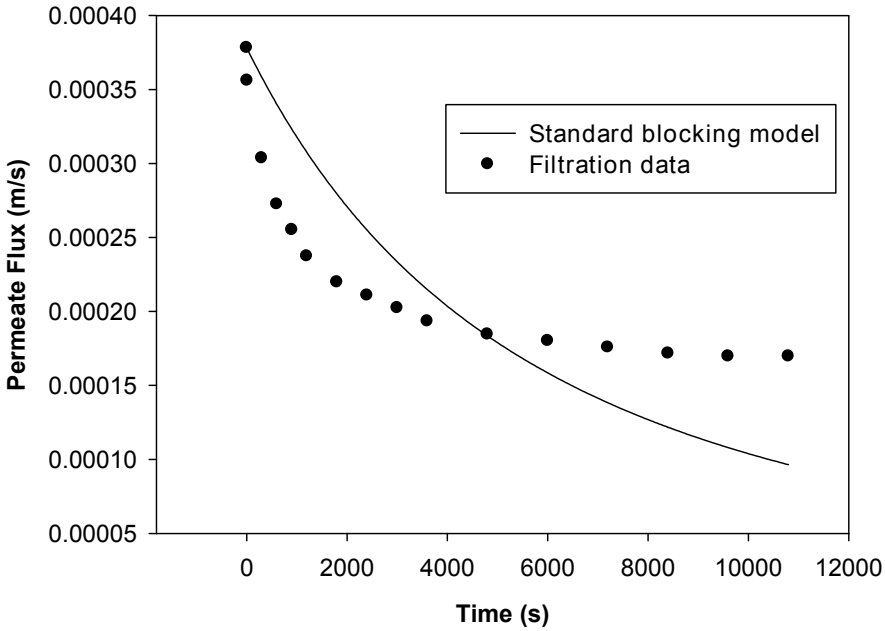

Figure 80. Standard blocking model fitting for F1 meat extract-calcium binary mixture 5 kD membrane filtration experiments.

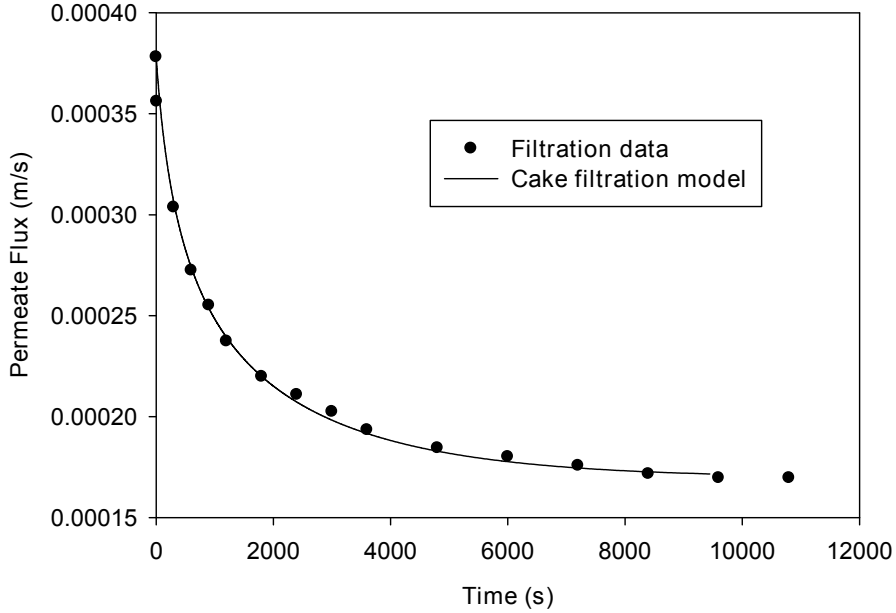

Figure 81. Cake filtration model fitting for F1 meat extract-calcium binary mixture 5 kD membrane filtration experiments.

Table 37. Blocking model R^2 fitting values for meat extract-calcium 5 kD membrane filtration experiments.

Experiment	Complete blocking	Intermediate blocking	Standard blocking	Cake filtration
F0	0.9596	0.9815	0.4282	0.9798
F1	0.9926	0.9947	0.7429	0.9610
F2	0.9788	0.9931	0.7076	0.7630
F3	0.9876	0.9937	0.7680	0.9275
F4	0.9796	0.9942	0.5712	0.9448
average	0.9796	0.9914	0.6436	0.9152

5.1.2 Blocking model fitting for alginate-calcium binary mixture filtration experiments

Here, the cake filtration model was the best fitting model, with an R^2 value of 0.8376. The standard blocking model gave the worst fitting, with an R^2 value of 0.0611. The intermediate and complete blocking model R^2 values were similar at 0.7885 and 0.7862, respectively (Table 38).

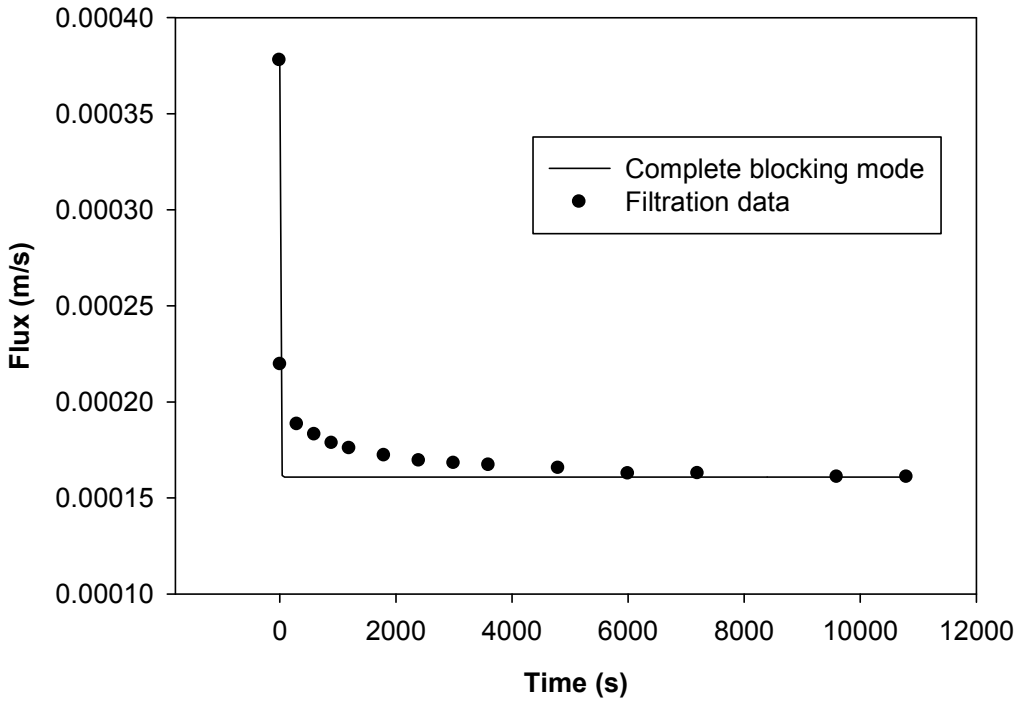

Figure 82. Complete blocking model fitting for F1 alginate-calcium binary mixture 5 kD membrane filtration experiments.

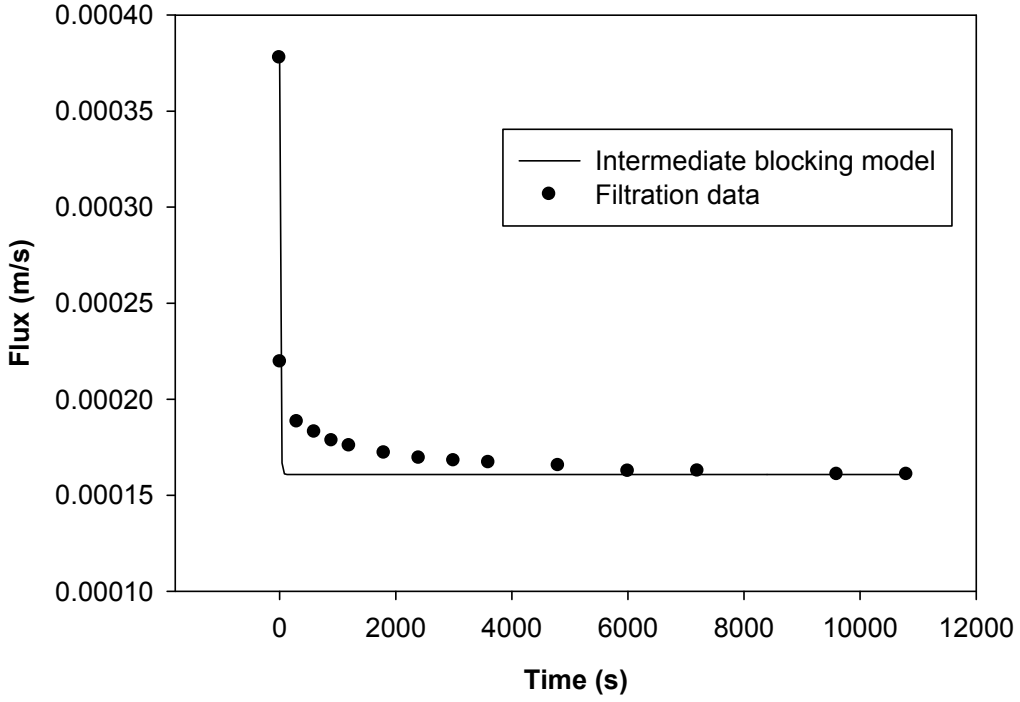

Figure 83. Intermediate blocking model fitting for F1 alginate-calcium binary mixture 5 kD membrane filtration experiments.

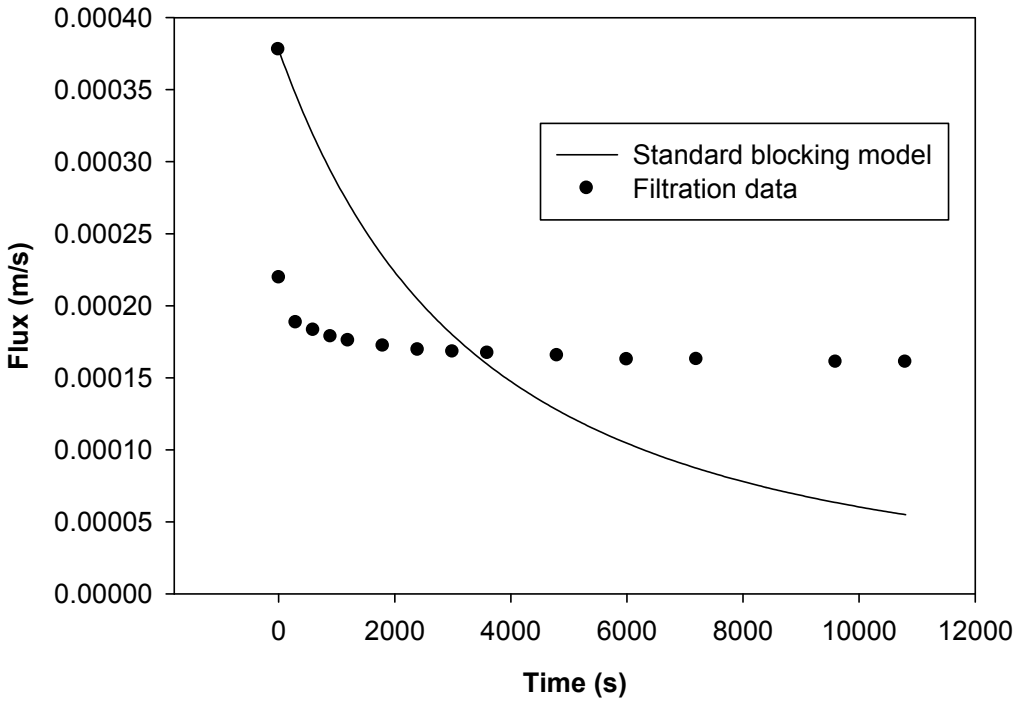

Figure 84. Standard blocking model fitting for F1 alginate-calcium binary mixture 5 kD membrane filtration experiments.

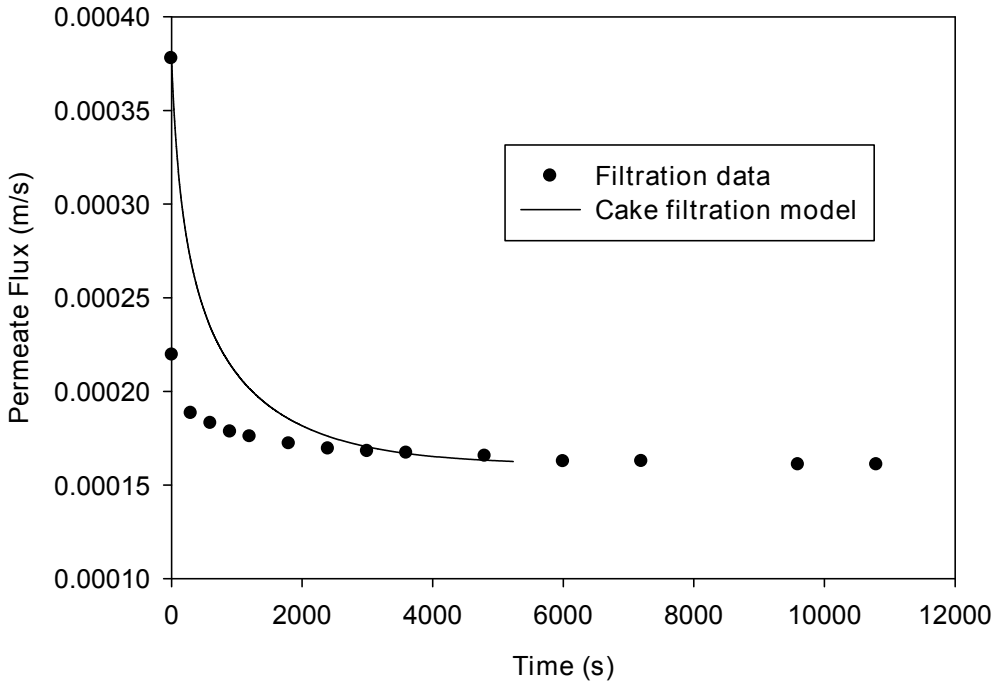

Figure 85. Cake filtration model fitting for F1 alginate-calcium binary mixture 5 kD membrane filtration experiments.

Table 38. Blocking model R^2 fitting values for alginate-calcium 5 kD membrane filtration experiments.

Experiment	Complete blocking	Intermediate blocking	Standard blocking	Cake filtration
F0	0.9511	0.9489	0.0000	0.7831
F1	0.8982	0.8696	0.0000	0.8541
F2	0.6850	0.7480	0.2443	0.9559
F3	0.5276	0.5876	0.0000	0.7104
F4	0.8693	0.8693	0.0000	08846
average	0.7862	0.7885	0.0611	0.8376

5.1.3 Blocking model fitting for artificial wastewater mixture 5 kD membrane filtration experiments

Here, the best fitting accuracy was obtained using the intermediate and the complete blocking models, with R^2 values of 0.9430 and 0.9133, respectively (Table 39). The cake filtration model came in third, with an R^2 value of 0.8144, whilst the worst fitting model was the standard blocking model, with an R^2 value of 0.1258 (Table 39).

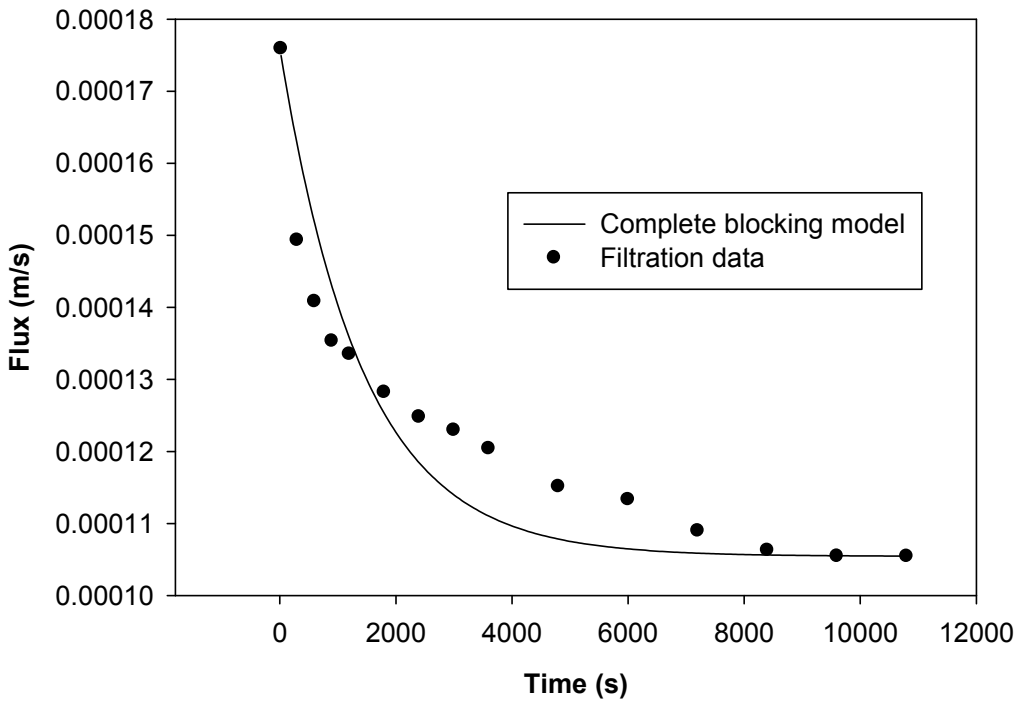

Figure 86. Complete blocking model fitting for F1 artificial wastewater mixture 5 kD membrane filtration experiments.

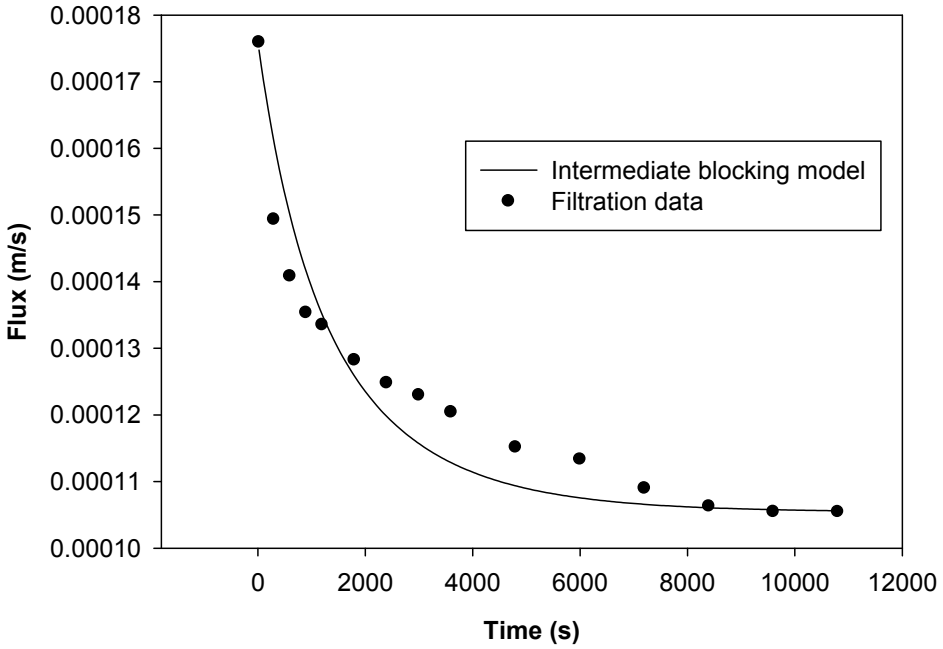

Figure 87. Intermediate blocking model fitting for F1 artificial wastewater mixture 5 kD membrane filtration experiments.

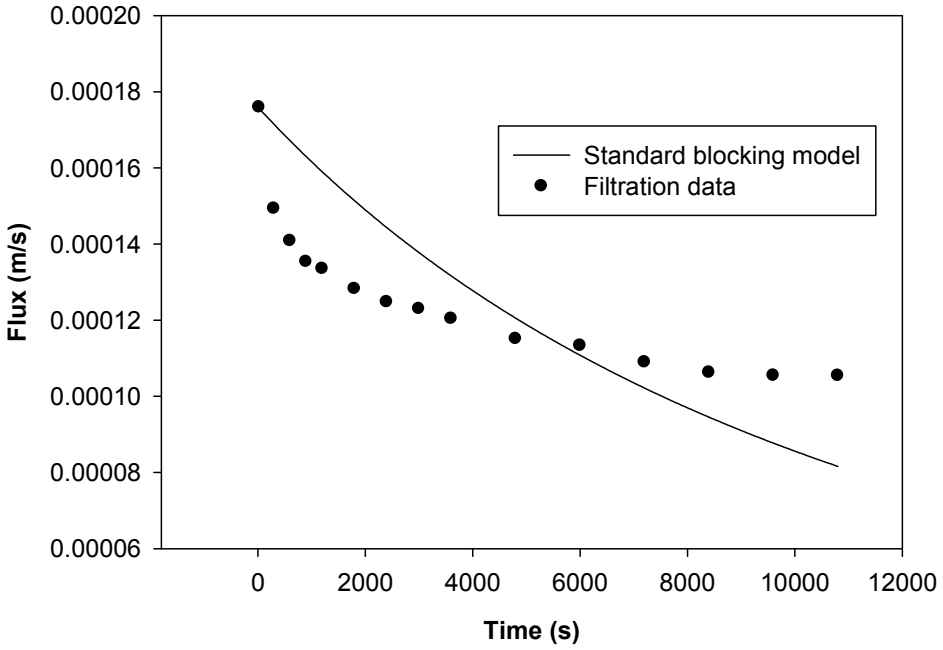

Figure 88. Standard blocking model fitting for F1 artificial wastewater mixture 5 kD membrane filtration experiments.

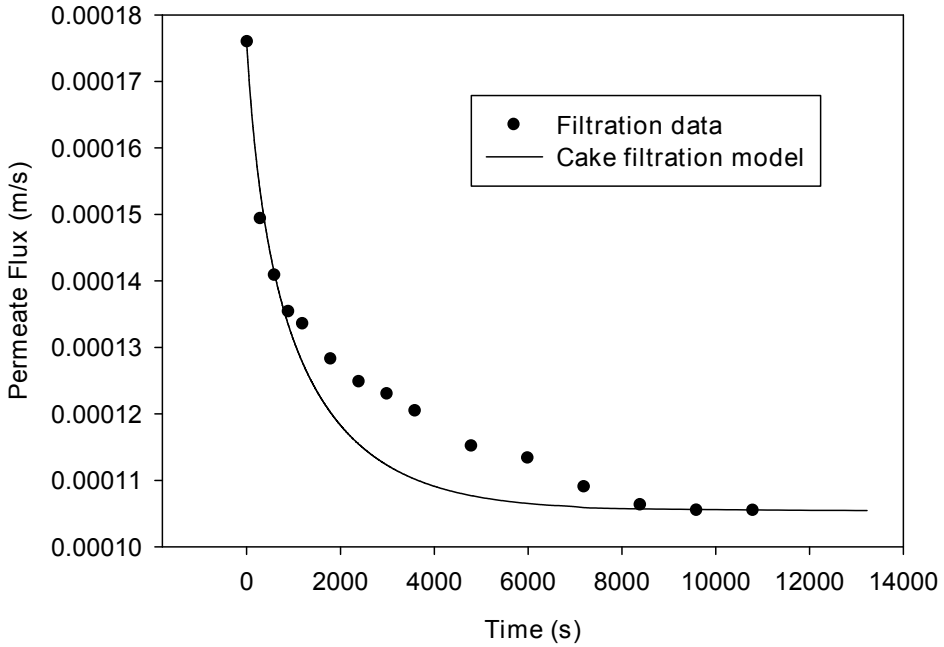

Figure 89. Cake filtration model fitting for F1 artificial wastewater mixture 5 kD membrane filtration experiments.

Table 39. Blocking model R^2 fitting values for artificial wastewater 5 kD membrane filtration experiments.

Experiment	Complete blocking	Intermediate blocking	Standard blocking	Cake filtration
F0	0.8704	0.9107	0.0554	0.6166
F1	0.9587	0.9779	0.5291	0.9859
F2	0.9612	0.9793	0.4792	0.9170
F3	0.9067	0.9355	0.0000	0.6661
F4	0.9212	0.9531	0.0000	0.9711
F5	0.9015	0.9269	0.1864	0.8356
F6	0.9106	0.9390	0.0000	0.8419
F7	0.9145	0.9345	0.0000	0.9354
F8	0.9694	0.9848	0.3269	0.7959
F9	0.9216	0.9571	0.0890	0.7953
F10	0.8531	0.8964	0.0000	0.5443
F11	0.9222	0.9475	0.0531	0.7102
F12	0.8525	0.8872	0.0000	0.9476
F13	0.9426	0.9698	0.2967	0.8926
F14	0.9117	0.9452	0.0481	0.9887
F15	0.9013	0.9377	0.0000	0.8126
F16	0.9066	0.9480	0.0752	0.5877
average	0.9133	0.9430	0.1258	0.8144

5.1.4 Blocking model fitting for artificial wastewater mixture 20 kD membrane filtration experiments

For the artificial wastewater crossflow experiments using the 20 kD ultrafiltration membrane, the fitting accuracy of all models, with the exception of the standard blocking model, were almost the same, with average R^2 values of 0.8875, 0.8805 and 0.8733 for the cake filtration, intermediate and complete blocking models, respectively (Table 40).

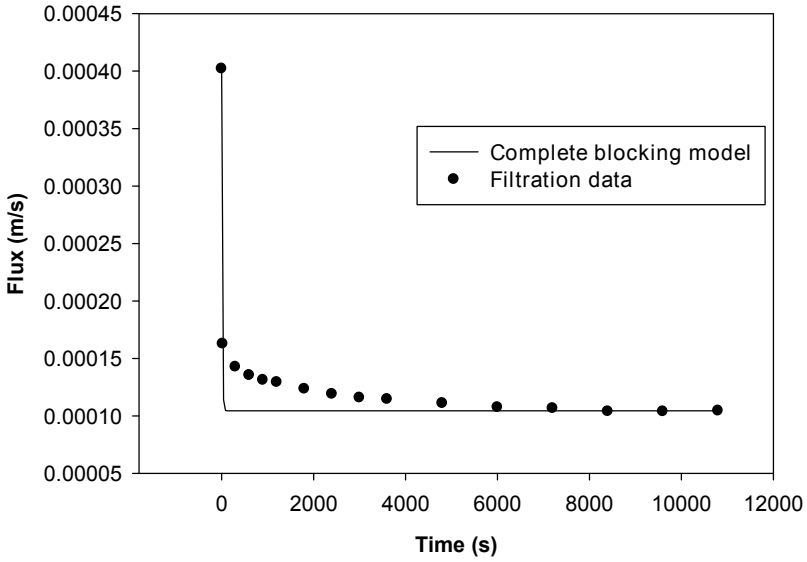

Figure 90. Complete blocking model fitting for F1 artificial wastewater mixture 20 kD membrane filtration experiments.

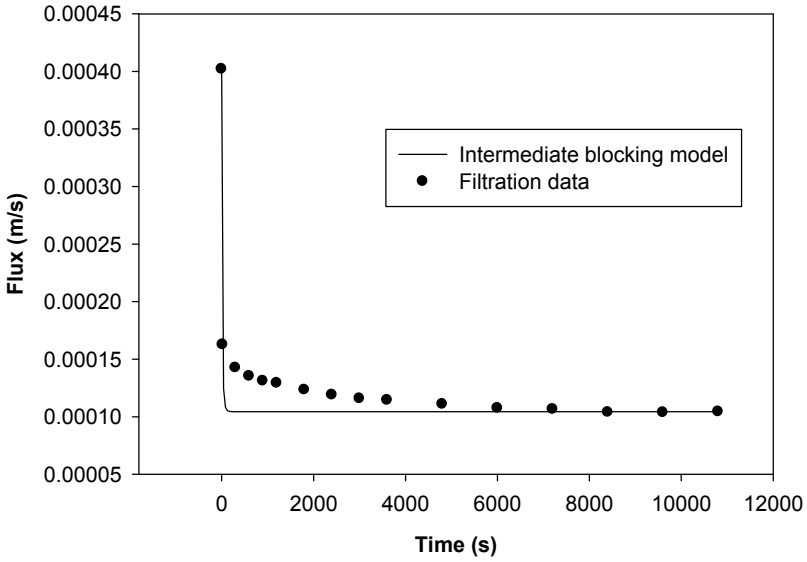

Figure 91. Intermediate blocking model fitting for F1 artificial wastewater mixture 20 kD membrane filtration experiments

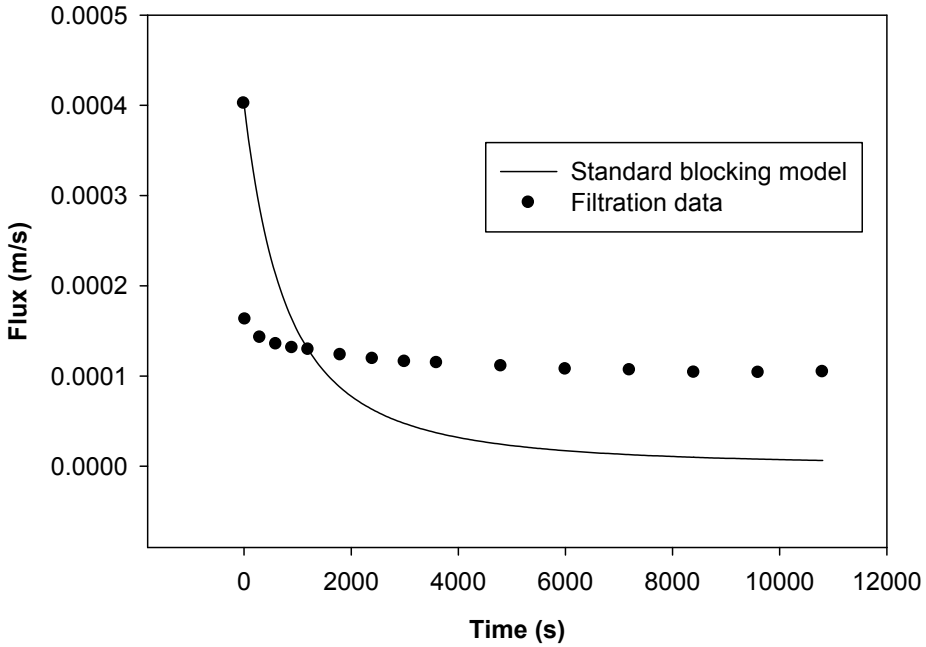

Figure 92. Standard blocking model fitting for F1 artificial wastewater mixture 20 kD membrane filtration experiments.

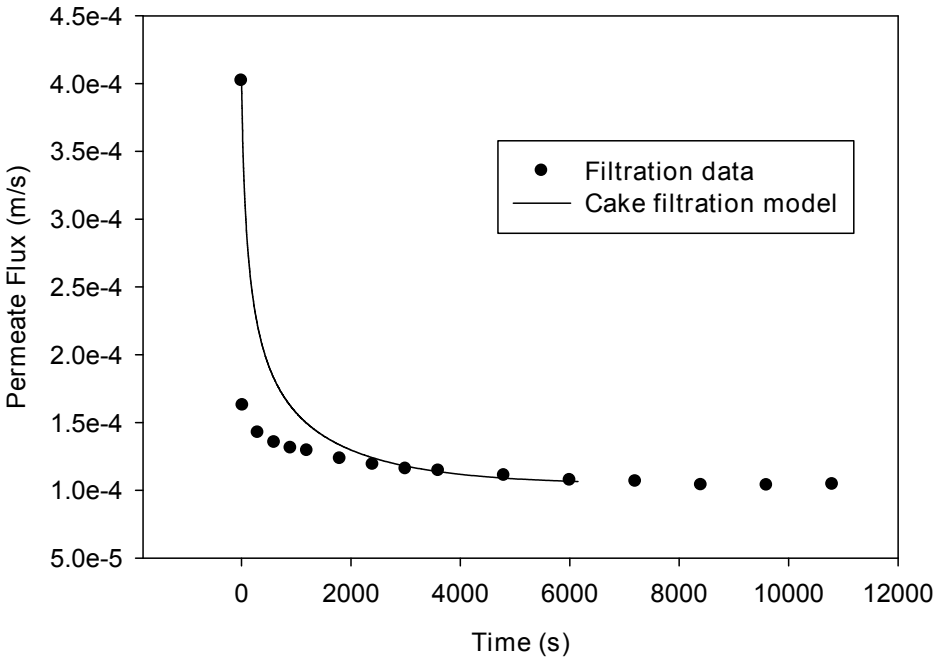

Figure 93. Cake filtration model fitting for F1 artificial wastewater mixture 20 kD membrane filtration experiments.

Table 40. Blocking model R^2 fitting values for artificial wastewater 20 kD membrane filtration experiments.

Experiment	Complete blocking	Intermediate blocking	Standard blocking	Cake filtration
F0	0.9414	0.9414	0.0000	0.8896
F1	0.6206	0.6800	0.0000	0.9831
F2	0.5470	0.6106	0.0000	0.7706
F3	0.8797	0.8797	0.0000	0.8874
F4	0.9257	0.9257	0.0000	0.9035
F5	0.8912	0.8912	0.0000	0.8272
F6	0.9530	0.9530	0.0000	0.8074
F7	0.9049	0.9049	0.0000	0.8886
F8	0.9023	0.9024	0.0000	0.9510
F9	0.8753	0.8754	0.0000	0.9358
F10	0.9513	0.9513	0.0000	0.9014
F11	0.9285	0.9285	0.0000	0.8716
F12	0.9861	0.9861	0.0000	0.7859
F13	0.8947	0.8947	0.0000	0.8713
F14	0.8530	0.8531	0.0000	0.9367
F15	0.8769	0.8769	0.0000	0.9225
F16	0.9147	0.9147	0.0000	0.9538
average	0.8733	0.8806	0.0000	0.8875

5.2 Effects of artificial wastewater component concentrations on the pore blocking model fitting accuracy

5.2.1 Artificial wastewater 5 kD membrane crossflow filtration experiments

The effects of varying the concentrations of the main four wastewater components, peptone, meat extract, alginate and calcium, on the blocking mechanisms was investigated in this section. Minitab software factorial design algorithms (Appendix D) were used to analyse the effect of changing component concentration levels on the blocking model accuracy by using the coefficients of determination, R^2, of the intermediate, complete, standard, and cake filtration blocking models calculated using matlab® route (Appendix B) .

5.2.1.1 Intermediate blocking model

The change in peptone concentration level had a minor, almost negligible effect on the goodness of fit of the intermediate blocking model (Figure 95). Changes in the meat extract concentration level had biggest effect on the fitting of the intermediate blocking model compared to the other three components. Increasing the meat extract concentration improved R^2 from 0.932 at the low concentration level to 0.958 at the high level on average (Figure 95). Increasing the concentration level of alginate reduced the R^2 from 0.952 at the low level to 0.936 at the high level (Figure 95). Similar to the alginate effect on the fit of the intermediate blocking model was the effect of increasing the calcium concentration; here, the R^2 was reduced from 0.957 at the low level to 0.931 at the high level (Figure 95).

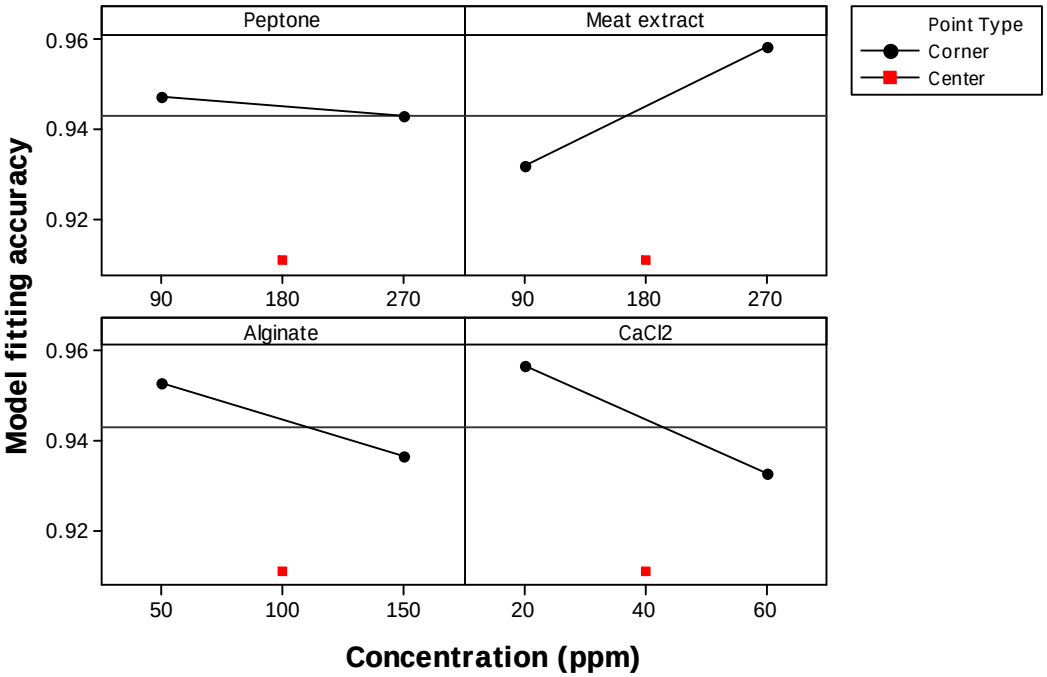

Figure 94. Main effects of wastewater components on intermediate blocking model R^2 values for the 5 kD ultrafiltration membrane.

The intermediate blocking model is considered to be accurate when the solute molecules are of the same size as the membrane pores; furthermore, it accounts for the possibility of molecules landing on top of each other rather than on the free membrane surface (Vela *et al.*, 2009). The fact that

increasing the meat extract concentration led to an improvement in the fit of the intermediate blocking model indicated that the meat extract particles were close in size to the membrane pore size of the 5 kD membrane. In contrast, alginate particle size was much larger than the membrane pore size; therefore, increasing alginate concentration had an adverse effect on the intermediate blocking model predictions. The bridging effect of calcium cations likely resulted in agglomeration and thus larger particle sizes for alginate and proteins which in turn reduced the fitting accuracy of the intermediate blocking model.

5.2.1.2 Complete blocking model

The change in peptone concentration level had a small effect on the accuracy of the complete blocking model fitting. At the high concentration of peptone the R^2 was 0.92 and at the low level it was 0.914 (Figure 96).

Changes in the meat extract concentration level had the second largest effect on the coefficient of determination of the complete blocking model. At the low meat extract level, the R^2 value was 0.904 and at the high level the value R^2 was 0.939. The higher concentration of meat extract resulted in a better fitting of the complete blocking model (Figure 96).

Similarly to the alginate effect on the fitting of the intermediate model, increasing the concentration of alginate reduced the goodness of fit of the complete blocking model. At the low alginate concentration level, the R^2 was 0.923 and it was 0.910 at the high level.

The largest effect on the goodness of fit of the complete blocking model resulted from changes in calcium concentration level. The high calcium concentration level resulted in lowering the R^2 value to 0.897, compared to an R^2 value of 0.935 at the high level (Figure 96).

As in the intermediate blocking model, the complete blocking model assumes that each particle arriving at the membrane surface blocks membrane pores by sealing them; nevertheless, unlike the intermediate blocking model, where particles can be deposited on top of each other, in the complete blocking model particles never settle over another molecule.

Similarly to the intermediate blocking model, increasing the meat extract concentration level increased the model fitting accuracy. Since small particle components such as meat extract have more chances to block membrane pores, increasing the fraction small particles, close to membrane pore size, will lead to better fitting of the complete blocking model.
Conversely, large molecular particles such as alginate are less likely to seal pore membrane, thus increasing the concentration of alginate had an adverse effect on the complete blocking model goodness of fit.

Further, increasing the calcium cation concentration encourages the formation of larger particles through ionic bonding and the alginate calcium bridging effect.

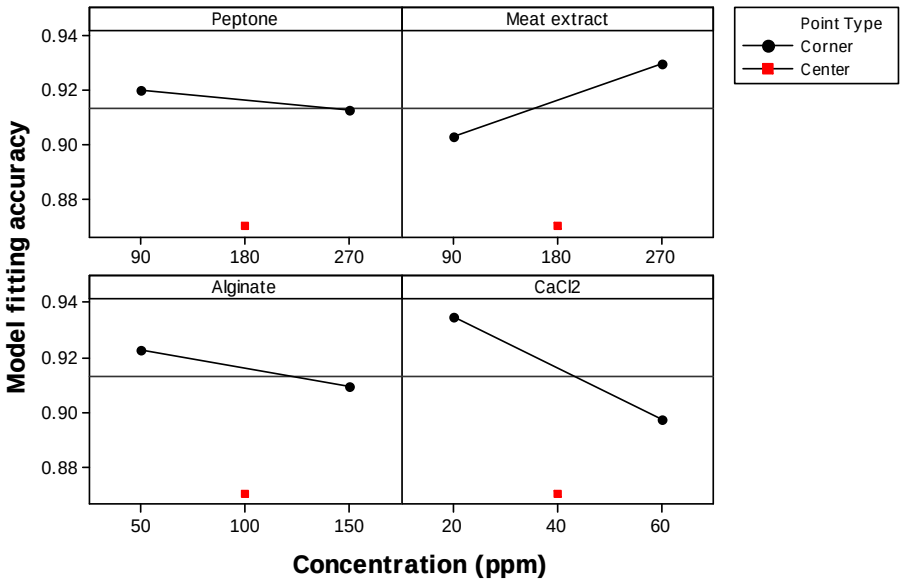

Figure 95. Main effects of wastewater components on complete blocking model R^2 values for the 5 kD ultrafiltration membrane.

5.2.1.3 Cake filtration model

Increasing the peptone concentration level reduced the accuracy of the cake filtration model. At a low peptone concentration, the R^2 value was 0.87, and at a high level, it was 0.79 (Figure 97).

The increase in meat extract concentration reduced the accuracy of the cake filtration model fitting. At a low meat extract concentration, the R^2 value was 0.84 whilst the higher meat extract concentration level resulted in an R^2 value of 0.81 (Figure 97).

The cake filtration model fitting accuracy increased with increasing alginate concentration. The value of R^2 at the high alginate concentration level was 0.88 and at the low level it was 0.78.

The change in calcium level did not have a large effect on the cake filtration model accuracy. The values of R^2 at high and low calcium levels were 0.84 and 0.81, respectively (Figure 97).

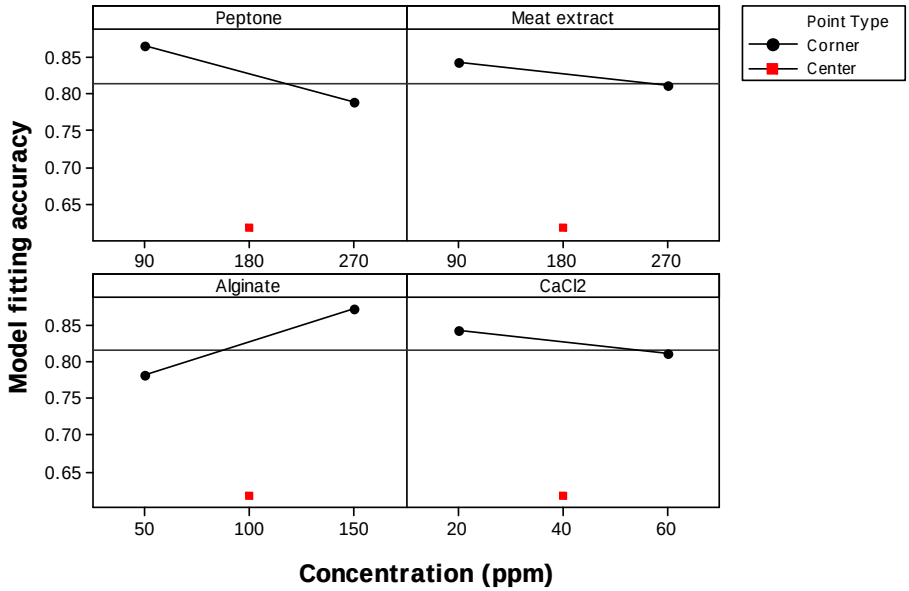

Figure 96. Main effects of wastewater components on cake–filtration model R^2 values for the 5 kD ultrafiltration membrane.

The cake filtration model assumes that the particles are larger than the membrane pores thus they do not enter the membrane pore; rather, particles form a cake layer on top of the membrane. Since peptone and meat extract molecules are not too large compared to the membrane pore size, increasing the concentration of these components reduced the fitting accuracy of the model. In contrast, increasing the concentration level of large molecules such as alginate increased the predictive accuracy of the cake filtration model. Although increasing the concentration of calcium should ideally increase the accuracy of the cake filtration model by reducing the fraction of small particles via ionic bonding and the alginate calcium bridging effect, there was only a small effect resulting from increasing the calcium concentration.

5.2.1.4 Standard blocking model

For the standard blocking model, the fitting accuracy did not change noticeably with the change of component concentrations. The value of R^2 was very low for this model; the maximum R^2 value obtained was 0.2 at the high concentration level of meat extract and the low level of calcium chloride, whilst the change in peptone and sodium alginate concentration levels had no effect on the accuracy of the standard blocking model (Figure 98).

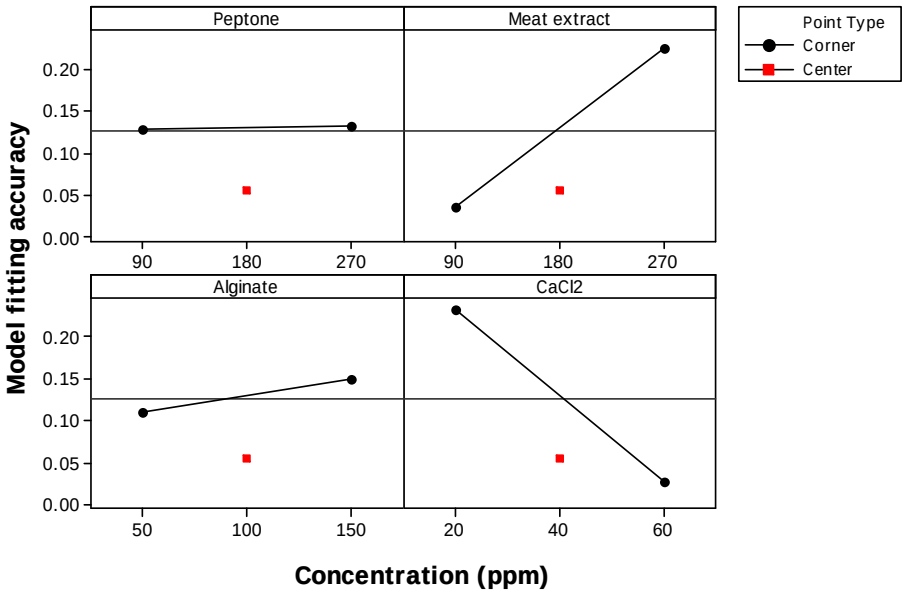

Figure 97. Main effects of wastewater components on standard blocking model R^2 values for the 5 kD ultrafiltration membrane.

5.2.2 Artificial wastewater 20 kD membrane crossflow filtration experiments

5.2.2.1 Intermediate blocking model

The change in peptone concentration had an effect on the accuracy of the intermediate blocking model fitting. The higher peptone concentration resulted in reducing the R^2 value to 0.879 from a value of 0.915 at the lower peptone level (Figure 99).

Changes in the meat extract concentration had a similar effect as peptone levels on the accuracy of the intermediate blocking model fitting. The R^2 value at the low meat extract level was higher, at 0.910, than its value at the high level, which was 0.875 (Figure 99).

The high alginate level resulted in a lower R^2 value for the intermediate blocking model than for the low level. The R^2 value was 0.90 at the low alginate level and 0.88 at the high alginate level (Figure 99).

The change in calcium concentration level had the greatest effect on the accuracy of the intermediate blocking model. The higher concentration of calcium resulted in a better fitting accuracy. The value of R^2 at the low calcium level was 0.865, which was lower than the value of R^2 at the high level, 0.915 (Figure 99).

Unlike the case with the 5 kD membrane, increasing the concentration level of peptone and meat extract did not improve the accuracy of the intermediate–blocking model prediction. Moreover, the improvement of the model prediction with increased calcium concentration may suggest that peptone and meat extract particles are much smaller than the 20 kD membrane pore size and that the bonding effect of the calcium cations brings these agglomerated

particles closer to the membrane size, thus increasing the intermediate blocking mechanisms.

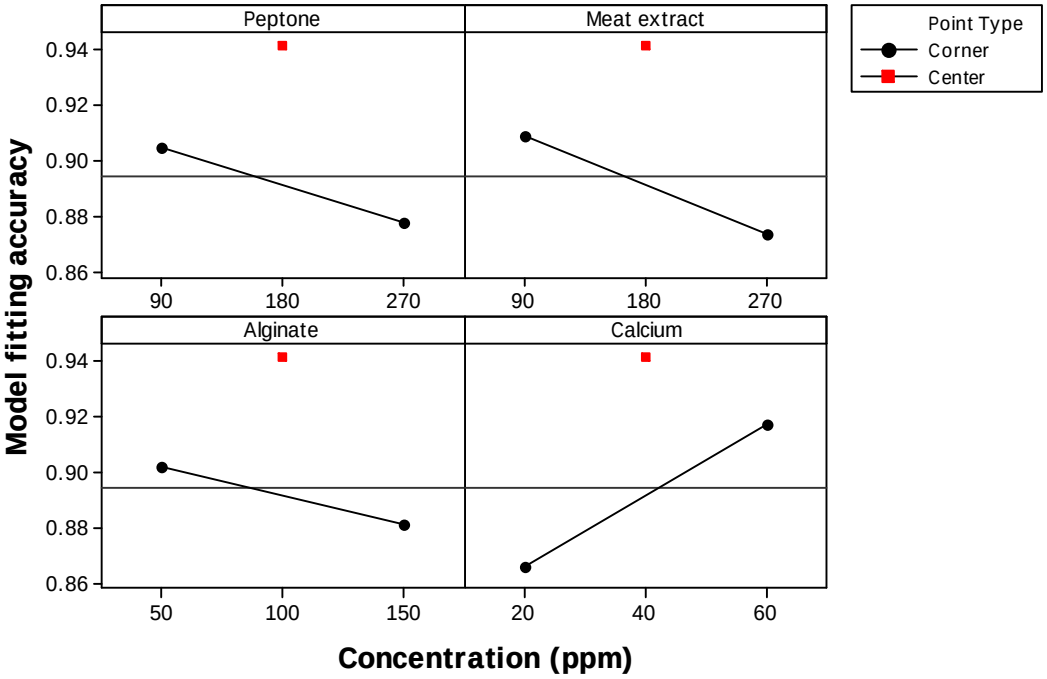

Figure 98. Main effects of wastewater components on intermediate blocking model R^2 values for the 20 kD ultrafiltration membrane.

5.2.2.2 Complete blocking model

Changes in peptone concentration had an effect on the accuracy of the complete blocking model fitting. The higher peptone concentration resulted in lowering the R^2 value to 0.865 from a value of 0.906 at the low peptone level (Figure 100).

Changes in the meat extract concentration had a similar effect on the accuracy of the complete blocking model fitting as for peptone. The value of R^2 at the low meat extract concentration level was higher, at 0.906, than its value at the high level, which was 0.863 (Figure 100).

The high alginate concentration level resulted in a lower R^2 value for the complete blocking model than low level; R^2 was 0.907 at low alginate concentration and 0.863 at high concentration (Figure 100).

The change in calcium concentration level had the greatest effect on the accuracy of the complete blocking model among all the components. The higher concentration of calcium resulted in a better fitting accuracy. The value of R^2 at the low calcium level was 0.856 but increased to 0.925 at the high level (Figure 100).

As with the intermediate blocking model, and unlike the case with the 5 kD membrane, increasing the concentration level of peptone and meat extract did not improve the accuracy of the complete blocking model predictions. Furthermore, the effect of increased calcium concentration in improving the model prediction suggests that peptone and meat extract particles are much smaller than the 20 kD membrane pore size and that the bonding effect of the calcium cations brings the agglomerated particles closer to the membrane size, thus increasing the influence of the complete blocking mechanism.

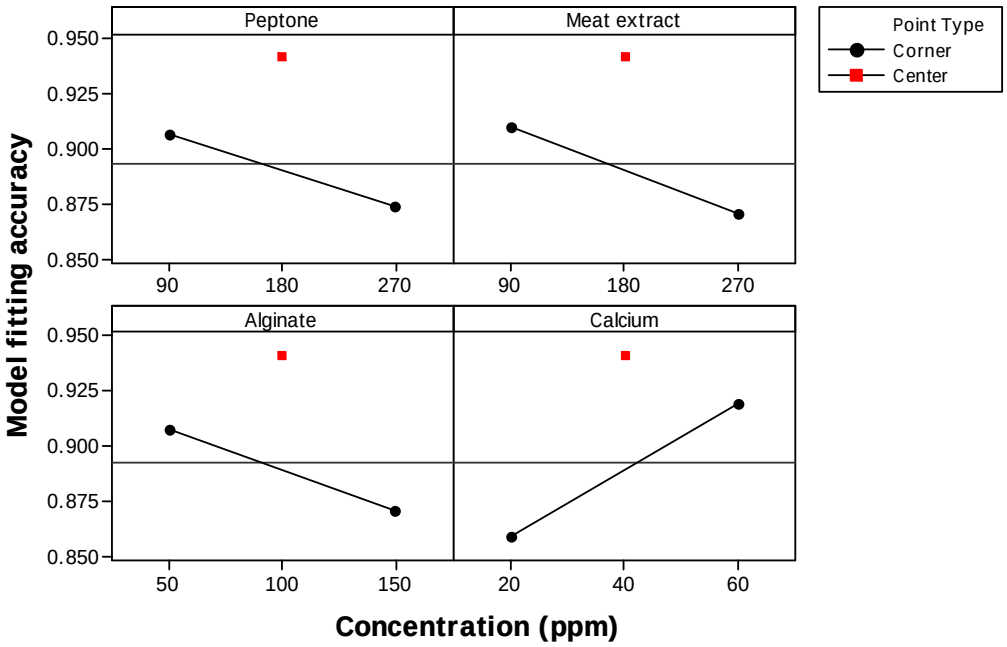

Figure 99. Main effects of wastewater components on complete blocking model R^2 values for the 20 kD ultrafiltration membrane.

5.2.2.3 Cake filtration model

The change in peptone concentration level affected the fitting accuracy of the cake filtration model. The lower concentration level of peptone improved the accuracy of the cake filtration model compared to the higher level. The value of R^2 at the low level was 0.91 and was 0.865 at the high level (Figure 101).
The higher meat extract concentration level resulted in a higher accuracy of prediction for the cake filtration model than lower level. The value of R^2 at the low level was 0.865 and it was 0.910 at the high level (Figure 101).

The lower concentration level of alginate yielded a better cake filtration model fitting than the higher level. The R^2 value at the low level was 0.915, which is much higher than its value at the high level, of 0.86 (Figure 101).
Changing the calcium concentration level had a marginal effect on the accuracy of the cake filtration model. The R^2 value at the low level was 0.88 compared to 0.89 at the high level (Figure 101).

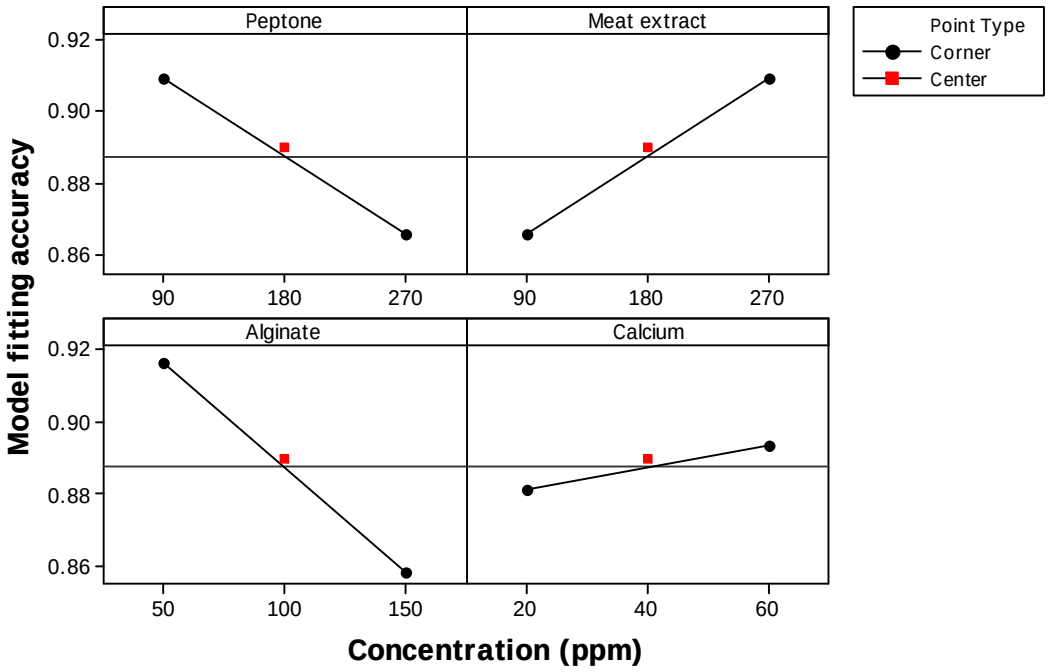

Figure 100. Main effects of wastewater components on cake filtration blocking model R^2 values for the 20 kD ultrafiltration membrane.

In the opposite of the effect with the 5 kD membrane, meat extract gave a better model fitting accuracy with increasing concentration. Moreover, increasing alginate concentration did not improve the model fitting accuracy, unlike the case with the smaller 5 kD membrane. Furthermore, calcium concentration level did not play a major role in the cake filtration model accuracy, suggesting that the bonding and bridging effect of calcium cations was not as important with the 20 kD membrane as it was in the case of the 5 kD membrane.

5.2.2.4 Standard blocking model

The standard blocking mechanisms did not play a role in the fouling of the 20 kD membrane. No change in the concentration level of any of the studied wastewater components had any effect on the fitting accuracy of the standard blocking model (Figure 102).

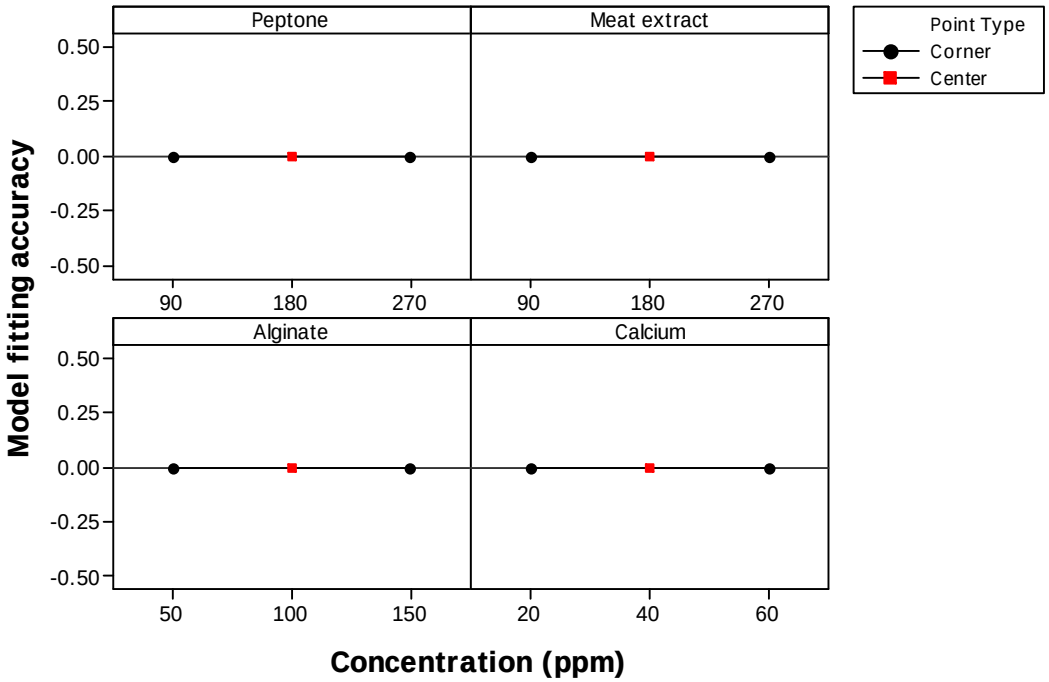

Figure 101. Main effects of wastewater components on standard blocking model R^2 values for the 20 kD ultrafiltration membrane.

5.2.3 Meat extract-calcium binary mixture crossflow filtration experiments

5.2.3.1 Intermediate blocking model

Changing the concentration level of meat extract did not have a noticeable effect on the fitting accuracy of the intermediate blocking model. The R^2 value at the low concentration level was 0.994 and it was 0.993 at the high level. Changing the concentration level of calcium also had no effect on the accuracy of the intermediate blocking model (Figure 103).

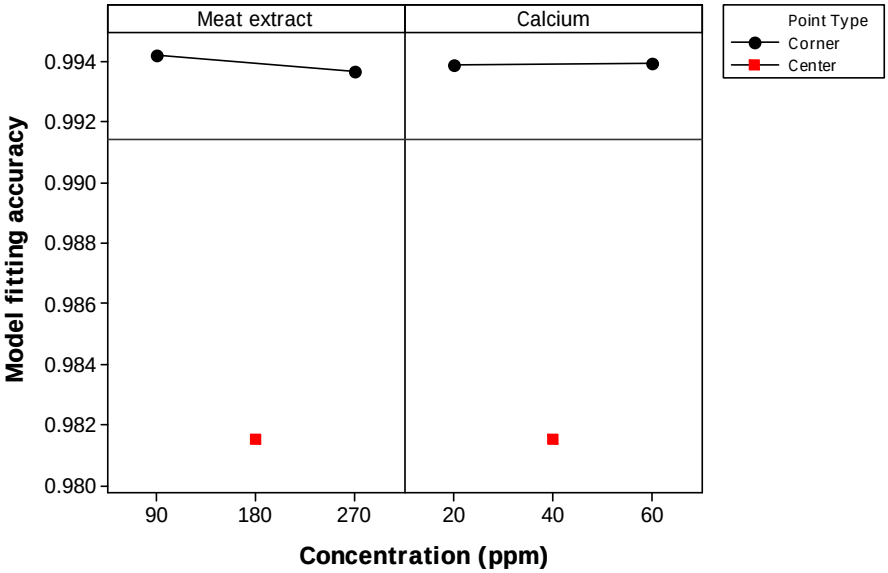

Figure 102. Main effects of meat extract-calcium binary mixture components on intermediate blocking model R^2 values for 5 kD membrane filtration.

5.2.3.2 Complete blocking model

Changing the concentration level of meat extract did not have a noticeable effect on the fitting accuracy of the complete blocking model. The R^2 value at low meat extract concentration level was 0.990 and its value at the high level was 0.980 (Figure 104).

The change in calcium concentration level also had no effect on the fitting accuracy of the complete blocking model. The values of R^2 for the high and

low concentrations of calcium were 0.983 and 0.985, respectively (Figure 104).

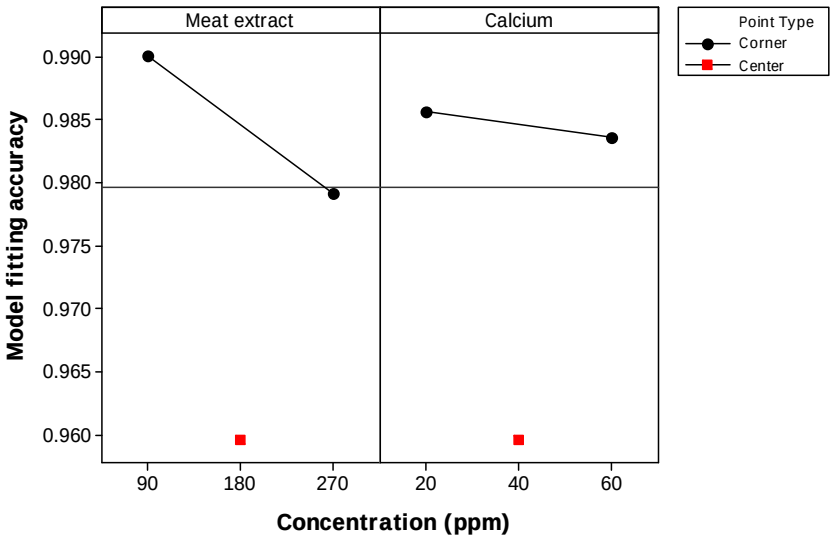

Figure 103. Main effects of meat extract-calcium binary mixture components on complete blocking model R^2 values for 5 kD membrane filtration.

5.2.3.3 Cake filtration model

Changing the concentration level of meat extract had a large effect on the fitting accuracy of the cake filtration model. The value of R^2 at low meat extract concentration was 0.944 while the value of R^2 at high meat extract concentration was 0.854 (Figure 105).

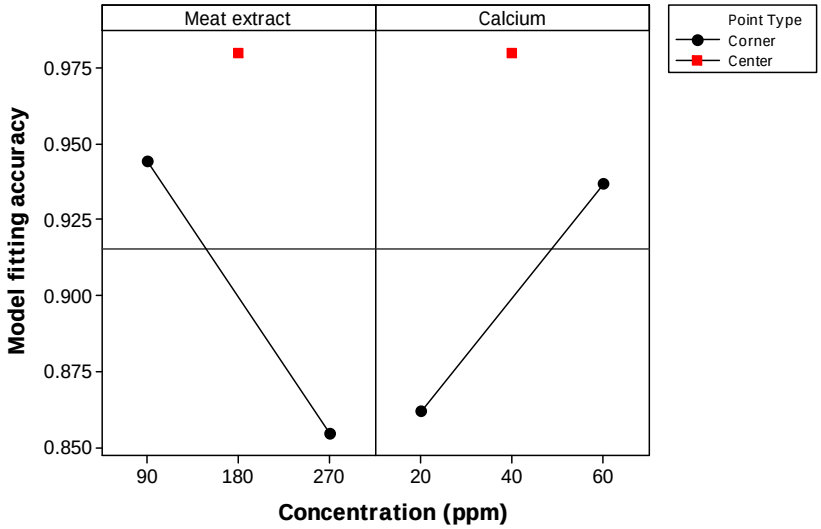

Figure 104. Main effects of meat extract-calcium binary mixture components on cake filtration blocking model R^2 values for 5 kD membrane filtration.

Increasing the calcium concentration improved the cake filtration model fitting accuracy. The R^2 value at the low calcium concentration level was 0.86 while it was 0.938 at the high level (Figure 105).

5.2.3.4 Standard blocking model

Changing the meat extract concentration had a minor effect on the accuracy of the standard blocking model. The values of R^2 were 0.75 at the low meat extract concentration level and 0.65 at the high level (Figure 106).

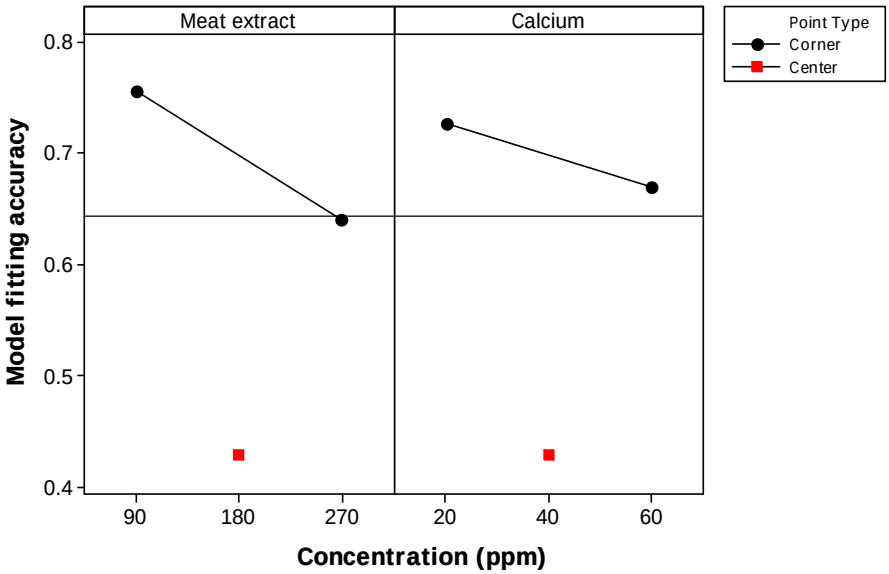

Figure 105. Main effects of meat extract calcium binary mixture components on standard blocking model R^2 values for 5 kD membrane filtration.

Changing calcium concentration level had a minor effect on the fitting accuracy of the standard blocking model. The R^2 value for the low and high concentration levels of calcium were 0.725 and 0.675, respectively (Figure 106). Compared to the other models, the standard model had the lowest fitting accuracy.

5.2.4 Sodium alginate-calcium binary mixture cross-flow filtration experiments

5.2.4.1 Intermediate blocking model

The change in the concentration of alginate had an effect on the fitting accuracy of the intermediate blocking model. Lowering the alginate concentration level improved the accuracy of the intermediate blocking model. The R^2 value at the low concentration level was 0.863, while the R^2 value at the high level was 0.725 (Figure 107).

Changing the calcium concentration had a large effect on the fitting accuracy of the intermediate blocking model. Increasing the concentration lowered the R^2 value from 0.92 at the low concentration level to 0.62 at the high level (Figure 107).

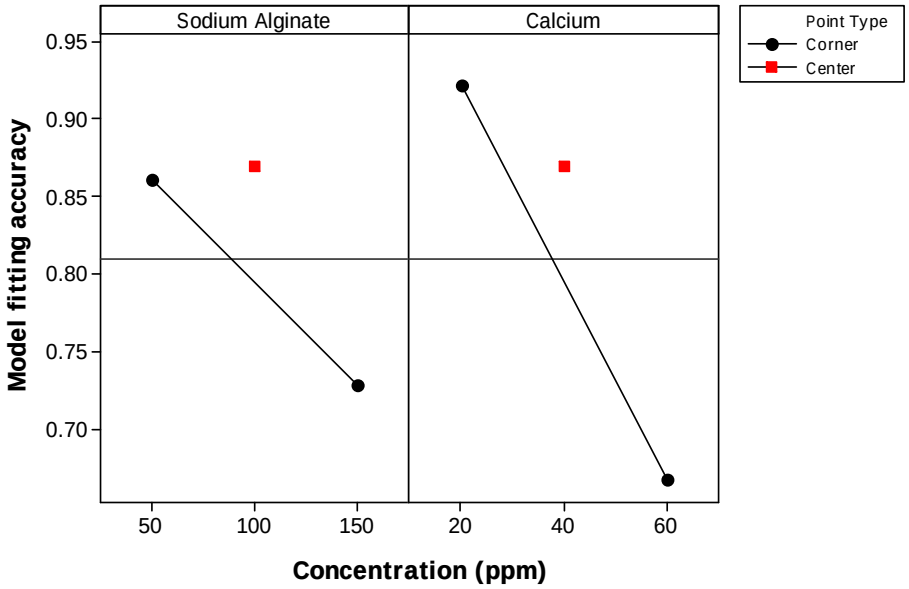

Figure 106. Main effects of alginate-calcium binary mixture components on intermediate blocking model R^2 values for 5 kD membrane filtration.

5.2.4.2 Complete blocking model

Increasing the alginate concentration had an adverse effect on the fitting accuracy of the complete blocking model, lowering the R^2 value from 0.83 at the low concentration level to 0.71 at the high level (Figure 108).

The change in the calcium concentration level had the largest effect on the fitting accuracy of the complete blocking model. The value of R^2 at the low concentration level of calcium was 0.94, while it was 0.61 at the high level (Figure 108).

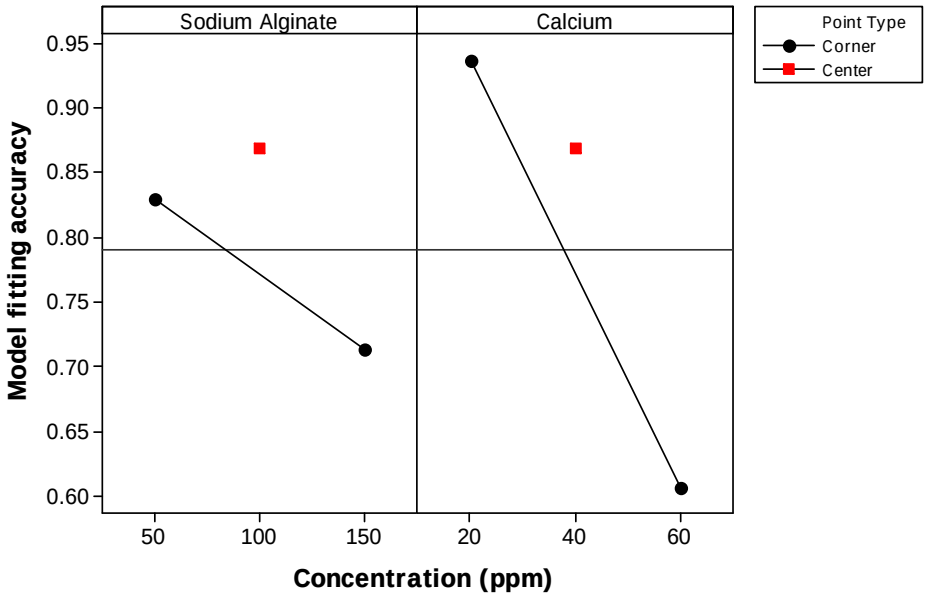

Figure 107. Main effects of alginate-calcium binary mixture components on complete blocking model R^2 values for 5 kD membrane filtration.

5.2.4.3 Cake filtration model

The change in the concentration level of alginate had an effect on the fitting accuracy of the cake filtration model. Increasing the concentration of alginate lowered the R^2 value from 0.87 at the low concentration level to 0.78 at the high level (Figure 109).

Increasing the concentration level of calcium marginally improved the fitting accuracy. The values of R^2 were 0.82 at the low concentration level and 0.83 at the high level (Figure 109).

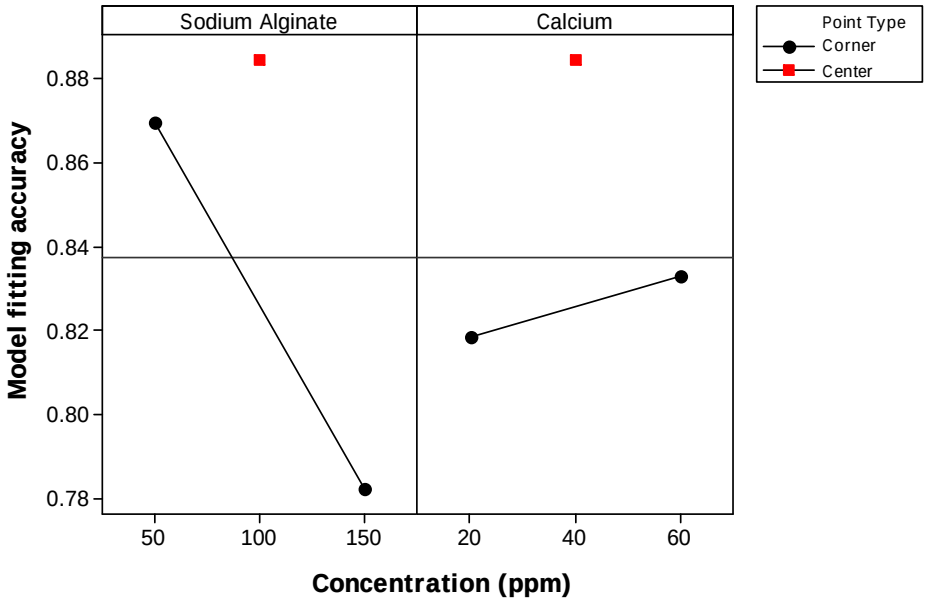

Figure 108. Main effects of alginate-calcium binary mixture components on cake filtration blocking model R^2 values for 5 kD membrane filtration.

5.2.4.4 Standard blocking model

The fitting accuracy of the standard blocking model was very low. Changing the concentrations of alginate or calcium did not have a noticeable effect on the fitting accuracy of the standard blocking model (Figure 110).

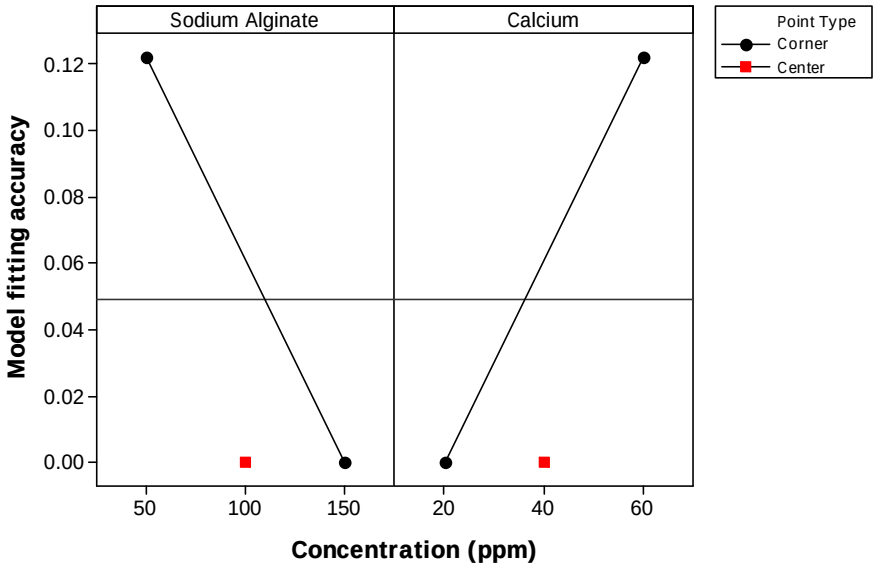

Figure 109. Main effects of alginate-calcium binary mixture components on standard blocking model R^2 values for 5 kD membrane filtration.

5.3 Concentration polarisation model

The assumption of uniform non-interacting particles in the feed is a major shortfall in this theory due to the well established concept of interaction between cations and several wastewater components such as proteins and polysaccharides, as well as the self interaction of wastewater components.

A second assumption that maybe a source of error in the model predictions for flux is 100% particle rejection by the membrane, which is unrealistic, as real wastewater contains many components with particle sizes smaller than the pores of the membrane, and certainly a microfiltration membrane, so the flux will be theoretically reduced by other blocking mechanisms such as complete and intermediate blocking, perhaps more greatly than by the resistance of the concentration polarisation layer.

In their theory of concentration polarisation, Song and Elimelech (1995) introduced the filtration number, N_F, a dimensionless number.

$$N_F = \frac{4\pi \cdot a_p^3}{3kT} \Delta P_p \qquad (5.2)$$

The filtration number represents a ratio between the energy needed to move the particle from the membrane surface back into the bulk suspension and the particle's thermal energy.

A critical value of 15 is assigned to the filtration number. If the filtration number is less than the critical value, then a concentration polarisation layer exists over the membrane surface, and if the filtration number value is larger than the critical value a cake layer with maximum packing starts to form on the membrane surface.

The calculation procedure is to solve equation (5.2) by substituting ΔP for ΔP_p then solve equation (5.3) for θ, which is a porosity dependent factor.

$$\frac{4\pi \cdot a_p^3}{3kT} \Delta P_p = \int_0^{\theta_w} \frac{1 + \frac{2}{3}\theta^5}{1 - \frac{3}{2}\theta + \frac{3}{2}\theta^5 - \theta^6} 3\theta^2 d\theta \qquad (5.3)$$

Finally the variable $A_s(\theta^*)$ is calculated using equation (5.4) (Song and Elimelech, 1995):

$$A_s(\theta^*) = \frac{N_F}{\theta_w^3} \qquad (5.4)$$

The flux when a cake layer is formed can be calculated from equation (5.5).

$$V = \left(\frac{3}{2}\right)^{2/3} \left(D^{2/3} \gamma^{1/3} L^{-1/3}\right) \left(\frac{\Delta P}{As(\theta_{\max}) kTC_0}\right)^{1/3} \qquad (5.5)$$

In all the artificial wastewater experiments performed in this study, the filtration number (N_F) value was larger than 15, indicating the formation of a cake layer.

As can be seen from equation (5.2), the filtration number depends here only on the particle size as all other variables, such as pressure and temperature, were constant in the artificial wastewater experiments performed in this study. The change in the steady state flux with different particle sizes for the constant operating conditions used in the wastewater filtration experiments is presented in (Figure 110).

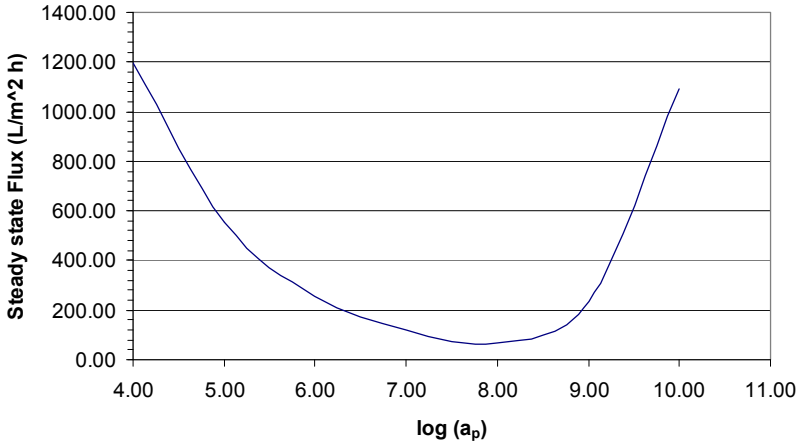

Figure 110. Steady state flux vs. particle diameter for artificial wastewater experiments calculated using the Song and Elimelech concentration polarisation equation.

Although the particle size analysis by the Malvern Mastersizer failed in the quality factor due to the high polydispersity of the wastewater feed, the results were used to compare the concentration polarisation model predictions to the experimental results (Table 41).

Table 41. Concentration polarisation model predictions for steady state flux versus experimental wastewater filtration results.

Experiment	J_{ss} (L/m^2 h)	Model J_{ss} (L/m^2 h)	Error (%)
F0	376	N/A	N/A
F1	475	N/A	N/A
F2	447	497	11
F3	551	N/A	N/A
F4	373	N/A	N/A
F5	482	491	2
F6	444	544	23
F7	452	473	5
F8	463	560	21
F9	418	449	7
F10	335	433	29
F11	427	439	3
F12	304	414	36
F13	385	478	24
F14	411	588	43
F15	440	497	13
F16	402	480	19

The model over predicted the steady state flux for all experiments. The best prediction was for experiment F5, with a 5% error, and the worst prediction was for experiment F14, with over 43% prediction error.

6.0 Conclusions and Recommendations

The microfiltration membrane could not reject the artificial wastewater components. The permeate flux reduced with time, nevertheless, the permeate Chemical Oxygen Demand (COD) was the same as the artificial wastewater feed. The flux reduction indicates a blocking of membrane pores and the permeate COD value indicates that the microfiltration pore size 0.2 μm was larger than the artificial wastewater component particles size.
Smaller pore size ultrafiltration membranes were used to carry on the experiments in this work to better examine the effect of different artificial wastewater components on the fouling of the ceramic membranes.

Flux analysis for 20 and 5 kD membranes showed a great influence of calcium concentration. As calcium concentration increased the flux reduction increased. Further, with the 5 kD membrane the largest flux reduction was obtained with high concentration of both calcium and alginate. This is a result of the fouling layer becoming more compacted and more resistance to permeate flow as a result of the calcium bridging effect on alginate.

Increasing calcium concentration level had the strongest effect on increasing membrane resistance. The average increase is membrane resistance for experiments conducted with a high calcium concentration of 60 ppm compared to the increase in membrane resistance for experiments conducted with low calcium concentration of 20 ppm was 100% and 32% for the 20 and 5 kD membrane, respectively.

It is clear from the comprehensive set of results and factorial design analysis of the artificial wastewater filtration experiments performed here that the concentration of calcium is a very important factor that must be considered in wastewater filtration. Furthermore, the soluble microbial products, especially polysaccharides, are one of the main components responsible for membrane fouling. The following can be concluded from the two level factorial design analysis:

- Polysaccharides are the major fouling compounds in EPS.
- While protein compounds are an important part of EPS membrane fouling, their effect increases in the presence of polysaccharides.
- Sodium alginate-calcium solutions fouled the membrane more severely, causing twice the increase of resistance (on average) than did meat extract-calcium solutions.
- Irreversible fouling was the major fouling type in alginate-calcium filtration experiments (95% in four of the five experiments), while 30 – 40 % of the fouling in the meat extract-calcium filtration experiments was reversible fouling.
- Clear relationships between the calcium to alginate ratio and both the extent and type of membrane fouling exist. However, when meat extract was the main foulant, no clear relationship between fouling level and meat extract to calcium ratio was observed.
- At calcium to alginate concentration ratios between 0.05 – 0.07, free calcium cations were found in the mixtures. At concentration ratios equal to or less than 0.05, nearly all calcium cations were bound by the alginate.
- For the meat extract–calcium solutions, 50% of the initial feed calcium was absorbed by the meat extract, regardless of the change in calcium feed concentration.

Choosing the appropriate cleaning method is an important factor for improving a membrane separation process. The cleaning chemicals and the frequency of cleaning are both functions of the process stream components and concentrations. Sodium hydroxide concentration in the cleaning solution was the most important factor in the recovery of the ceramic membrane used in artificial wastewater filtration. Further, higher cleaning temperature and longer cleaning time generally gave an increase in membrane recovery after filtration experiments nevertheless their effect was not as noticeable as increasing the sodium hydroxide concentration.

The fitting accuracy of the intermediate and complete blocking models was the highest for the filtration of the meat extract and calcium binary mixtures. The alginate-calcium binary mixture was best fitted with the cake filtration model. The artificial wastewater filtration data had the highest fitting accuracy with the intermediate and complete blocking for the 5 kD membrane and the cake filtration and intermediate blocking models for the 20 kD membrane.

The prediction accuracy of the complete, intermediate and standard blocking models increased with increasing meat extract concentration. The increase in calcium and alginate concentration lowered the prediction accuracy of complete, intermediate and standard blocking models. On the other hand, increases in calcium and alginate concentration had a positive effect on the predication accuracy of the cake filtration model for the 5 kD pore size membrane.

The effect of changing the artificial wastewater components concentration on the fitting accuracy of the blocking models for the 20 kD pore size membrane was almost the opposite of the 5 kD pore size membrane. Increasing the calcium concentration increased the predication accuracy of the intermediate and complete blocking models, while the increase in alginate concentration reduced the cake filtration model prediction accuracy.

In the case of the relatively smaller pore size 5 kD membrane the smaller particles size proteins blocked the pores completely or partially while large alginate particles formed a cake layer over the membrane. However, in the case of the relatively large size 20 kD membrane the increase in calcium concentration increased the particles size of the artificial wastewater by the calcium bridging effect on proteins and polysaccharides to produce a particles size able to completely or partially block the 20 kD membrane pores.

Furthermore understanding the mechanism and the scale at which different wastewater components effect the membrane fouling rate will help produce better operating procedures. Moreover, accurate prediction of the fouling rate

will enable membrane filtration operators to optimise the cleaning procedure and cleaning time intervals.

The blocking models compared in this study clearly indicated that complicated blocking mechanisms were responsible for fouling the membrane. It would be very interesting to combine several blocking mechanisms into one model to account for the complexity associated with real wastewater filtration. Further, a predictive model that takes into account the interaction between different wastewater components would surely give far better predictions of permeate flux and membrane fouling than existing models, which sometimes oversimplify the complexity of wastewater component interactions.

Nomenclature

a_P	Particle size (μm)
C_b	Bulk particle concentration (mg/L)
C_{ip}	Solute concentration in permeate (mg/L)
C_{ir}	Retentate particle concentration (mg/L)
COD	Chemical oxygen demand (ppm)
D	Diffusion coefficient (m^2/s)
IC	Inorganic carbon concentration (ppm)
J	Permeate flux (L/m^2 hr)
J_{cw}	Clean water permeate flux (L/m^2 hr)
J_o	Initial clean membrane water flux (L/m^2 hr)
J_{pss}	Steady state permeate flux (L/m^2 hr)
K_{gl}	Cake filtration model fitting parameter (s/m^2)
k_c	complete blocking model fitting parameter (1/m)
K_{CF}	Crossflow filtration blocking models constant
k_i	Intermediate blocking model fitting parameter (1/m)
k_s	Standard blocking model fitting parameter ($s^{-0.5}$ $m^{-0.5}$)
L	Membrane filter length (m)
N_F	Dimensionless filtration number
R_c	Cake layer resistance (1/m)
R_{cw}	Clean membrane resistance (1/m)
R_i	Membrane rejection for specie i (%)
R_m	Membrane resistance (1/m)
R_{ss}	Steady state membrane resistance (1/m)
T	Absolute temperature (K)
t	Time (s)
TC	Total carbon concentration (ppm)
V	Permeate total volume (L)
v	Permeate volume per unit membrane area (m^3/m_2)
X_i	Component i concentration level for factorial design analysis (ppm)
β_i	Factorial design interaction parameter

γ	Shear rate (1/s)
ΔP	Transmembrane pressure drop (Pa)
θ	Porosity dependent factor (%)
θ_w	Value of θ at the membrane surface
K	Boltzmann constant (J/K)
μ	Fluid dynamic viscosity (Pa s)

References

Aptel, P, 1994, "Membrane pressure driven processes in water treatment", Membrane processes in separation and purification, 263-281.

Abrahamse, A.J., Lipreau, C., Li, S. and Heijman, S.G.J. 2008, "Removal of divalent cations reduces fouling of ultrafiltration membranes", *Journal of Membrane Science,* **323**(1), 153-158.

Al-Halbouni, D., Dott, W. and Hollender, J. 2009, "Occurrence and composition of extracellular lipids and polysaccharides in a full-scale membrane bioreactor", *Water Research,* **43**, (1), 97-106.

Arabi, S. and Nakhla, G. 2008, "Impact of calcium on the membrane fouling in membrane bioreactors", *Journal of Membrane Science,* **314**(1-2), 134-142.

Aspelund M.T., Rozeboom G., Heng M. and Glatz C.E., 2008, “Improving permeate flux and product transmission in the microfiltration of a bacterial cell suspension by flocculation with cationic polyelectrolytes”, *Journal of Membrane Science*, **324**(1-2), 198-208.

Baeyens, J., Hosten, L. and Van Vaerenbergh, E. 1997, *Wastewater treatment*, Kluwer Academic Publishers, The Netherlands.

Bin, Z., Baosheng, S., Min, J., Taishi, G. and Zhenghong, G. 2008, "Extraction and analysis of extracellular polymeric substances in membrane fouling in submerged MBR", *Desalination,* **227**(1-3), 286-294.

Bodzek, M., Waniek, A. and Konieczny, K. 2002, "Pressure driven membrane techniques in the treatment of water containing THMs", *Desalination*, **147**(1-3), 101-107.

Bolton, G., LaCasse, D. and Kuriyel, R., 2006, “Combined models of membrane fouling: Development and application to microfiltration and ultrafiltration of biological fluids”, *Journal of Membrane Science*, **277**, 75-84

Bowen, W.R., Calvo, J.I., and Hernández, A., 1995, "Steps of membrane blocking in flux decline during protein microfiltration", Journal of Membrane Science, **101**(1-2), 153-165.

Brindle, K., and Stephenson, T., 1996. ‘‘The application of membrane biological reactors for the treatment of wastewaters.’’ *Biotechnol. Bioeng*., **49**, 601–610.

Bruus J.H., Nielsen P.H. and Keiding K., 1992, On the stability of activated sludge flocs with implications to dewatering, *Water Research*, **26**(12), 1597-1604.

Chang, I.S., Le Clech, P., Jefferson, B. and Judd, S. 2002, "Membrane fouling in membrane bioreactors for wastewater treatment", *Journal of Environmental Engineering,* **128**, 1018.

Chua, H.C., Arnot, T.C., and Howell, J.A., 2002, “Controlling fouling in membrane bioreactors operated with a variable throughput”, *Desalination*, **149**, 225–229.

Costa, A.R., de Pinho, M.N. and Elimelech, M. 2006, "Mechanisms of colloidal natural organic matter fouling in ultrafiltration", *Journal of Membrane Science,* **281**(1-2), 716-725.

Coulson, J.M., Richardson, J.F., Backhurst, J.R. and Harker, J.H., 1991, “*Coulson & Richardson’s Chemical Engineering Volume 2: Particle Technology and Separation Processes*”, Butterworth-Heinemann, Oxford, 869-876.

Draget, K.I., Smidsrød, O. and Skjåk-Bræk, G. 2002, "Alginates from algae", *Biopolymers,* **6**, 215–240.

Evenblij, H., Geilvoet, S., Van der Graaf, J. and Van der Roest, H. 2005, "Filtration characterisation for assessing MBR performance: three cases compared", *Desalination,* **178**(1-3), 115-124.

Faibish, R.S. and Cohen, Y., 2001, “Fouling-resistant ceramic-supported polymer membranes for ultrafiltration of oil-in-water microemulsions”, *Journal of Membrane Science*., **185**, 129–143.

Fane, A.G., Fell, C.J.D. and and Nor, M.T. 1981, "Ultrafiltration/ Activated sludge system---development of a predictive model", *Polymer Science Technology,* **13**, 631-658.

Field, R.W., Wu, D., Howell, J.A., and Gupta, B.B., 1995, "Critical flux concept for microfiltration fouling", Journal of Membrane Science, **100**(3), 259-272.

Forster, C.F. 1971, "Activated sludge surfaces in relation to the sludge volume index", *Water Research,* **5**(10).

Frølund, B., Palmgren, R., Keiding, K. and Nielsen, P.H. 1996, "Extraction of extracellular polymers from activated sludge using a cation exchange resin", *Water Research,* **30**(8), 1749-1758.

Gan, Q., Howell, J.A., Field, R.W., England, R., Bird, M.R., and McKechinie, M.T., 1999, "Synergetic cleaning procedure for a ceramic membrane fouled by beer microfiltration", Journal of Membrane Science, **155**(2), 277-289.

Güell, C., Czekaj, P. and Davis, R. 1999, "Microfiltration of protein mixtures and the effects of yeast on membrane fouling", *Journal of Membrane Science,* **155**(1), 113-122.

Hermia, J. 1982, "Constant Pressure Blocking Filtration Laws-Application to Power-Law Non-Newtonian Fluids", *Chemical Engineering Research and Design,* **60**(a), 183-187.

Ho, W.S.W. and Sirkar, K.K.S. (ed.) 1992, *Membrane Handbook*, Van Nostrand Reinhold, New York, New York.

Hong, S. and Elimelech, M. 1997, "Chemical and physical aspects of natural organic matter (NOM) fouling of nanofiltration membranes", *Journal of Membrane Science,* **132**(2), 159-181.

Horan, N. and Eccles, C. 1986, "Purification and Characterization of Extracellular Polysaccharide from Activated Sludges", *Water Research WATRAG,* **20**(11), 1427-1432.

Houghton, J., Quarmby, J. and Stephenson, T. 2001, "Municipal wastewater sludge dewaterability and the presence of microbial extracellular polymer", *Water Science and Technology,* **44**(2), 373-379.

Hwang, K. J. and Lin, T. T., 2002, “Effect of morphology of polymeric membrane on the performance of cross-flow microfiltration”, *Journal of Membrane Science*, **199**, 41-52.

Jarusutthirak, C., Amy, G. and Croué, J.P. 2002, "Fouling characteristics of wastewater effluent organic matter (EfOM) isolates on NF and UF membranes", *Desalination,* **145**(1-3), 247-255.

Jermann, D., Pronk, W., Meylan, S. and Boller, M. 2007, "Interplay of different NOM fouling mechanisms during ultrafiltration for drinking water production", *Water Research,* **41**(8), 1713-1722.

Jiraratananon, R., Uttapap, D. and Sampranpiboon, P., 1998, "Crossflow microfiltration of a colloidal suspension with the presence of macromolecules", *Journal of Membrane Science*, **140**(1), 57-66.

Judd, S. and Jefferson, B. 2003, *Membranes for industrial wastewater recovery and re-use,* Elsevier, Oxford.

Katsoufidou, K., Yiantsios, S.G. and Karabelas, A.J. 2007, "Experimental study of ultrafiltration membrane fouling by sodium alginate and flux recovery by backwashing", *Journal of Membrane Science,* **300**(1-2), 137-146.

Kim, I.S. and Jang, N. 2006, "The effect of calcium on the membrane biofouling in the membrane bioreactor (MBR)", *Water Research,* **40**(14), 2756-2764.

Kimura, K., Yamato, N., Yamamura, H. and Watanabe, Y. 2005, "Membrane fouling in pilot-scale membrane bioreactors (MBRs) treating municipal wastewater", *Environmental Science & Technology,* **39**(16), 6293-6299.

Lesjean, B., Rosenberger, S., Laabs, C., Jekel, M., Gnirss, R. and Amy, G. 2005, "Correlation between membrane fouling and soluble/colloidal organic substances in membrane bioreactors for municipal wastewater treatment.", *Water Science and Technology,* **51**(6/7), 1-8.

Li, X., Gao, F., Hua, Z., Du, G. and Chen, J. 2005, "Treatment of synthetic wastewater by a novel MBR with granular sludge developed for controlling membrane fouling", *Separation and Purification Technology,* **46**(1-2), 19-25.

Li, Q. and Elimelech, M. 2004, "Organic Fouling and Chemical Cleaning of Nanofiltration Membranes: Measurements and Mechanisms", *Environmental science and technology,* **38**(17), 4683-4693.

Lu, S. G., Imai, T., Ukita, M., Sekine, M., Higuchi, T. and Fukagawa, M., 2001, "A Model for Membrane Bioreactor Process Based on the Concept of Formation and Degradation of Soluble Microbial Products", *Water Research*, **35**(8), 2038-2048

Lubbecke, S., Vogelpohl, A., and Dewjanin, W., 1995, ''Wastewater treatment in a biological high-performance system with high biomass concentration.'' *Water Research*., **29**, 793–802.

Mohammadi, T., Kazemimoghadam, M. and Saadabadi, M., 2003, "Modeling of membrane fouling and flux decline in reverse osmosis during separation of oil in water emulsions", Desalination,**157**(1-3), 369-375.

Negaresh, E., Le-Clech, P. and Chen, V. 2007, "Fouling mechanisms of model polymeric substances", *Asia-Pacific Journal of Chemical Engineering,* **2**(5), 394-399.

Neyens, E., Baeyens, J., Dewil, R. and De heyder, B. 2004, "Advanced sludge treatment affects extracellular polymeric substances to improve activated sludge dewatering", *Journal of Hazardous Materials,* **106**(2-3), 83-92.

Nguyen, T.P., Hankins, N.P. and Hilal, N. 2007, "Effect of chemical composition on the flocculation dynamics of latex-based synthetic activated sludge", *Journal of Hazardous Materials,* **139**(2), 265-274.

Nguyen, T.P., Hilal, N., Hankins, N.P. and Novak, J.T., 2008a, "The relationship between cation ions and polysaccharide on the floc formation of synthetic and activated sludge", *Desalination,* **227**(1-3), 94-102.

Nguyen, T.P., Hilal, N., Hankins, N.P. and Novak, J.T. 2008b, "Determination of the effect of cations and cationic polyelectrolytes on the characteristics and final properties of synthetic and activated sludge", *Desalination,* **222**(1-3), 307-317.

Örmeci, B. and Vesilind, P.A., 2000, “Development of an improved synthetic sludge: a possible surrogate for studying activated sludge dewatering characteristics”, *Water Research,* **34**(4), 1069-1078.

Osmonics Inc., 2002. The Osmonics Filtration Spectrum

Availble at:http://www.liquidfiltration-products.com/LiquidFiltration/Osmonicsfiltraspec.html

Palintest Ltd, 2007, Palintest Photometer 7100 Manual, Palintest Instruments, UK

Prádanos, P., Hernández, A., Calvo, J.I., and Tejerina, F., 1996, "Mechanisms of protein fouling in cross-flow UF through an asymmetric inorganic membrane", *Journal of Membrane Science*, **114**(1), 115-126.

Rosenberger, S., Evenblij, H., te Poele, S., Wintgens, T. and Laabs, C. 2005, "The importance of liquid phase analyses to understand fouling in membrane assisted activated sludge processes—six case studies of different European research groups", *Journal of Membrane Science,* **263**(1-2), 113-126.

Rosenberger, S. and Kraume, M. 2003, "Filterability of activated sludge in membrane bioreactors", *Desalination,* **151**(2), 195-200.

Sanin, F.D. and Vesilind, P.A., 1999, “A comparison of physical properties of synthetic sludge with activated sludge”, *Water Environment Research,* **71**(2), 191-196.

Schäfer, A.I., Fane, A.G. and Waite, T.D. 1998, "Nanofiltration of natural organic matter: Removal, fouling and the influence of multivalent ions", *Desalination,* **118**(1-3), 109-122.

Shimizu, Y., Shimodera, K. I., and Watanabe, A., 1993, “Cross flow microfiltration of bacterial cells”*J. Ferment. Bioeng*., **76**, 493-500

Singh, R. 2006, *Hybrid membrane systems engineering for water purification : technology, systems design and operation,* Elsevier, Oxford.

Sobeck, D.C. and Higgins, M.J. 2002, "Examination of three theories for mechanisms of cation-induced bioflocculation", *Water Research,* **36**(3), 527-538.

Song, L. and Elimelech, M. 1995, "Theory of concentration polarization in crossflow filtration", *Journal of the Chemical Society, Faraday Transactions,* **91**(19), 3389-3398.

Song, L. 1998, "Flux decline in crossflow microfiltration and ultrafiltration: mechanisms and modeling of membrane fouling", *Journal of Membrane Science,* **139**(2), 183-200.

Steiner, A., McLaren, D. and Forster, C. 1976, "The nature of activated sludge flocs", *Water Research,* **10**(1), 25-30

Tarleton, E. and Wakeman, R. 1993, "Understanding Flux Decline in Crossflow Microfiltration-Part I-Effects of Particle and Pore Size", *Chemical Engineering Research and Design,* **71**(a), 399-410.

Tarnacki, K., Lyko, S., Wintgens, T., Melin, T. and Natau, F. 2005, "Impact of extra-cellular polymeric substances on the filterability of activated sludge in membrane bioreactors for landfill leachate treatment", *Desalination,* **179**(1-3), 181-190.

van de Ven, W.J.C., Sant, K.v., Pünt, I.G.M., Zwijnenburg, A., Kemperman, A.J.B., van der Meer, W.G.J. and Wessling, M. 2008, "Hollow fiber dead end ultrafiltration: Influence of ionic environment on filtration of alginates", *Journal of Membrane Science,* **308**(1-2), 218-229.

Varian Australia Pty. Ltd., 1989, SpectrAA 200 Manual, Australia

Vela, V., Cinta, M. and Blanco, Á., 2009, "Analysis of membrane pore blocking models adapted to crossflow ultrafiltration in the ultrafiltration of PEG", *Chemical Engineering Journal,* **149**(1-3), 232-241.

Water Environment Federation 2005, *Membrane systems for wastewater treatment,* McGraw-Hill, London.

Yamamoto, K., issa, M., Mahmood, T., and Matsuo, T., 1989, “Direct solid liquid separation using hollow fiber membrane in an activated sludge aeration tank” Water Science and Technology, **21**, 43-54.

Ye, Y., Clech, P.L., Chen, V. and Fane, A. 2005a, "Evolution of fouling during crossflow filtration of model EPS solutions", *Journal of Membrane Science,* **264**(1-2), 190-199.

Ye, Y., Le Clech, P., Chen, V., Fane, A.G. and Jefferson, B. 2005b, "Fouling mechanisms of alginate solutions as model extracellular polymeric substances", *Desalination,* **175**(1), 7-20.

Yoon, S., Lee, C., Kim, K. and Fane, A.G. 1998, "Effect of calcium ion on the fouling of nanofilter by humic acid in drinking water production", *Water Research,* **32**(7), 2180-2186.

Zhong, Z., Xing, W., Liu, X., Jin, W. and Xu, N., 2007, "Fouling and regeneration of ceramic membranes used in recovering titanium silicalite-1 catalysts", *Journal of Membrane Science,* **301**(1-2), 67-75.

Zhou, J., Yang, F., Meng, F., An, P. and Wang, D., 2007, "Comparison of membrane fouling during short-term filtration of aerobic granular sludge and activated sludge", *Journal of Environmental Sciences,* **19**(11), 1281-1286.

Appendix A: Artificial Wastewater Experimental Results

The artificial wastewater experiments filtration result for 20 kD membrane

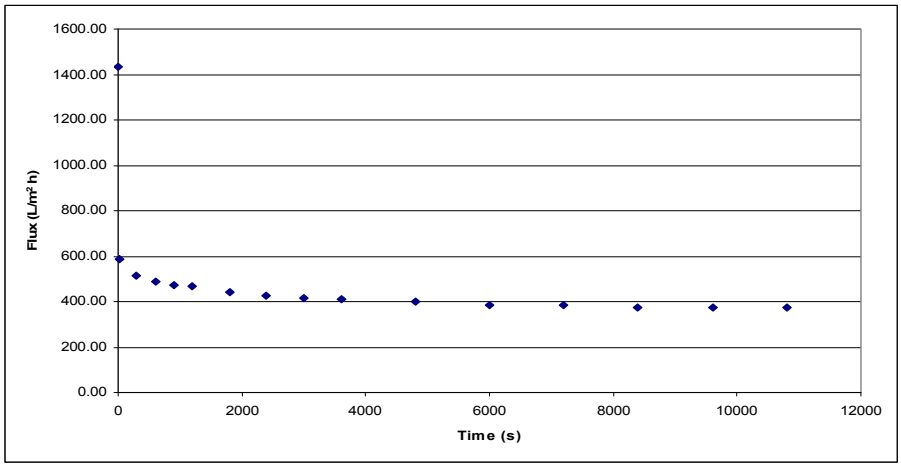

Flux vs. time for experiment F0

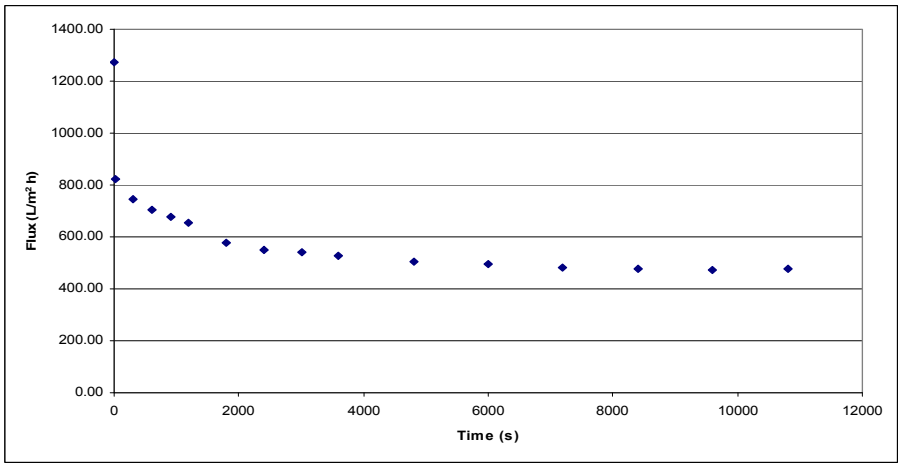

Flux vs. time plot for experiment F1

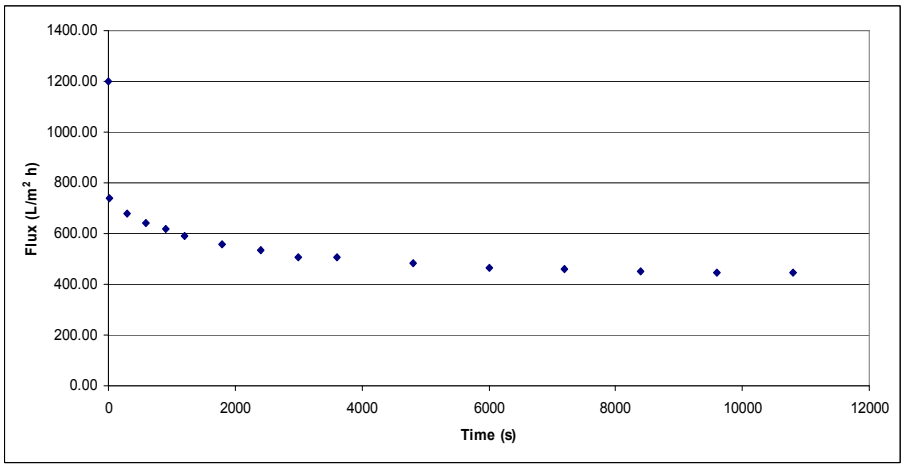

Flux vs. time plot for experiment F2

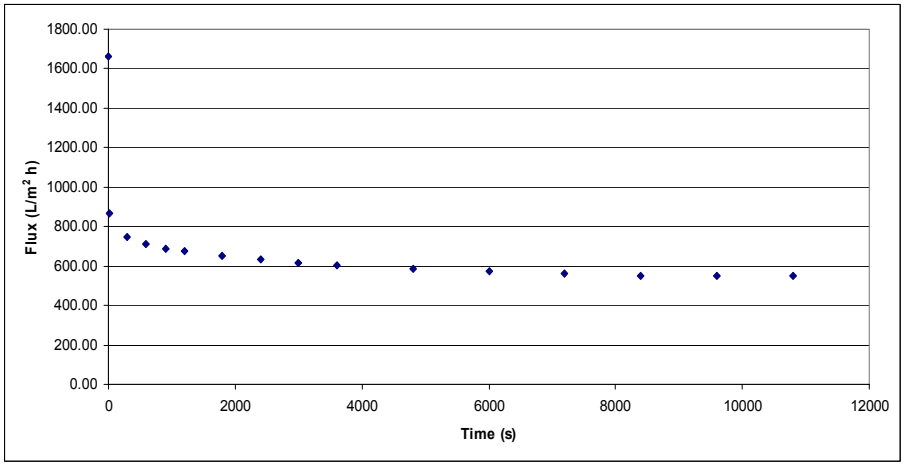

Flux vs. time plot for experiment F3

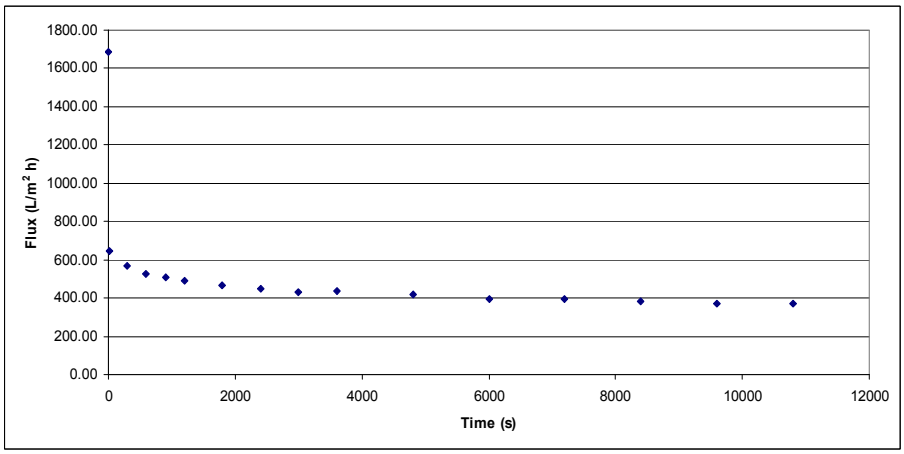

Flux vs. time plot for experiment F4

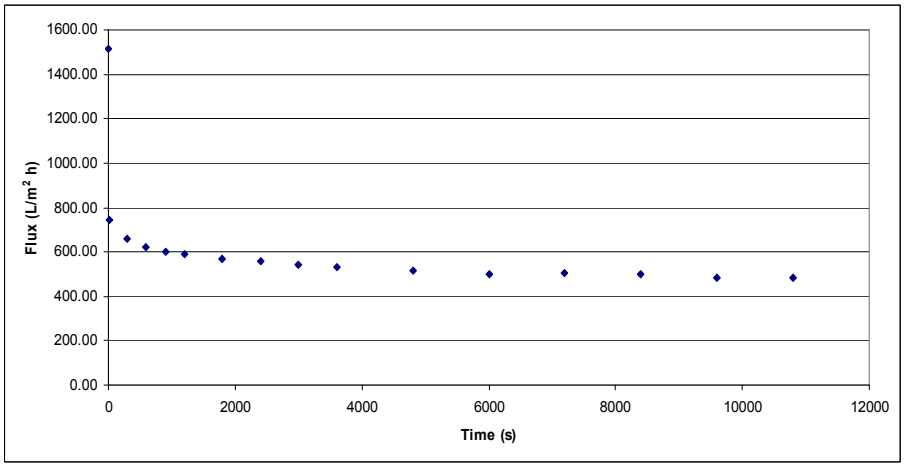

Flux vs. time plot for experiment F5

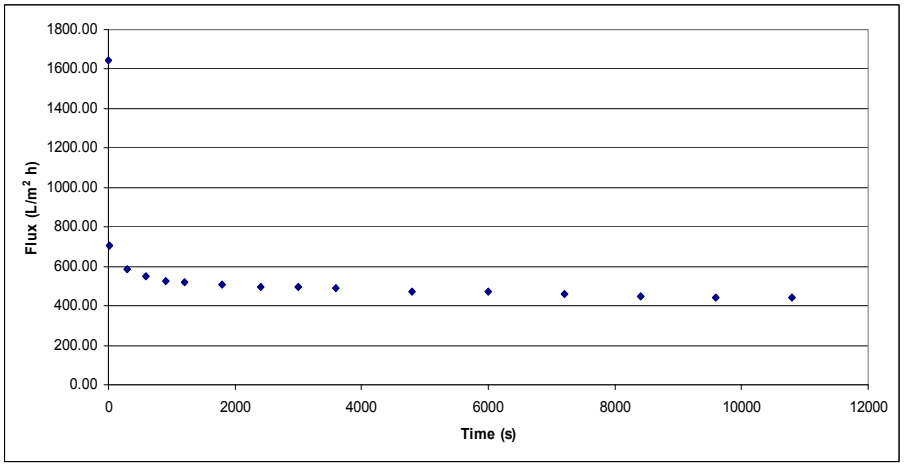

Flux vs. time plot for experiment F6

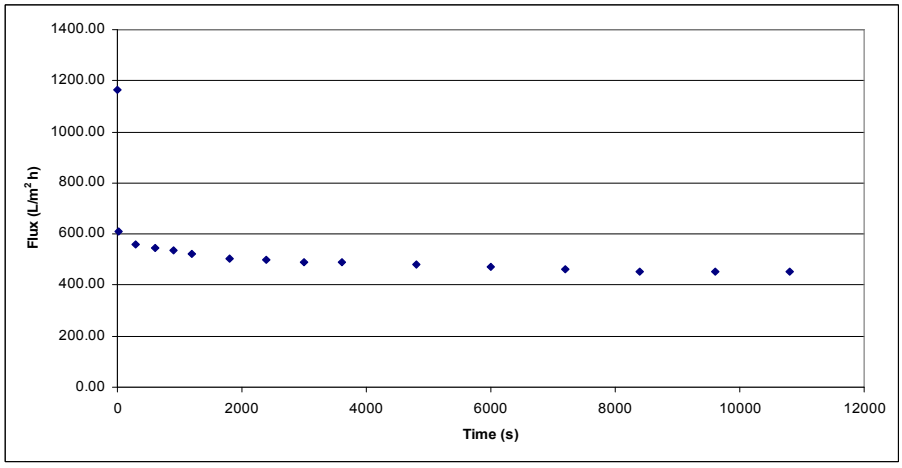

Flux vs. time plot for experiment F7

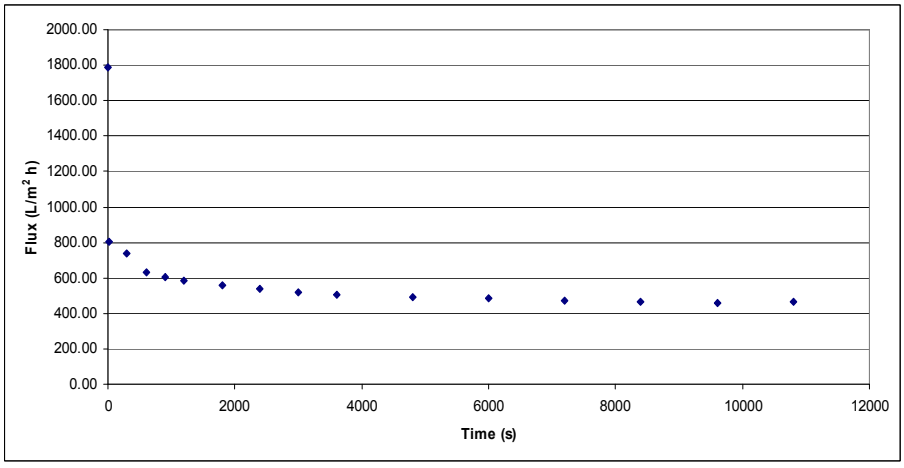

Flux vs. time plot for experiment F8

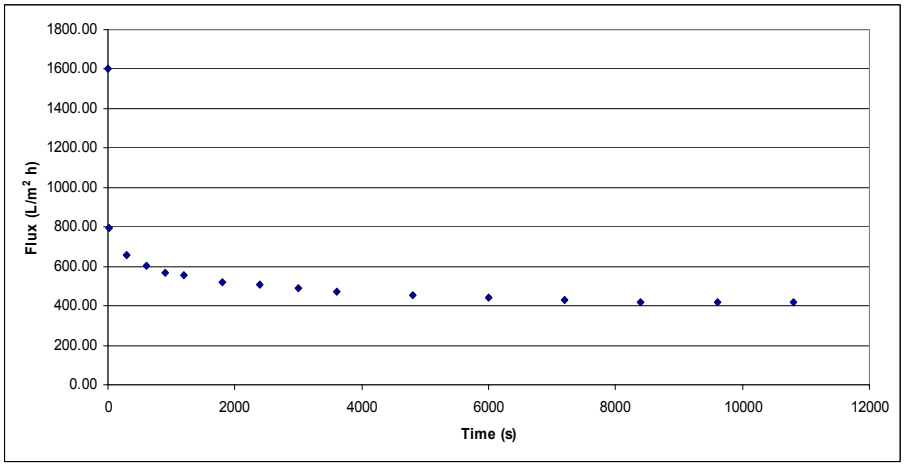

Flux vs. time plot for experiment F9

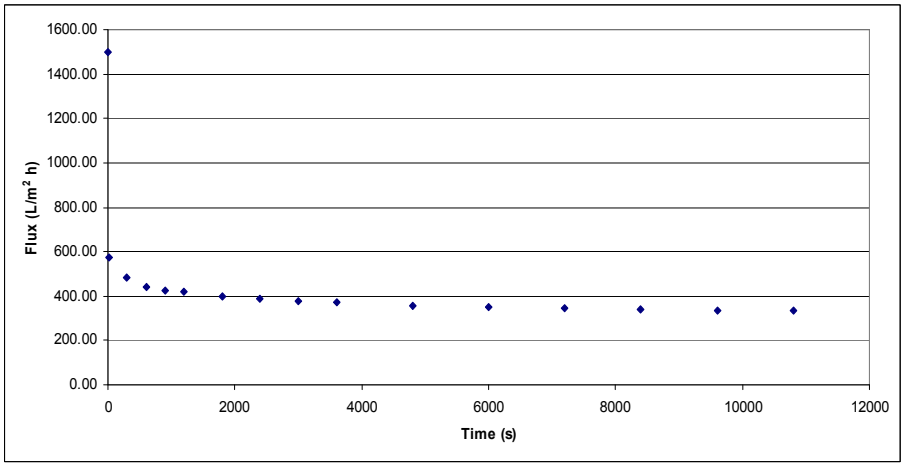

Flux vs. time plot for experiment F10

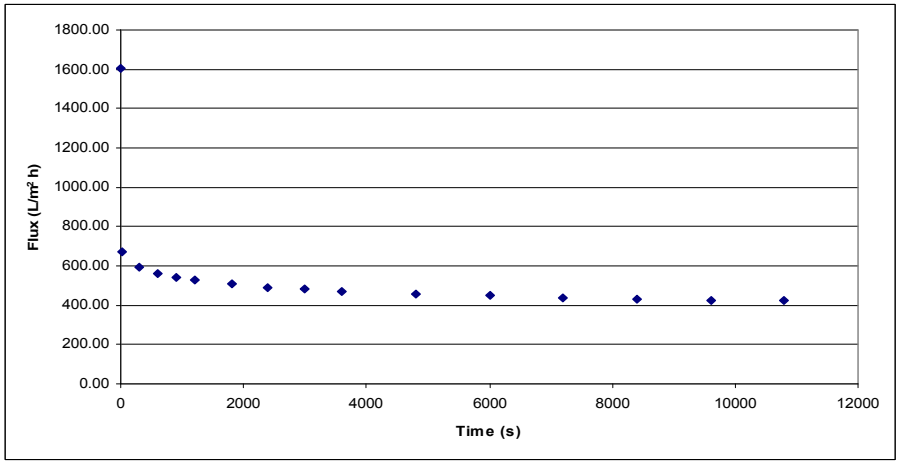

Flux vs. time plot for experiment F11

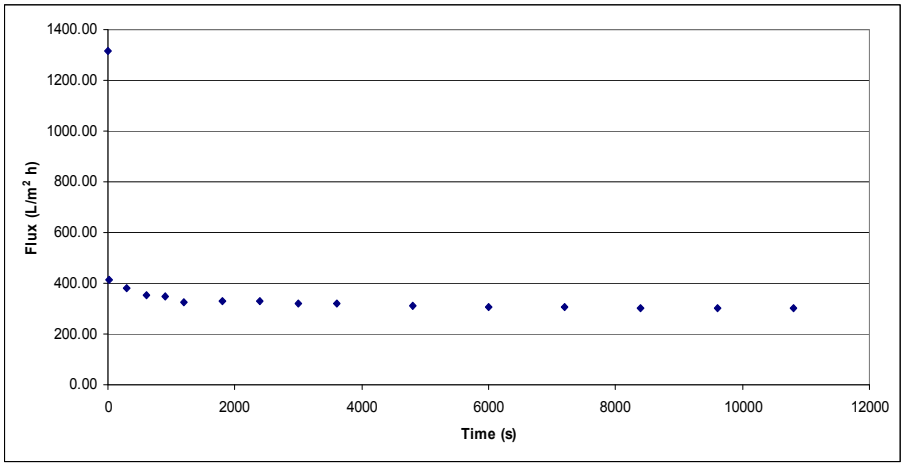

Flux vs. time plot for experiment F12

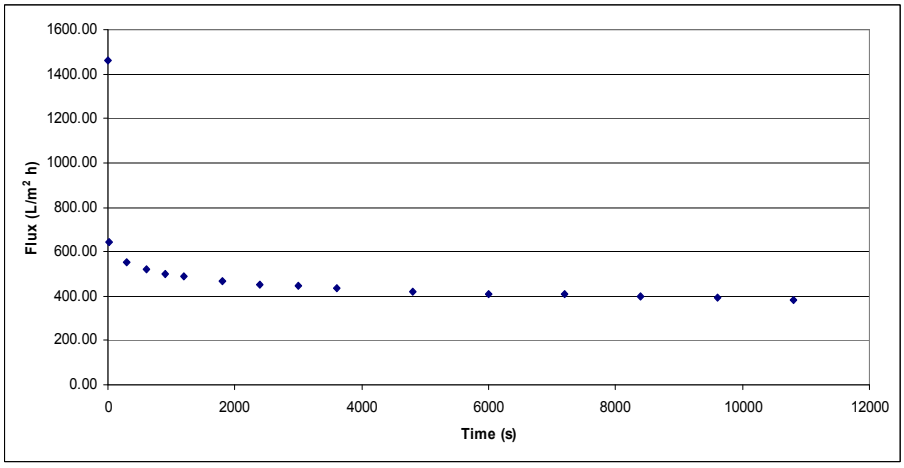

Flux vs. time plot for experiment F13

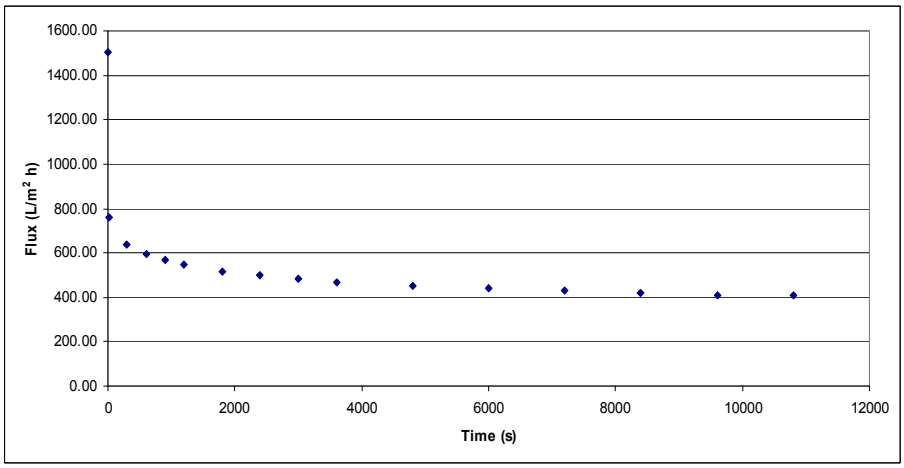

Flux vs. time plot for experiment F14

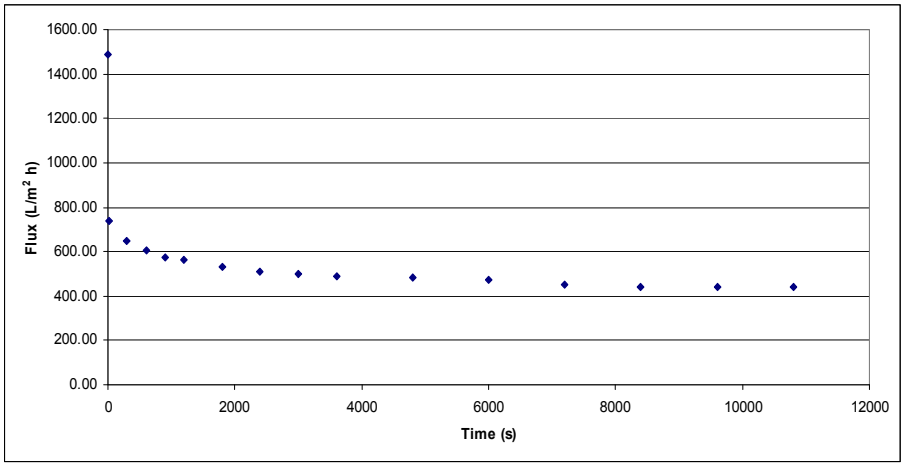

Flux vs. time plot for experiment F15

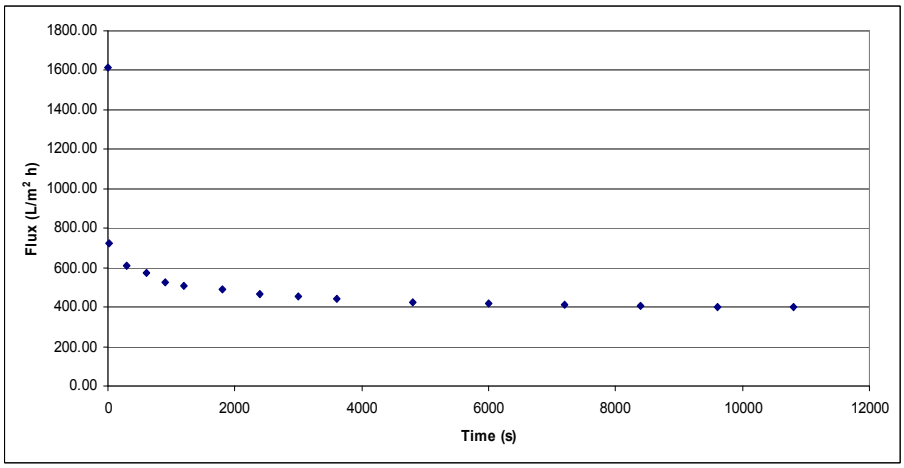

Flux vs. time plot for experiment F16

The artificial wastewater experiments filtration result for 5 kD membrane

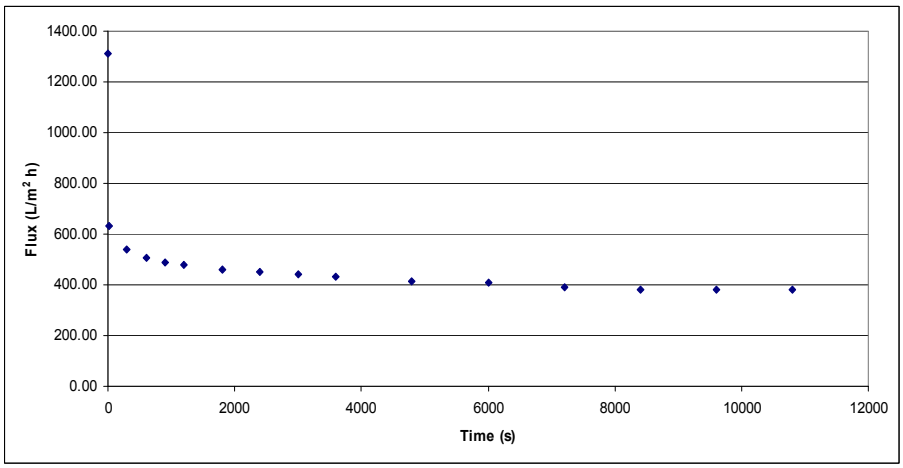

Flux vs. time plot for experiment F0

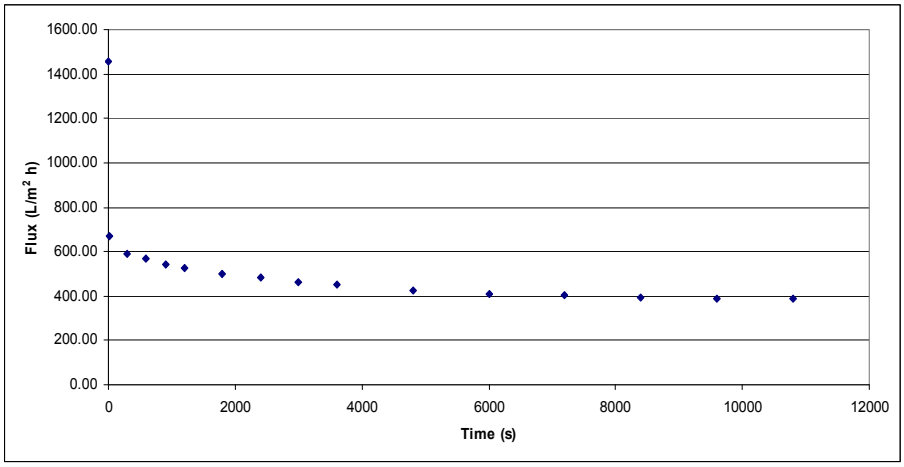

Flux vs. time plot for experiment F1

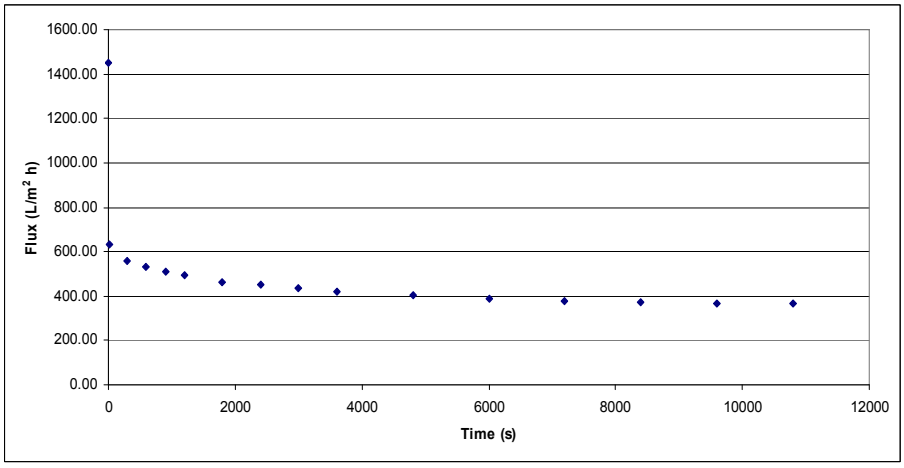

Flux vs. time plot for experiment F2

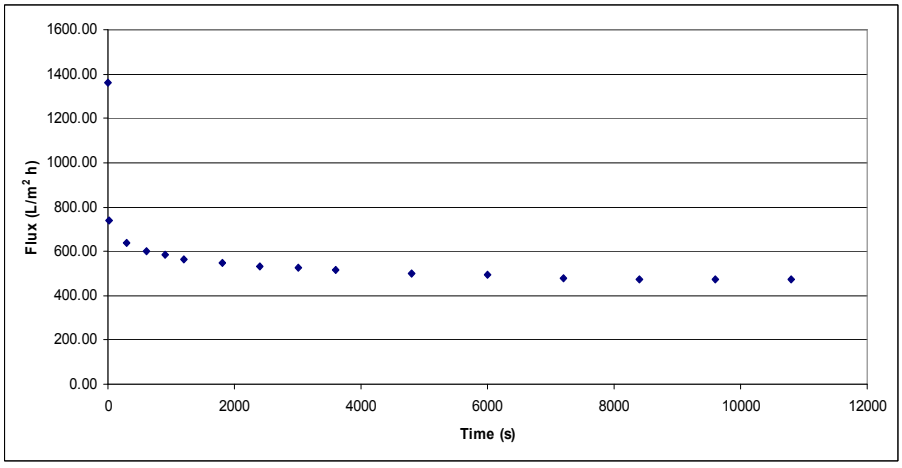

Flux vs. time plot for experiment F3

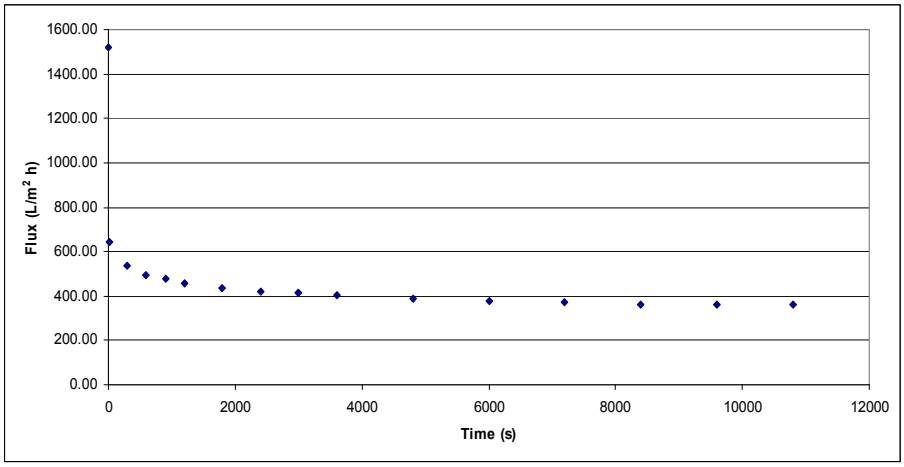

Flux vs. time plot for experiment F4

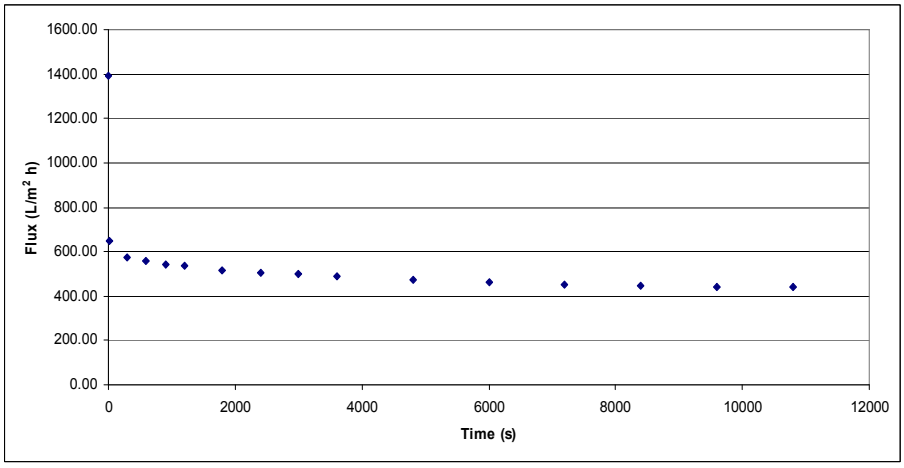

Flux vs. time plot for experiment F5

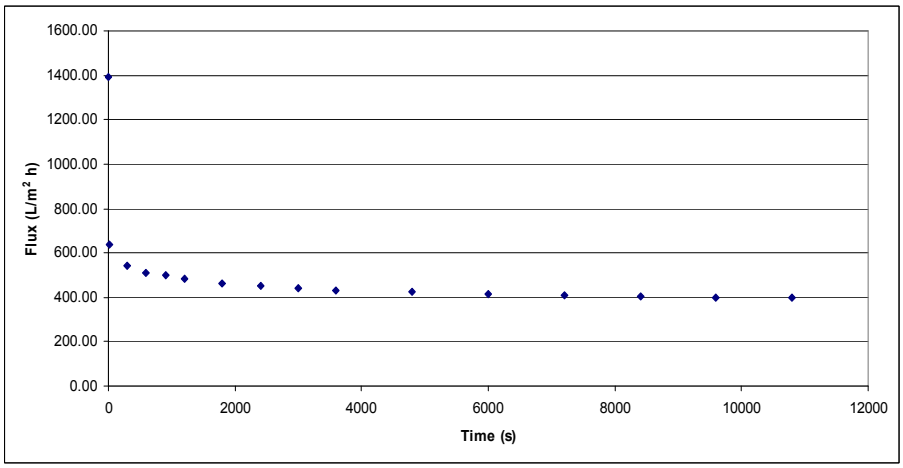

Flux vs. time plot for experiment F6

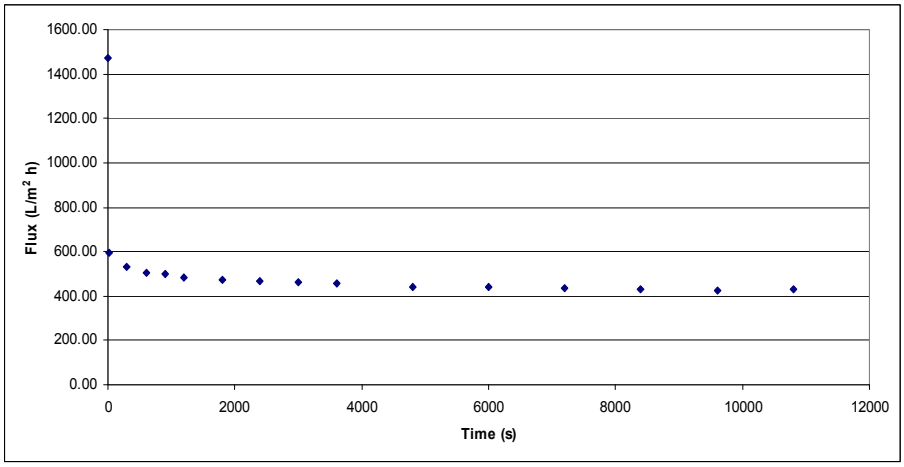

Flux vs. time plot for experiment F7

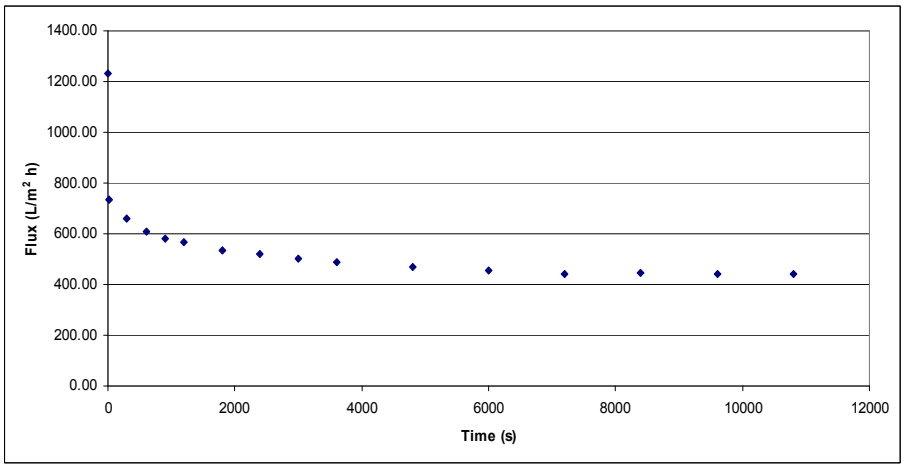

Flux vs. time plot for experiment F8

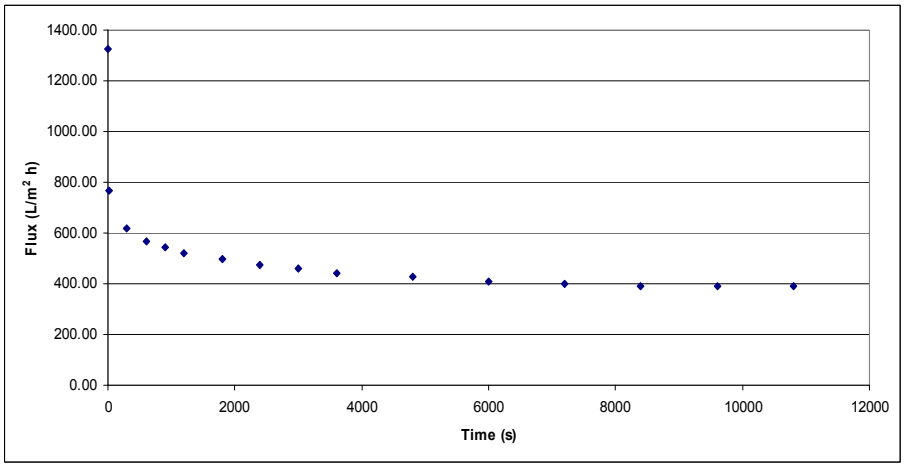

Flux vs. time plot for experiment F9

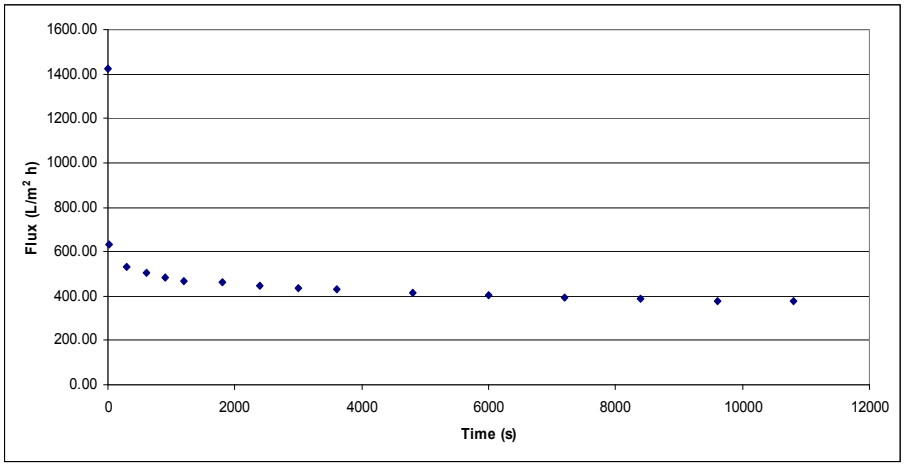

Flux vs. time plot for experiment F10

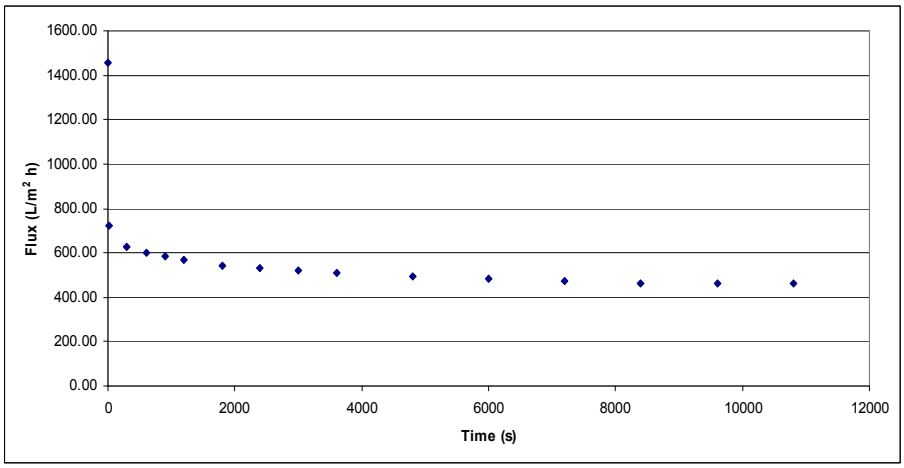

Flux vs. time plot for experiment F11

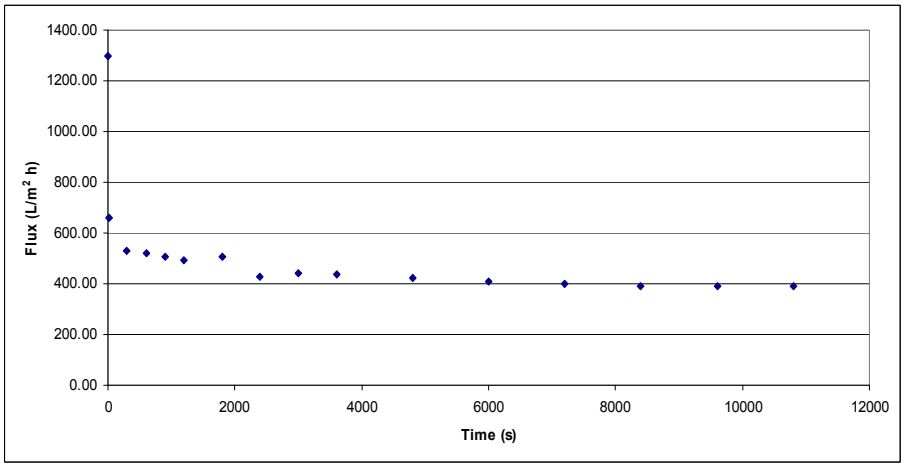

Flux vs. time plot for experiment F12

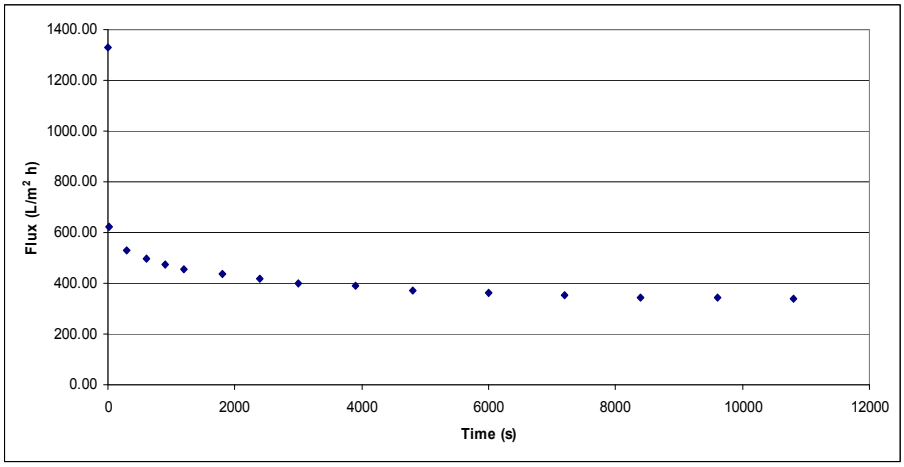

Flux vs. time plot for experiment F13

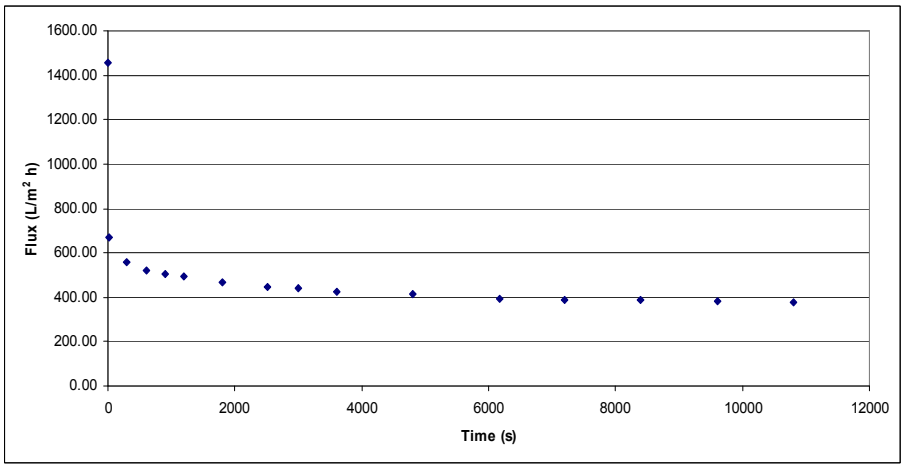

Flux vs. time plot for experiment F14

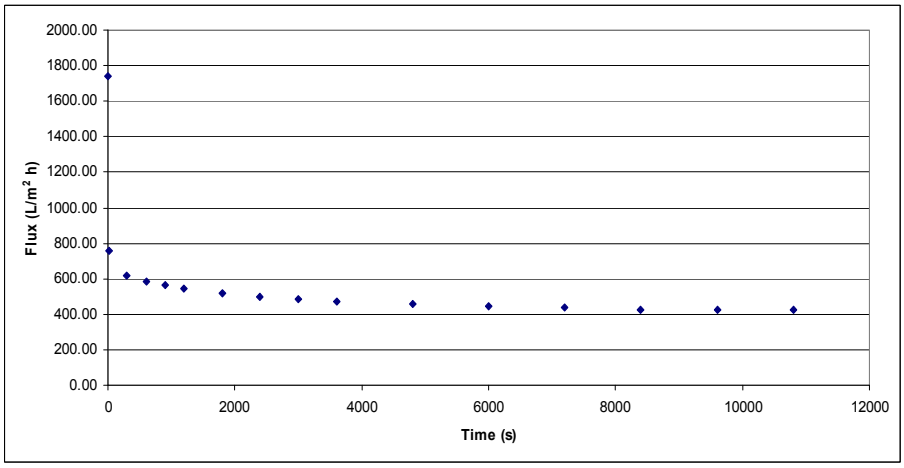

Flux vs. time plot for experiment F15

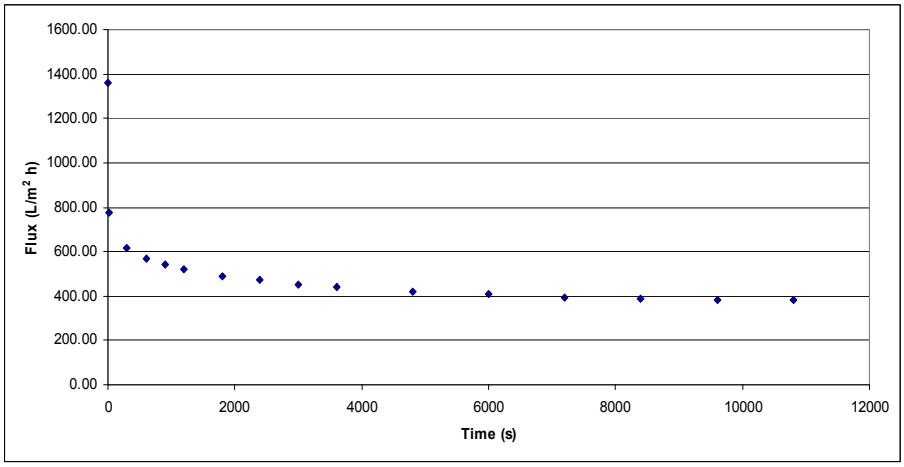

Flux vs. time plot for experiment F16

Appendix B: The Matlab modelling programmes.

The Main programme

```
clc
clf

fit_JCake; % Run the Cake filtration model
fit_JComplete; % Run the Complete blocking model
fit_JIntermediate; % Run the Intermediate blocking model
fit_JStandard; % Run the Standard blocking model

% Setup the main graph
%[ax,h3]=suplabel('Blocking mechanisms fitting' ,'t');
%set(h3,'FontSize',20)

% Creat a table for the fitting results
table=[SSE_Cake; SSE_Complete; SSE_Intermediate; SSE_Standard];
fprintf('\n')
fprintf('  Cake SSE        Complete SSE         Intermediate SSE          Standard SSE\n')
fprintf(' %2.3e       %2.3e             %2.3e              %2.3e\n',table)
fprintf('\n')
table2=[Rsq_Cake; Rsq_Complete; Rsq_Intermediate; Rsq_Standard];
fprintf('\n')
fprintf('  Cake Rsq        Complete Rsq         Intermediate Rsq          Standard Rsq\n')
fprintf('   %2.3f\t        %2.3f\t             %2.3f\t              %2.3f\n',table2)
fprintf('\n')
```

Complete blocking model fitting programme:

```
%*********************************************************************%
%Complete blocking model fitting program.
%the Complet blocking model equation used in this program from the
work
%of Vela et al., 2009.
%The program use the LSQCURVEFIT function which solves non-linear
least
%squares problems.
%*********************************************************************%

clear
clf
clc
%loading The filtration experiment data
load JMExF0.dat;
%set time data to x in (s)
x=JMExF0(:,1);
%set permeate flux data to y in (m/s)
```

```
y=JMExF0(:,2);
%Jo is the initial flux
global Jo
Jo=JMExF0(1,2);
%Jpss is the steady stat flux
global Jpss
Jpss=JMExF0(16,2);

%Initial guess
%the better your initial condition guesses are, the faster
%the lsqcurvefit command will converge onto a solution
initialConditions = 1.0;


options= optimset('TolFun',1e-20);

%newParameters is an array containing the optimal values that will
%generate a curve that will best fit your data
%error is the sum of the error squared.  the lower this number is,
the better
[newParameters,error] = lsqcurvefit(@JComplete,
initialConditions,x,y,[],[],options);

%use new parameters to get new output values
y2 = JComplete(newParameters,x);

%check the error
diff=y-y2;
diff_sq=diff.^2;
SSE_Complete=sum(diff_sq);

%SST and R-squired calculation
y_sum=sum(y);
n=numel(y);
yavg=y_sum/n;
diff2=y-yavg;
diff2_sq=(diff2).^2;
SST_Complete=sum(diff2_sq);
Rsq_Complete=1-(SSE_Complete/SST_Complete);
```

%plot the new data using the color red
subplot(2,2,2)
plot(x,y,'o',x,y2,'r')
title('Complete blocking model fit')
xlabel({'Time (s)'})
ylabel({'J (m/s)'})
hold on

Complete blocking function sub programme:

```
function output= JComplete (param,input)

global Jo % the initial flux
global Jpss % the steady state flux

a = param(1);

% this is the Complete blocking model equation here
output =Jpss + (Jo - Jpss)*exp(-a.*input.*Jo);
```

Intermediate blocking model fitting programme:

```
---------------------------------------------------------------------

%*********************************************************************%
%Intermediate blocking model fitting program.
%the Intermediate blocking model equation used in this program from
the work
%of Vela et al., 2009.
%The program use the LSQCURVEFIT function which solves non-linear
least
%squares problems.
%*********************************************************************%

clear
clf
clc
%loading The filtration experiment data
load JMExF0.dat;
%set time data to x in (s)
x=JMExF0(:,1);
%set permeate flux data to y in (m/s)
y=JMExF0(:,2);
%Jo is the initial flux
global Jo
Jo=JMExF0(1,2);
%Jpss is the steady stat flux
global Jpss
Jpss=JMExF0(16,2);

%Initial guess
%the better your initial condition guesses are, the faster
%the lsqcurvefit command will converge onto a solution
initialConditions = 1.0;

%newParameters is an array containing the optimal values that will
%generate a curve that will best fit your data

options= optimset('TolFun',1e-20);

%error is the sum of the error squared.  the lower this number is,
the better
[newParameters,error] = lsqcurvefit(@JIntermediate,
initialConditions,x,y,[],[],options);


%use new parameters to get new output values
y2 = JIntermediate(newParameters,x);

% Check the error
diff=y-y2;
diff_sq=diff.^2;
SSE_Intermediate=sum(diff_sq);

% SST and Rsqr calculation
y_sum=sum(y);
n=numel(y);
```

```
yavg=y_sum/n;
diff2=y-yavg;
diff2_sq=(diff2).^2;
SST_Intermediate=sum(diff2_sq);
Rsq_Intermediate=1-(SSE_Intermediate/SST_Intermediate);
```

%plot the new data using the color red
subplot(2,2,3)
plot(x,y,'o',x,y2,'r')
title('Intermediate blocking model fit')
xlabel({'Time (s)'})
ylabel({'J (m/s)'})
hold on

Intermediate blocking function sub programme:

```
function output= JIntermediate (param,input)

global Jo % the initial flux
global Jpss % the steady state flux

a = param(1);

% this is the Intermediate blocking model equation here
output =(Jo*Jpss*exp(Jpss*a.*input))/(Jpss + Jo*(exp(Jpss*a.*input)-
1));
```

Standard blocking model fitting programme:

```
%*********************************************************************%
%Standard blocking model fitting program.
%the Standard blocking model equation used in this program from the
work
%of Vela et al., 2009.
%The program use the LSQCURVEFIT function which solves non-linear
least
%squares problems.
%*********************************************************************%

clear
clf
clc
%loading The filtration experiment data
load JMExF0.dat;
%set time data to x in (s)
x=JMExF0(:,1);
%set permeate flux data to y in (m/s)
y=JMExF0(:,2);
%Jo is the initial flux
global Jo
Jo=JMExF0(1,2);
%Jpss is the steady stat flux
global Jpss
Jpss=JMExF0(16,2);

%Initial guess
%the better your initial condition guesses are, the faster
```

```
%the lsqcurvefit command will converge onto a solution
initialConditions = 0.01;

%newParameters is an array containing the optimal values that will
%generate a curve that will best fit your data

options= optimset('TolFun',1e-20);

%error is the sum of the error squared.  the lower this number is,
the better
[newParameters,error] = lsqcurvefit(@JStandard,
initialConditions,x,y,[],[],options);


%use new parameters to get new output values
y2 = JStandard(newParameters,x);

% Check the error
diff=y-y2;
diff_sq=diff.^2;
SSE_Standard=sum(diff_sq);

% SST ans Rsqr calculation
y_sum=sum(y);
n=numel(y);
yavg=y_sum/n;
diff2=y-yavg;
diff2_sq=(diff2).^2;
SST_Standard=sum(diff2_sq);
Rsq_Standard=1-(SSE_Standard/SST_Standard);
```

%plot the new data using the color red
subplot(2,2,4)
plot(x,y,'o',x,y2,'r')
title('Standard blocking model fit')
xlabel({'Time (s)'})
ylabel({'J (m/s)'})
hold on

Standard blocking function sub programme:

```
function output= JStandard (param,input)

global Jo % Initial flux
global Jpss % steady state flux

a = param(1);

% this is the Standard blocking model equation here
output =Jo./(1+Jo^2*a.*input).^2;
```

Cake filtration model fitting programme:

```
%*****************************************************************
***%
%Cake blocking model fitting program.
%the Cake blocking model equation used in this program from the work
%of Vela et al., 2009.
```

```
%The program use the LSQCURVEFIT function which solves non-linear
least
%squares problems.
%*********************************************************************
***%

clear
clf
clc
%loading The filtration experiment data
load JMExF0.dat;
%set time data to y in (s)
y=JMExF0(:,1);
%set permeate flux data to x in (m/s)
x=JMExF0(:,2);
%Jo is the initial flux
global Jo
Jo=JMExF0(1,2);
%Jpss is the steady stat flux
global Jpss
Jpss=JMExF0(16,2);

%Initial guess
%the better your initial condition guesses are, the faster
%the lsqcurvefit command will converge onto a solution
initialConditions = 10000;

%newParameters is an array containing the optimal values that will
%generate a curve that will best fit your data

options= optimset('TolFun',1e-20);

%error is the sum of the error squared.  the lower this number is,
the better
[newParameters,error] = lsqcurvefit(@JCake,
initialConditions,x,y,[],[],options);

%use new parameters to get new output values
y2 = JCake(newParameters,x);

%Check the error
diff=y-y2;
diff_sq=diff.^2;
SSE_Cake=sum(diff_sq);

%SST and Rsqr calculation
y_sum=sum(y);
n=numel(y);
yavg=y_sum/n;
diff2=y-yavg;
diff2_sq=(diff2).^2;
SST_Cake=sum(diff2_sq);
Rsq_Cake=1-(SSE_Cake/SST_Cake);

%plot the new data using the color red
subplot(2,2,1)
plot(x,y,'o',x,y2,'r')
title('Cake blocking model fit')
xlabel({'Time (s)'})
ylabel({'J (m/s)'})
```

hold on

Cake filtration function sub programme:

```
function output= JCake (param,input)

global Jo % initial flux
global Jpss % steady state flux

a = param(1);

% this is the Cake blocking model equation here

output = (1/(a*Jpss^2))*log(((input./Jo)*((Jo-Jpss)/(input-Jpss)))-
Jpss*((1./input)-(1/Jo)));
```

Appendix C: Published Work

Alazmi, R., Nassehi, V. and Wakeman, R., 2010. Calcium cation interactions with polysaccharides and proteins in wastewater UF membrane fouling. *Membrane Technology*, **2010**(1), 6-12.

FEATURE

Calcium cation interactions with polysaccharides and proteins in wastewater UF membrane fouling

Radhi Alazmi and Vahid Nassehi, Advanced Separations Technologies Group, Department of Chemical Engineering, Loughborough University, Loughborough, UK, and Richard Wakeman, Consultant Chemical Engineer, Exeter, UK

The role of divalent calcium cations in bio-flocculation and their interactions with wastewater components such as biopolymers (proteins, polysaccharides, nucleic acids and lipids) are crucial in membrane fouling. In this work, the interactions between calcium cations and sodium alginate (a model polysaccharide) and meat extract (a complex protein mixture) were investigated. Dead-end stirred cell and crossflow ultrafiltration experimental matrices were carried out. The alginate–calcium interaction was found to be a more severe foulant of the membrane than the meat-extract–calcium. The alginate–calcium membrane fouling was almost completely irreversible, while 40% of the membrane fouling was reversible with the meat-extract–calcium filtration experiments. Membrane fouling by alginate and meat extract was greater when the two coexisted in the feed stream than when they existed as individual components.

In traditional activated sludge wastewater treatment processes, aggregation of microbials into flocs – bio-flocculation – is an important and desirable process. Bio-flocculation improves solid/liquid separation which, in turn, leads to improved settling and dewatering in the bioreactor.

Several research studies have been dedicated to exploring the roles of cations in bio-flocculation and the mechanisms by which bio-flocculation occurs.[1–3] The influence of different cations (monovalent, divalent and trivalent) on membrane fouling has been studied extensively for both submerged and crossflow membrane bioreactors.[4–7]

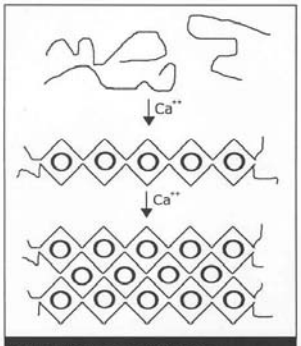

Figure 1. Alginate–calcium cations 'egg-box' model.[1]

Three theories exist that describe the roles of cations in bio-flocculation – the Derjaguin, Landau, Verwey and Overbeek (DLVO) theory, the alginate theory and the divalent cation bridging (DCB) theory.

In the DLVO theory, particles are surrounded by a double layer of counter-ions, composed of a tightly associated layer of counter-ions, the so-called Stern layer, and a second layer of less tightly associated counter-ions known as the diffuse layer. The negative cloud surrounding the particles results in repulsion forces between particles. According to this theory, increasing cation concentration should compress the double layer, thus allowing particles to aggregate.

In the alginate theory, alginate, which is a polysaccharide made up of linear copolymers of 1–4 linked β-D-mannuronic and α-L-guluronic acids monomers,[8] forms a gel in the presence of Ca^{++}. The gel forms an 'egg-box' structure as shown in **Figure 1**, which is unique to the alginate composition.[9] Polysaccharides such as alginate are unprotonated at a typical activated sludge pH. The unprotonated carboxyl groups thus contribute to the bio-floc negative charge.[10, 11]

The DCB theory emphasises the role of cations such as Ca^{++} and Mg^{++} in bridging between the negatively charged functional groups that exist on the extracellular polymeric substances (EPS), as illustrated in **Figure 2**. The bridging allows biopolymers to aggregate and encourages bio-flocculation.[1]

There is some disagreement among researchers on the definitions of reversible and irreversible membrane fouling, and some consider limiting the classification of membrane fouling to irreversible and reversible is somewhat simplistic.[12] Nevertheless, researchers consider that irreversible fouling involves a foulant that cannot be removed with physical cleaning but may be removed by chemical cleaning.[13–15]

Although some studies could not find a clear relationship between the concentration of EPS and membrane fouling,[16] it is generally accepted that EPS (polysaccharides, proteins, humic substances and lipids), which are biopolymers produced by microorganisms by cell lysis or active transport, are the major fouling substances in the

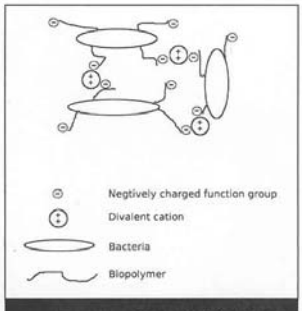

Figure 2. Divalent cation bridging.[1]

Appendix D: Factorial Design Calculations

Numbers of factors (components) = 4

Component	High Level (mg/l)	Low Level (mg/l)	Factor
Na Alginate	150	100	X_1
Peptone	270	180	X_2
Meat Ex.	270	180	X_3
CaCl2	60	20	X_4

Number of experiments needed to examine all possible combinations of high and low factors levels are:

Number of runs = 2^k , where k is the number of factors (components)

Number of runs= 2^4 = 16

The factorial design experimental matrix is:

Run	X_1	X_2	X_3	X_4
F5	150	270	90	20
F3	50	270	90	20
F1	150	90	270	20
F8	50	90	270	20
F10	150	270	270	60
F16	50	90	270	60
F0	100	180	180	40
F15	50	270	90	60
F11	50	90	90	20
F2	150	270	270	20
F12	150	90	90	60
F9	50	270	270	60
F14	50	90	90	60
F13	50	270	270	20
F6	150	270	90	60
F7	150	90	90	20
F4	150	90	270	60

A response is measured (Y) in all filtration experiments such as membrane resistance increase, permeate flux reduction, blocking model fitting accuracy…etc.

Membrane resistance increase (Y):

Run	Y (%)
F5	225
F3	195
F1	293
F8	185
F10	313
F16	278
F0	263
F15	328
F11	227
F2	313
F12	231
F9	243
F14	285
F13	300
F6	263
F7	264
F4	320

The factorial design equation for the sixteen experiments run to be solve is:

$$Y = \beta_0 + \beta_1 X_1 + \beta_2 X_2 + \beta_3 X_3 + \beta_4 X_4 + \beta_{12} X_1 X_2 + \beta_{13} X_1 X_3 + \beta_{14} X_1 X_4 + \beta_{23} X_2 X_3 + \beta_{24} X_2 X_4 + \beta_{34} X_3 X_4 + \beta_{123} X_1 X_2 X_3 + \beta_{124} X_1 X_2 X_4 + \beta_{134} X_1 X_3 X_4 + \beta_{234} X_2 X_3 X_4 + \beta_{1234} X_1 X_2 X_3 X_4$$

where β_0 is the intercept coefficient

β_i is the mean effect of factor X_i

β_{ij} is the two-way interaction effect between factor X_i and X_j

β_{ijk} is the three-way interaction effect between factors X_i, X_j and X_k

β_{ijkn} is the four-way interaction effect between factors X_i , X_j , X_k and X_n

Minitab® Software factorial design output files

Artificial wastewater 20 kD membrane crossflow experiments:

09/01/2009 04:53:59 PM

```
Welcome to Minitab, press F1 for help.
```

Factorial Design

```
Full Factorial Design

Factors:        4   Base Design:          4, 16
Runs:          17   Replicates:               1
Blocks:      none   Center pts (total):       1

All terms are free from aliasing


Saving file as: C:\Program Files\MTBWIN\Data\UF 20 kDa experiments.MPJ
```

Fractional Factorial Fit: Rss versus Peptone, Meat Ex, Alginate, CaCl2

```
Estimated Effects and Coefficients for Rss (coded units)

Term                            Effect      Coef
Constant                                  268.38
Peptone                         -17.25     -8.63
Meat Ex                           9.25      4.63
Alginate                         -1.00     -0.50
CaCl2                            99.25     49.63
Peptone*Meat Ex                  17.75      8.88
Peptone*Alginate                 13.50      6.75
Peptone*CaCl2                   -20.25    -10.13
Meat Ex*Alginate                -27.50    -13.75
Meat Ex*CaCl2                    13.75      6.88
Alginate*CaCl2                   79.50     39.75
Peptone*Meat Ex*Alginate         -5.50     -2.75
Peptone*Meat Ex*CaCl2             4.75      2.37
Peptone*Alginate*CaCl2          -26.50    -13.25
Meat Ex*Alginate*CaCl2            4.00      2.00
Peptone*Meat Ex*Alginate*
CaCl2                            25.50     12.75
Ct Pt                                     21.63

Analysis of Variance for Rss (coded units)

Source                DF      Seq SS     Adj SS     Adj MS      F      P
Main Effects           4     40938.8    40938.8    10234.7      *      *
2-Way Interactions     6     32691.7    32691.7     5448.6      *      *
3-Way Interactions     4      3084.3     3084.3      771.1      *      *
4-Way Interactions     1      2601.0     2601.0     2601.0      *      *
Curvature              1       440.1      440.1      440.1      *      *
Residual Error         0         0.0        0.0        0.0
Total                 16     79755.9
```

Minitab® Software factorial design output files

Artificial wastewater 5 kD membrane crossflow experiments:

09/01/2009 05:35:41 PM

```
Welcome to Minitab, press F1 for help.

Retrieving project from file: D:\DOCUMENTS AND SETTINGS\EEZEE
EEZEE\DESKTOP\MEMBRANE EXPERIMENTS\UF 5 KDA EXPERIMENTS.MPJ
```

Fractional Factorial Fit: Rss1 versus Peptone, Meat Ex, ...

Estimated Effects and Coefficients for Rss1 (coded units)

Term	Effect	Coef
Constant		266.44
Peptone	12.12	6.06
Meat Ex	28.38	14.19
Alginate	22.63	11.31
Calcium	32.38	16.19
Peptone*Meat Ex	11.12	5.56
Peptone*Alginate	-10.63	-5.31
Peptone*Calcium	-3.87	-1.94
Meat Ex*Alginate	35.63	17.81
Meat Ex*Calcium	-16.63	-8.31
Alginate*Calcium	-24.38	-12.19
Peptone*Meat Ex*Alginate	-6.13	-3.06
Peptone*Meat Ex*Calcium	-40.38	-20.19
Peptone*Alginate*Calcium	14.87	7.44
Meat Ex*Alginate*Calcium	22.12	11.06
Peptone*Meat Ex*Alginate* Calcium	15.88	7.94
Ct Pt		-3.44

Analysis of Variance for Rss1 (coded units)

Source	DF	Seq SS	Adj SS	Adj MS	F	P
Main Effects	4	10048.7	10048.7	2512.19	*	*
2-Way Interactions	6	9565.4	9565.4	1594.23	*	*
3-Way Interactions	4	9513.8	9513.8	2378.44	*	*
4-Way Interactions	1	1008.1	1008.1	1008.06	*	*
Curvature	1	11.1	11.1	11.12	*	*
Residual Error	0	0.0	0.0	0.00		
Total	16	30147.1				